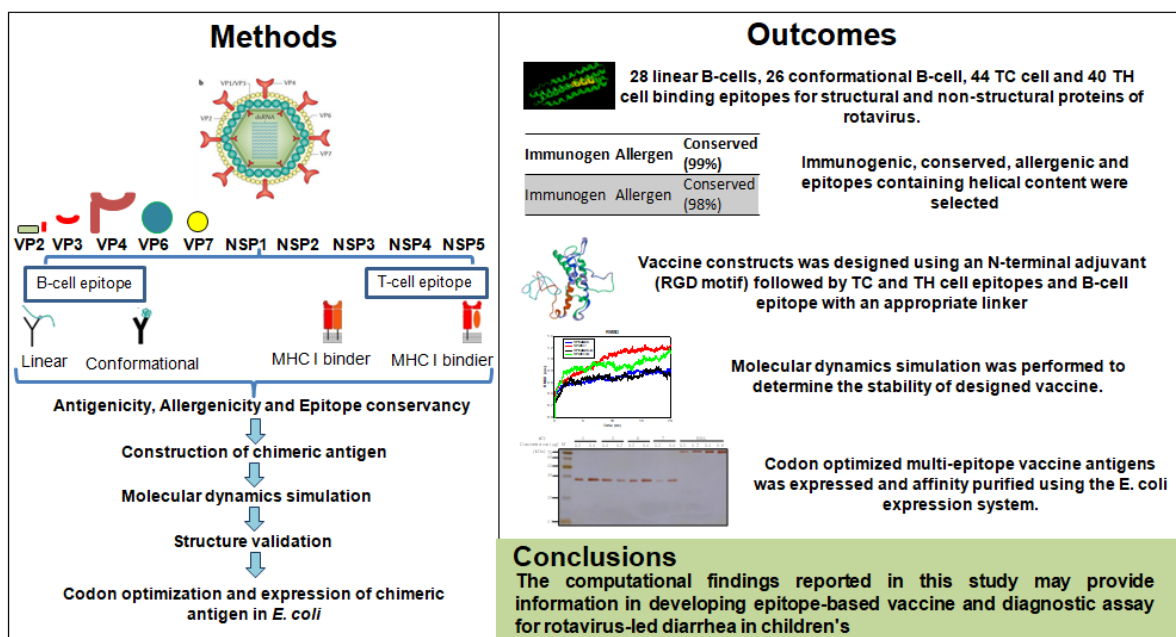# CHAPTER 6

IDENTIFICATION OF B- AND T-CELL EPITOPES OF ROTAVIRUS PROTEOME AND DEVELOPMENT OF CHIMERIC ANTIGEN FOR DIAGNOSIS OF ROTAVIRUS

Graphical Abstract

6.1. Introduction

Rotavirus-associated infection accounts for 39% of diarrhoeal deaths that occur mainly in low and middle-income countries and 22% of all rotavirus-related deaths worldwide can be attributed to India [1]. More than 100 countries have included the rotavirus vaccine into their immunization programmes since it is the most effective intervention in preventing severe rotavirus disease [2,3]. Although Rotarix and RotaTeq were licensed in 2006, India was unable to afford to include the vaccine in its universal immunization programme (UIP) due to concerns about cost and long-term price sustainability [4,5]. The effectiveness of Rotarix® and RotaTeq® in high-and middle-income countries were observed high ranging from 85% to 98% [2, 6]. However, average efficacies (51%–64%) were found in the low-income Asian and African countries [7,8].

The efficacy and effectiveness for Rotavac against severe gastroenteritis was 56% during the first year of life [9] and 49% in the subsequent year [10]. RotaSIIL is a heat-stable oral vaccine that can retain stability up to 18 months during storage at 40ºC [11]. The vaccine efficacy against severe rotavirus gastroenteritis in an immunized Indian children was 33% [12] and 67% in Niger [13]. The results of an Indian manufactured vaccines showed similar efficacy with the existing commercial vaccines for rotavirus in developing country populations. Live-attenuated strains of RV vaccines have the inherent potential to interchange genetic materials with the circulating strains that might generate a virulent RV strains [14]. Although at a lower rate, live-attenuated oral RV vaccines are associated with the risk of developing intussusception (IS) [15,16] in an age-dependent manner [17,18]. An estimated of about 1–6 cases of IS during the administration of first or second dose for Rotarix® and RotaTeq® per 100,000 immunized children have been reported [15]. Similar rates of IS have been observed for an Indian manufactured vaccines, Rotavac® [9] and RotaSIIL® [12]. Recombinant vaccines could overcome the adverse consequences of live-attenuated vaccines. The common recombinant subunit vaccines are Hepatitis B vaccine which consists of hepatitis B virus surface antigen and recent recombinant vaccine against human papillomaviruses [19]. Novel next generation vaccination involving a rational design of B- and T-cell epitope-based vaccine have made substantial progress in the clinical trials. The recombinant epitope-based malaria vaccine that successfully reached phase-III trials might become the first commercial vaccine for parasitic disease [20].

With the inclusion of indigenous RV vaccines in UIP, important aspects need to be examined including impact of the vaccine on disease burden, efficacy, safety and cost effectiveness. With the diverse strains of RV identified so far, rapid and accurate detection of RVA has been a major challenge, particularly in low- and middle-income countries. As mentioned in Chapter 2, the diagnosis methods detect either the surface antigen or its genome. RT-PCR, despite being highly sensitive, it is not affordable for use in surveillance studies especially in poor and resource-limited countries [21,22]. Although latex agglutination and electropherotyping tests are affordable, their low sensitivity and specificity limit their use in rotavirus detection in surveillance. Therefore, ELISA is an ideal diagnostic method currently used for detection of VP6 antigen of RVA in stool samples of diarrheic children. VP6 protein is highly immunogenic, abundant, and conserved among the rotavirus proteins thereby making it suitable for use as a universal

diagnostic assay [23]. Moreover, for more sensitive and effective diagnostic assays, peptides from other proteins of rotavirus that are highy reactive with anti-RV antibodies are of immense importance. The anti-peptide antibodies that are often targeted against more than two epitopes may serve as homogenous antibodies with increased specificity, affordability, and user-friendly procedure [24]. Further, combining multiple antigenic peptides may be a solution for the problem of low titer anti-peptide serum [24,25]. For serodiagnosis of various viruses, such antibodies have been in use; hepatitis C virus [26], infectious bronchitis virus [27], infectious bursal disease virus [28] and peste-des-petits ruminants virus [29].

Immunoinformatic approaches have been used for prediction of an antigenic epitope for vaccine development and high-affinity antibodies for therapeutic and diagnostic applications [30,31]. Some examples of computational immunoinformatic tools that has the potential to help experimental researchers to validate the in silico designed epitope-based vaccine includes but not limited to SARS-CoV-2 [32], Zika virus [33], and Nipah virus [34]. In silico identified protein regions with high probability of being effective epitopes might help in designing effective experimental assays with improved precision [35]. This part of work involves the application of extensive computational immunoinformatic tools to identify potential B and T- cell epitopes to enable us to design a multi-epitope vaccine construct containing predicted antigenic fragments of rotavirus proteins.

The final vaccine constructs carry a tripeptide Arg-Gly-Asp (RGD) cell adhesion motif at the N-terminal end to improve the immunogenicity. Allergenicity, antigenicity, epitope conservancy, structural modelling, docking and molecular dynamics simulation of vaccine constructs were carried out to ensure vaccine property of multi-epitope protein. Codon optimized vaccine antigens were expressed, and affinity purified in E. coli. The present observations of computational bioinformatics are expected to help researchers to select epitopes for further experimental validations and develop recombinant subunit vaccine against rotavirus.

6.2. Materials and methods

A schematic representation of an *in-silico* strategy followed for prediction of B- and T-cell epitope using proteome of rotavirus is presented in Figure 6.1.
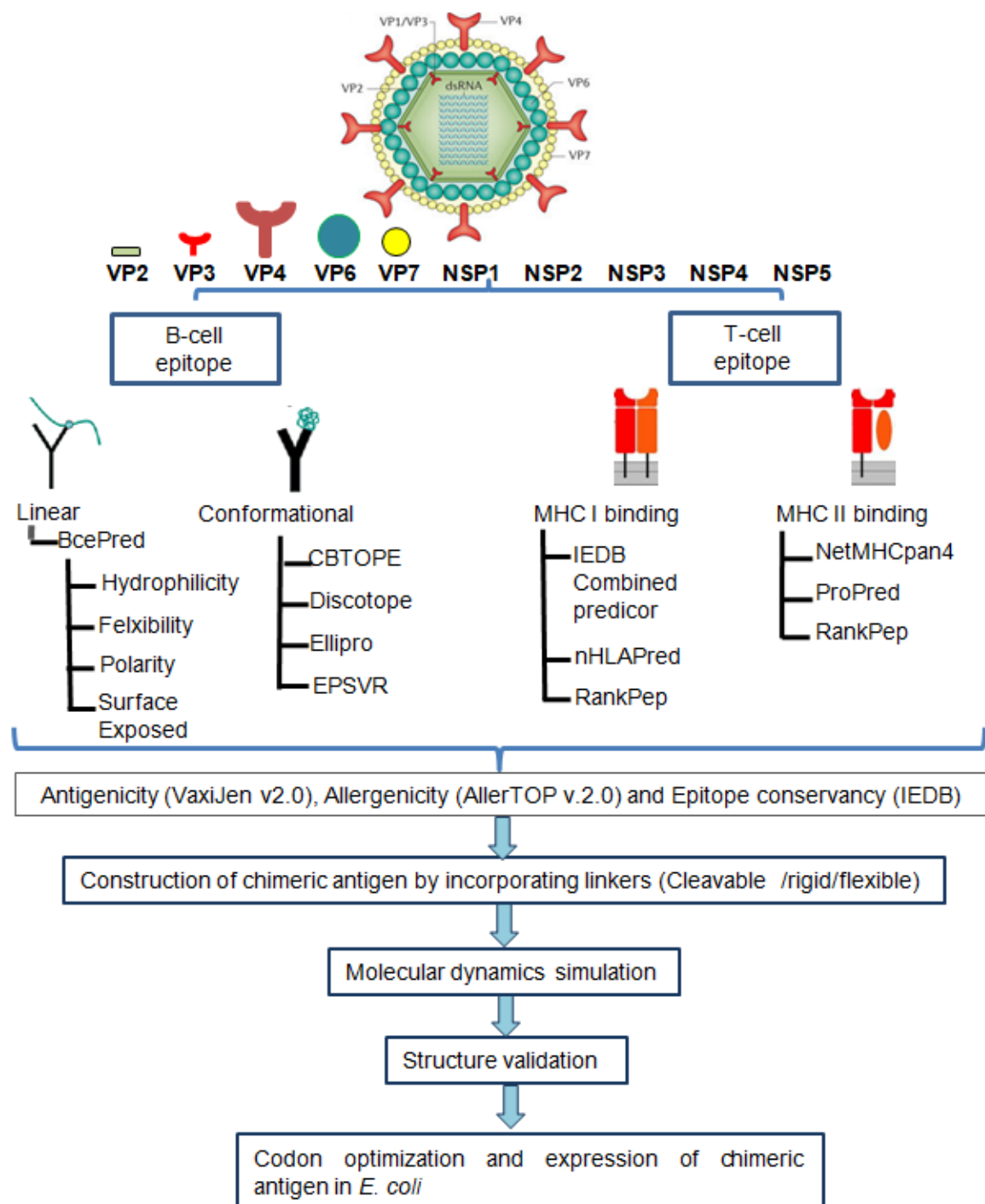
Figure 6.1. Schematic representation of an *in-silico* strategy followed for prediction of B- and T-cell epitope using proteome of rotavirus.

6.2.1. Rotavirus protein sequence and selection of antigenic protein

In this study, the prototype simian group A rotavirus SA11 strain was used as reference strain to download sequences of structural (VP1, VP2, VP3, VP4, VP6 and VP7) and non-structural proteins (NSP1, NSP2, NSP3, NSP4 and NSP5); VP6 protein sequences

of Adult diarrhoeal rotavirus (ADRV) and Cowden strain of porcine were included as group B and group C reference strains. The accession numbers of rotavirus proteins used for various bioinformatics analyses have been given in Table 6.1. All retrieved rotavirus protein sequence was analyzed for antigenicity using VaxiJen v2.0 server (http://ddg-pharmfac.net/vaxijen). VaxiJen is the first server used for prediction of whole protein antigenicity in an alignment-independent manner with high prediction accuracy of 70%–89% [36].

6.2.2. B-cell epitope prediction

Antigenic/immunogenic epitopes are specific region of an antigen that is recognized by the immune B-cell antibodies. We have predicted linear B-cell epitope using Bcepred server [37,38]. Bcepred predict B-cell epitopes based on combination of four parameters such as flexibility, hydrophilicity, polarity, and exposed surface with a prediction accuracy of about 58.7% (http://crdd.osdd.net/raghava/bcepred). We used full-length or partial crystallographic {VP4 {VP8 (PDB ID: 2P3I), VP5 (PDB ID: 2B4H)}, VP6 (PDB ID: 1QHD), VP7 (PDB ID: 3FMG), NSP2 (PDB ID: 1L9V), NSP3 (PDB ID: 1KNZ)} and modelled structures of rotavirus proteins to identify and predict a conformational B-cell epitopes [37]. Four different servers have been used to develop a reliable identification of conformational B-cell epitopes of rotavirus proteins [33,34,35,39]. CBTOPE server (http://crdd.osdd.net/raghava/cbtope) predicts B-cell epitope of an antigen using SVM-based model [40]. B-cell epitope prediction using DiscoTope 2.0 server (http://tools.iedb.org/discotope/) is based on estimation of surface accessibility with a default threshold setting value. ElliPro (http://tools.iedb.org/ellipro/) predicts B-cell epitopes using the structure of an antigen. EPSVR (http://sysbio.unl.edu/EPSVR/) uses a Support Vector Regression (SVR) method to predict B-cell epitopes and shown to exhibit high performance with AUC value 0.597 as compared to the existing prediction servers [41]. Agadir score (http://agadir.crg.es/) was calculated for selection of potent epitopes based on its helical content [42].

6.2.3. Prediction of cytotoxic T lymphocytes and helper T-cell epitope

Cytotoxic T lymphocytes (CTL) epitopes of 9-mer peptide length were predicted using three different tools [37]. Proteasomal cleavage/TAP transport/MHC class I combined predictor (http://tools.iedb.org/processing) is a tool that predicts CTL epitopes based on

combination of prediction scores obtained for each of proteasomal processing, TAP transport, and MHC binding. The top 2% binders with an IC50 less than or equal to 500nM was considered [43]. nHLAPred (http://crdd.osdd.net/raghava/nhlapred) predicts MHC I binding peptide using a neural network method [44]. Rankpep (http://imed.med.ucm.es/tools/rankpep.html) is used for prediction of peptides binding to MHC I and MHC II molecules using position specific scoring matrices and the top 2% MHC binders were selected [45]. Similarly, helper T-cell (HTL) epitopes were identified by NetMHCIIpan 3.1 (http://cbs.dtu.dk/services/NetMHCIIpan-3.1/). The threshold value for peptides with strong binding affinity was set as top 2%. ProPred (http://crdd.osdd.net/raghava/propred/) have been used to identify 9-mer promiscuous MHC II peptides based on quantitative matrices and the top 3% predicted peptides were selected as best binders [46]. Rankpep server predicted MHC class-II binding peptides top 5% best binders were selected in this study. A total of 27 HLA supertypes alleles with maximum population coverage (approximately >97%) were selected to identify and predict MHC I and II binding peptides [47,48,49,50,51].

6.2.4. Epitope immunogenicity, conservancy analysis and allergenicity assessment

Antigenicity of predicted epitopes in our vaccine constructs were assessed by VaxiJen v2.0. The identification of immunogenic epitopes is of great importance in understanding cellular immune responses and vaccine development. IEDB Class I immunogenicity tool (http://tools.iedb.org/immunogenicity/) was used to characterize the immunogenic potential of predicted 9-mer MHC I binding peptide [52]. We have predicted the immunogenicity (http://tools.iedb.org/CD4epi score) of MHC II binding epitopes using 7-allele method, immunogenicity method and combined method [41,53]. AllerTOP v2.0 (http://www.ddg-pharmfac.net/AllerTOP/) was used to predict the allergenic properties and the route of exposure of vaccine construct [42]. A web-based IEDB tool (http://tools.iedb.org/conservancy/) was used to predict the conservancy of epitopes that were included in the vaccine constructs [54].

6.2.5. Molecular docking and CTL/HTL mediated immunogenicity prediction

It is important to determine the strength of interaction of peptide-MHC molecules and the T-cell receptors. Molecular docking approach was used to identify and select the best CTL/HTL epitopes binding to MHC molecules. The 3D structure of peptide was

generated by PEP-FOLD 2.0 (http://bioserv.rpbs.univ-paris-diderot.fr/services/PEP-FOLD/) and N- and C-terminals ends were capped [55]. We retrieved the PDB files of MHC molecules from Protein Data Bank for docking purpose. MHC allele lacking a crystal structure was modeled by I-TASSER (https://zhanglab.ccmb.med.umich.edu/I-TASSER/). MHC-peptide docking simulation was performed using ClusPro v.2.0 docking program (www.cluspro.bu.edu) with default settings [56]. Interaction energy was analyzed by prodigy (http://milou.science.uu.nl/services/PRODIGY/) [57].

6.2.6. Designing epitope-based vaccine constructs

Using the information of predicted epitopes, a multi-epitope-based vaccine was designed using high scoring peptide sequence consisting of T- and B-cell epitopes. Predicted immune epitopes were joined by cleavable and flexible linkers [32,33,39]. Integrin binding motif (RGD) fused with EAAAK linker was added as adjuvant and forms the component of final multi-epitope vaccine [58].

6.2.7. Structure prediction and validation

Physiochemical properties of vaccine constructs were analyzed using ProtParam [59]. Secondary structure of designed vaccine was predicted using the sequence of amino acid as input data by PSIPRED v3.3 (http://bioinf.cs.ucl.ac.uk/psipred/). Position-specific iterated BLAST (PSI--BLAST) was employed to select sequences exhibiting homology to vaccine constructs [60]. Modeling of vaccine constructs was done byI-TASSER [61], Phyre [62] and RaptorX. The best structures selected based on similarity of structure modelled by all three methods (I-TASSER, RaptorX, Phyre2) was used for validation and molecular dynamics simulation. We validated modelled structure by RAMPAGE server that provides a Ramachandran plots for glycine and proline amino acid residues. Ramachandran plot shows the distribution of torsion angles [psi(ψ) and phi (ϕ)] in a protein structure based on calculated van der Waal radius of the side chain [63].

6.2.8. Molecular dynamics simulation of epitope-based vaccine

Molecular dynamics (MD) is a computer simulation method that provides detailed information on the fluctuations and conformational changes of atoms and molecules. MD simulation of epitope-based vaccine was performed using GROMACS, v4.6.5 [64]. We

used single point charge water molecules and CHARMM27 force field to determine the intermolecular interactions. Solvation was done in a cubic box-type and appropriate number of chloride and sodium ions was used to neutralize peptide charges. Energy minimization was done using the steepest decent algorithm for 50000 steps with the maximum force of 1000 kJ/mol/nm. Equilibration of NVT (constant Number of particles, Volume and Temperature) and NPT (constant Number of particle, Pressure and Temperature) ensemble was done for 100 ps using Particle Mesh Ewald algorithm. After equilibrations of NVT at 300 K and NPT at 1 bar and production MD run was performed for 20 ns using LINCS (Linear Constant Solver) algorithm [64]. Root mean square deviation and root mean square fluctuation were performed to calculate standard deviation and fluctuation of the protein backbone with respect to time.

6.2.9. Codon optimization, synthesis, expression, and affinity purification of chimeric constructs in *E. coli*

Codon optimized epitope-based vaccine namely constructs 1, 2, 6 and 7 was cloned into the Champion pET directional TOPO expression cloning vector (pET100/D-TOPO, Thermofischer Scientific) to achieve high level expression in *E. coli*. Expression of N-terminal 6X-His-tagged multi-subunit chimeric antigens was induced at culture OD600 of 0.6 using different concentration of IPTG at 18°C, 25°C and 37°C. Ni^{2+}-affinity purification of soluble protein was carried out using Tris-NaCl buffer with 5 mM imidazole in the binding buffer and eluted with 250 mM imidazole, pH 7.4. The purified protein was dialyzed in a Tris buffer supplemented with NaCl. The purity of protein was analyzed on silver stained SDS-PAGE and different concentrations of BSA were loaded to determine the approximate concentration of purified proteins estimated using Bradford assay.

6.3. Results and discussion

6.3.1. Sequence retrieval and selection of antigenic rotavirus proteins

The prototype simian agent 11 (SA11) was used as group A rotavirus reference strain to retrieve protein sequences in FASTA format due to availability of complete genome sequence (Table 6.1). Rotavirus pathogenesis is multifactorial, and the outcome of disease is determined by both host and viral factors. Genetic analysis of selected virus

reassortants identified several proteins of rotaviruses but not limited to VP3, VP4, VP6, VP7, NSP1, NSP2, NSP3, and NSP4 that are involved in virulence. The VP6 protein sequences of adult diarrhoeal rotavirus (ADRV) and Cowden strain of porcine were included as group B and group C prototype strains. Among 12 rotavirus proteins, only 9 proteins were predicted as antigenic using VaxiJen v.2.0 with probability of antigenicity scores in the range of 0.4043–0.5734 (Table 6.1). Rotavirus NSP4 was predicted as non-antigen by VaxiJen which might be due to the limitation of server. NSP4 protein has pleiotropic properties including viral enterotoxin, intracellular role in viral replication and morphogenesis [65]. Recombinant NSP4 protein is known to induce age and dose-dependent diarrhoea in suckling mice mimicking a rotavirus disease caused during natural infection [66]. NSP4 and 9 other rotavirus proteins predicted as antigens were analyzed for the identification of B- and T-cell epitopes using well established immunoinformatic prediction methods (Figure 6.1).

Table 6.1: Physico-chemical analysis and prediction of antigenicity of rotavirus proteins

Protein	Rotavirus protein sequence	Protein PDB ID	Length	Mol. Wt. (Da)	pI value	Highly repeated amino acid	Antigenicity (VaxiJen v2.0 score)
VP1	YP_002302227.1	-	1088	125207.83	8.35	Leu (L) 9.9%	Non-antigen (0.3592)
VP2	YP_002302226.1	-	882	102740.82	5.70	Leu (L) 10.9%	Antigen (0.4043)
VP3	YP_002302228.1	-	835	98069.11	7.89	Ile (I) 9.9%	Antigen (0.5068)
VP4	YP_002302230.1	2B4H	776	86774.57	5.15	Ser (S) 9.8%	Antigen (0.5283)
VP6	YP_002302229.1	1HQD	397	44873.00	5.81	Asn (N) 9.3%	Antigen (0.4939)
VP7	YP_002302222.1	3FMG	326	37197.79	4.68	Thr (T) 11.3%	Antigen (0.4739)
NSP1	YP_002302219.1	-	496	58564.75	8.48	Leu (L) 10.3%	Antigen (0.4938)
NSP2	YP_002302221.1	IL9V	317	36569.28	9.02	Lys (K) 9.5%	Antigen (0.5734)
NSP3	YP_002302220.1	1KNZ	315	36424.50	5.64	Ser (S) 9.2%	Antigen (0.5038)
NSP4	YP_002302223.1	-	175	20331.84	7.69	Thr (T) 11.4%	Non-antigen (0.3564)
NSP5	YP_002302224.1	-	198	21722.10	6.73	Ser (S) 19.2%	Antigen (0.5083)
VP6 (Group B)	M55982.1	-	391	43671.00	5.40	Ile (I) 9.5%	Antigen (0.4989)
VP6 (Group C)	AAA47097.1	-	395	44664.64	5.85	Asn (N) 8.9%	Antigen (0.4511)

6.3.2. B-cell epitope mapping

B cells are primarily involved in the production of antibodies to provide a protective immune defense against the foreign pathogens through the complement activation, antibody-mediated cytotoxicity, and Fc-mediated endocytosis. Additionally, B cells can exert antibody independent functions like antigen presentation, cytokine secretion, and immunoregulation [67]. The possible presence of linear B-cell epitopes in structural (VP2, VP3, VP4, VP6, VP7) and non-structural (NSP1, NSP2, NSP3, NSP4, NSP5) proteins were predicted by Bcepred using parameters such as antigenicity, surface

accessibility, turns, flexibility and hydrophilicity. Bcepred prediction method uses a dataset of 1029 experimentally proven continuous B cell epitopes and 1029 non-epitopes covering a protein derived from viruses, bacteria, protozoa and fungi. Therefore, Bcepred server is a reliable method used to predict the linear B-cell epitopes with an accuracy of 58.70% based on amino acid properties namely hydrophilicity, flexibility, polarity and exposed surface [36]. A total of 31 linear B-cell epitopes (9–15-mer length) were predicted for all proteins including 3 and 4 epitopes for group B and group C VP6 protein, respectively (Table 6.2). We have developed a heat map to show the distribution of predicted linear B-cell epitopes across structural and nonstructural proteins of rotavirus Figure 6.4A). We have selected 14 continuous B-cell epitopes with 2 epitopes each from VP6 group B and group C for inclusion in the vaccine construct based on epitope conservancy and agadir score of predicted epitopes. A maximum of 6 linear B-cell epitopes were predicted for VP4, 1 epitope was predicted for NSP5 and no epitope was predicted for NSP1 (Table 6.3). A conformational B-cell epitope is made of discontinuous stretches of amino acid residues that are tightly held together in tertiary conformation and as over 90% of epitopes are conformational epitopes [68]. Rotaviral proteins lacking crystallographic structures were modeled using multiple-threading approach server I-TASSER. The c-score of best modeled structures were 0.010, -0.84, -1.41, -1.33, -1.71, -1.17 and -2.83 for VP2, VP3, VP4, VP7, NSP3, NSP4 and NSP5, respectively (Figure 6.3). The best selected modeled structures were energy minimized and validated structures were used for prediction of conformational B-cell epitopes using four different independent tools to achieve maximum accuracy of computed epitope mapping; CBTOPE, DiscoTope 2.0, Ellipro and EPSVR (Table 6.3). The epitopes predicted by at least two different tools and found as antigenic, non-allergenic with agadir score and good conservancy across antigens have been selected as potential discontinuous B-cell epitope. Maximum 4 discontinuous 9 to 20-mer epitopes were predicted for VP4, while only 1 epitope each was predicted for NSP2, and VP4 (Table 6.8). The localization of selected linear B-cell epitope in their native rotavirus protein structure was carried out using structural superimposition (Figure 6.2). Agadir algorithm analyzes the stability of isolated α-helices and the alpha-helical tendency of the peptide in solution [48]. We found the epitope of rotavirus proteins VP3 (aa238-249), VP7 (aa168–184), NSP2 (aa298-312), NSP3 (aa108-120), and NSP5 (aa170-183) that are predicted to function as both linear and conformational B-cell epitopes (Table 6.2 & 6.3).

Table 6.2. Summary of linear B-cell epitopes predicted by Bcepred. Four physico-chemical properties namely, hydrophilicity (Property 1), flexibility (Property 2), polarity (Property 3) and exposed surface (Property 4) were considered for prediction of B-cell epitopes. The selected epitopes used for designing multi-epitope vaccine constructs are highlighted in bold

RV Protein	Position	Linear B-cell epitopes	Length	Bcepred Parameter	Agadir Score	Conservancy analysis by IEDB tool
VP2	**189-200**	**AVENKNSRDAGK**	**12**	**1,2,3&4**	**0.33**	**98.82%**
	275-284	YIPERIRNDV	10	3&4	0.62	97.65%
	633-643	LNLYQKKMKSI	11	2,3&4	0.55	65.29%
	664-673	MYRLRDRLRL	10	3&4	0.32	95.29%
	690-701	NMEQIERASDKI	12	2&4	0.35	61.76%
VP3	**238-249**	**TIKLKQERWLGK**	**12**	**2,3&4**	**0.36**	**46.08%**
	658-666	ACRSAKEFA	9	4	0.33	55.76%
	819-827	SIYLRKIKG	9	2,3&4	0.38	74.65%
VP4	20-32	DEIQEIGSTKSQN	13	1&2	0.43	4.67%
	241-253	**RDVIHYRAQANED**	**13**	**1&4**	**0.29**	**4.00%**
	208-220	**IPRSEESKCTEYI**	**14**	**1,2&4**	**0.41**	**4.67%**
	262-271	**WKEMQYNRDI**	**10**	**4**	**0.48**	**97.33%**
	657-667	**PDIVTEASEKF**	**11**	**1&2**	**0.4**	**76.67%**
	725-736	KTLKNLNDNYGI	12	3&4	0.25	96.00%
VP6	**9-21**	**KTLKDARDKIVEG**	**13**	**2,3&4**	**0.63**	**88.52%**
	98-108	DEMVRESQRNG	11	1,2,3&4	0.51	57.38%
	109-119	IAPQSDSLRKL	11	2&3	0.45	47.54%
	139-149	**WNLQNRRQRTG**	**11**	**1,2,3&4**	**0.69**	**98.36%**
	373-384	**NYSPSREDNLQR**	**12**	**1,2,3&4**	**0.3**	**96.72%**
VP7	174-185	YYQQTDEANKWI	12	1&4	0.31	44.78%
	308-320	**QVMSKRSRSLNSA**	**13**	**2&4**	**0.28**	**73.88%**
NSP2	**267-281**	**QNWYAFTSSMKQGNT**	**15**	**1&2**	**0.32**	**72.34%**
	298-312	NPFKGLSTDRKMDEV	15	1,2&4	0.3	89.36%
NSP3	51-66	DFVMDDSGVKNNLIGK	16	1&2	0.4	23.91%
	108-120	**LSSKGIDQKMRVL**	**13**	**1&2**	**0.48**	**96.74%**
	226-235	YNNKLERDLQ	10	1&4	0.39	40.22%
NSP4	87-99	EQITTKDEIEKQM	13	1,3&4	0.59	42.86%
	101-111	RVVKEMRRQLE	11	2,3&4	0.51	41.07%
	117-128	**TTREIEQVELLK**	**12**	**4**	**0.58**	**96.43%**
	144-155	MTKEINQKNVRT	12	3&4	0.38	26.79%
NSP5	**170-183**	**KCKNCKYKKKYFAL**	**14**	**3&4**	**0.55**	**74.47%**

Table 6.2. contd…..

| RV Protein	Position	Linear B-cell epitopes	Length	Bcepred Parameter	Agadir Score	Conservancy analysis by IEDB tool
VP6_Group B	9-20	ACVKLQKRVLGL	12	4	0.39	42.86%
	74-86	**ISTDDYDDMRSGI**	**13**	**1&2**	**0.28**	**76.19%**
	197-211	**GMDSEHRFTVELKTR**	**15**	**1,2&4**	**0.57**	**34.38%**
VP6_Group C	10-19	TVSDLKKKV	9	2,3&4	0.51	69.57%
	93-104	**EAVCDDEIVREA**	**12**	**1,2&4**	**0.48**	**86.96%**
	130-141	NNSSQSIKNWSA	12	1&2	0.58	60.87%
	143-156	**SRRENPVYEYKNPM**	**14**	**3&4**	**0.3**	**60.87%**
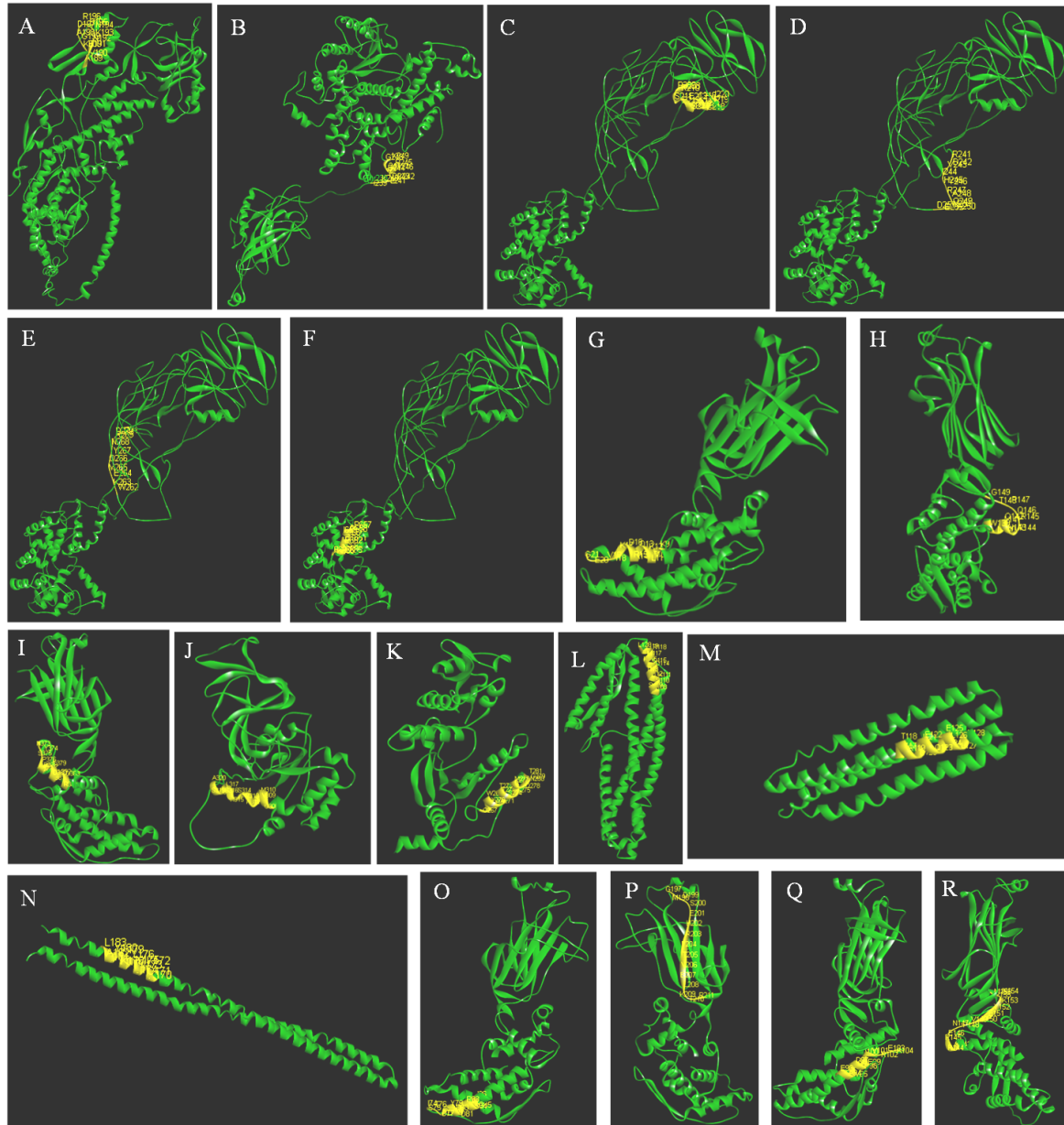
Figure 6.2. Localization of selected linear B-cell epitope in native rotavirus protein.
A. VP2; 189-AVENKNSRDAGK-200, B. VP3; 238-TIKLKQERWLGK-249, C. VP4;
208- IPRSEESKCTEYI-220, D. VP4; 241-RDVIHYRAQANED-253, E. VP4; 262-
WKEMQYNRDI- 271, F. VP4; 657-PDIVTEASEKF-667, G. VP6; 9-
KTLKDARDKIVEG-21, H. VP6; 139- WNLQNRRQRTG-149, I. VP6; 373-
NYSPSREDNLQR-384, J. VP7; 308-QVMSKRSRSLNSA- 320, K. NSP2; 267-
QNWYAFTSSMKQGNT-281, L. NSP3; 108-LSSKGIDQKMRVL-120, M. NSP4; 117-
TTREIEQVELLK-128, N. NSP5; 170-KCKNCKYKKKYFAL-183, O. VP6 (Group A);
74-ISTDDYDDMRSGI-86, P. VP6 (Group B); 197-GMDSEHRFTVELKTR-211, Q.
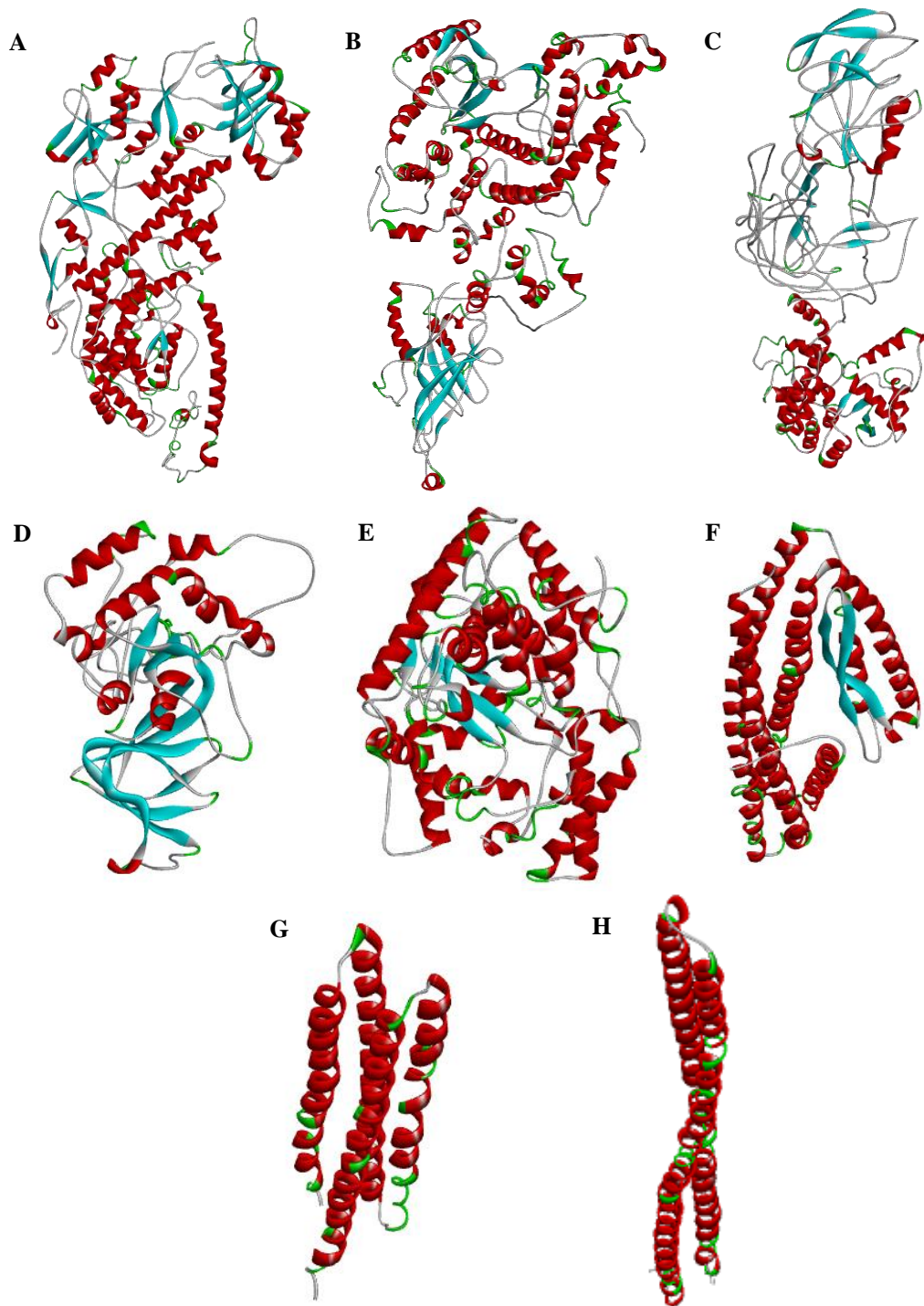VP6 (Group C); 93-EAVCDDEIVREA-104, R. VP6 (Group C); 143-
SRRENPVYEYKNPM-156.

Figure 6.3. Structure modeling of rotavirus proteins using I-TASSER. A. VP2, B. VP3, C. VP4, D. VP7, E. NSP1, F. NSP3, G. NSP4 and H. NSP5.

Table 6.3. **Summary of predicted conformational B-cell epitopes.** Four servers were used based on amino acid sequence dependent, CBTOPE (1) and three structure-dependent tools, Ellipro (2), Discotope (3) and EPSVR (4). The selected epitopes used for designing multi-epitope vaccine constructs are highlighted in bold

RV Protein	PDB/I model	Conformational B-cell Epitope	Server	No. of residues	Aagadir Score	Conservancy analysis by IEDB tool
VP2	I-TASSER	K72,Q73,L74,L75,E76,V77,L78,K79,T80,K81,E82,E83,H84	2,3&4	13	0.5	38.24%
		K339,E340,L341,V342,S343,T344,E345,A346,Q347,I348,Q349,K350,M351	**1,3&4**	**13**	**0.41**	**97.65%**
		A441,F442,G443,M444,Q445,R446,M447,H448,Y449,R450,N451,G452,D453,P454,Q455	1,2,3&4	15	0.38	98.24%
		D807,S808,N809,D810,F811,Y812,L813,V814,A815,N816,Y817,D818,W819,I820,P821,T822	3&4	16	0.47	60.59%
VP3	I-TASSER	Y29,E30,N31,A32,F33,L34,I35,S36,N37,L38,T39,T40,H41,N42,I43,L44,Y45	2,3&4	17	0.33	96.31%
		R176,M177,T178,T179,S180,L181,P182,I183,A184,R185,L186,S187,N188,R189,V190,F191,R192	**2,3&4**	**17**	**0.53**	**98.16%**
		T238,I239,K240,L241,K242,Q243,E244,R245,W246,L247,G248,K249,R250	2&3	13	0.51	46.08%
VP4	2B4H	**T413,Q414,F415,T416,D417,F418,V419,S420,L421,N422,S423,L424**	**3&4**	**12**	**0.27**	**93.33%**
VP6	1HQD	**Y24,S25,N26,V27,S28,D29,L30,I31,Q32,Q33,F34,N35,Q36**	**1&3**	**13**	**0.57**	**90.16%**
		D74,A75,N76,Y77,V78,E79,T80,A81,R82,N83,T84,I85,D86,Y87	**3&4**	**14**	**0.58**	**44.26%**
		E260,E262,L264,L265,N266,G267,Q268,I269,I270,N271,T272,Y273,Q274,A275,R276,F277,G278,T279	1,3&4	18	0.52	93.44%
VP7	I-TASSER	T101,L102,S103,Q104,L105,F106,L107,T108,K109,G110,W111,P112,T113,G114	1,3&4	14	0.27	29.85%
		M168,D169,I170,T171,L172,Y173,Y174,Y175,Q176,Q177,T178,D179,E180,A181,N182,K183,W184	1,3&4	17	0.38	29.10%
		R286,I287,N288,W289,K290,K291,W292,W293,Q294,V295	**3&4**	**10**	**0.61**	**26.87%**
	3FMG	**D169,I170,T171,L172,Y173,Y174,Y175,Q176,Q177,T178,D179,E180,A181,N182,K183,W184**	**1,3&4**	**16**	**0.32**	**29.10%**

Table 6.3.contd…..

RV Protein	PDB/I model	Conformational B-cell Epitope	Server	No. of residues	Aagadir Score	Conservancy analysis by IEDB tool
NSP2	IL9V	**N298,P299,F300,K301,G302,L303,S304,T305,D306,R307,K308,M309,D310,E311,V312,S313**	**2,3&4**	**16**	**0.39**	**89.36%**
NSP3	I-TASSER	R105,M106,M107,L108,S109,S110,K111,G112,I113,D114,Q115,K116,M117,R118,V119,L120	2,3&4	16	0.47	22.83%
		F78,G79,S80,A81,I82,R83,N84,R85,N86,W87	4	10	0.51	45.65%
	1KNZ	**K77,F78,G79,S80,A81,I82,R83,N84,R85,N86**	**2,3&4**	**10**	**0.36**	**45.65%**
NSP4	I-TASSER	**I51,P52,T53,M54,K55,I56,A57,L58,K59**	**1,3&4**	**9**	**0.36**	**91.74%**
		E157,E158,W159,E160,S161,G162,K163,N164,P165,Y166,E167	1,2&4	11	0.24	21.43%
NSP5	I-TASSER	K19,N20,E21,S22,S23,S24,T25,T26,S27,T28,L29,S30,G31,K32,S33,I34,G35,R36	2,3&4	18	0.23	59.57%
		A66,S67,N68,D69,P70,L71,T72,S73,F74,S75,I76,R77,S78,N79,A80,V81,K82,T83,N84,A85	**1,2,3&4**	**20**	**0.5**	**89.36%**
		N173,C174,K175,Y176,K177,K178,K179,Y180,F181,A182,L183,R184	2,3&4	12	0.3	75.53%
VP6_Group B	I-TASSER	**E154,N155,P156,L157,Y158,A159,D160,I161,I162,E163,Q164,I165,V166,H167,R168**	**1,2&4**	**15**	**0.59**	**35.71%**
VP6_Group C	I-TASSER	**F364,P365,W366,E367,Q368,T369,L370,S371,N372,Y373,T374,V375,A376,Q377,E378**	**1&4**	**15**	**0.32**	**59.57%**

6.3.3. Computational mapping of T-cell epitopes

In a given population some representative alleles called supertypes are found more frequently than others and have commonly shared binding specificity and these are of empirical use for epitope based vaccine development [47]. 27 alleles (Table 6.4a) of major Human Leukocyte Antigen class I (HLA-I) supertypes are known to have more than 97% population coverage (African Americans, Caucasians, Hispanics, Asians, North American Natives) [48,49]. Similarly, for HLA-II, 27 alleles (Table 6.4b) have been shown to provide more than 99% population coverage [50,51].

Cytotoxic T lymphocyte (CTL) belongs to the CD8+ subset of T cells that are associated with killing of cells-infected with intracellular virus, bacterial or protozoal parasites. CD8+ T cells bind epitopes that are presented by the MHC class I molecule while the CD4+ T cells recognize epitopes that are presented by MHC class I molecule. T cells are required for both cell- and antibody-mediated immune protection systems. A total of 39 CTL epitopes (9-mer) were predicted for rotavirus proteome using three different tools namely IEDB Proteasomal cleavage/TAP transport/MHC class I combined predictor, nHLAPred and RankPep (Table 6.5a). Similarly, a heat map was generated to indicate the distribution of predicted HLA-class I (Figure 6.4B) and II epitopes (Figure 6.4C) of structural and non-structural proteins of rotavirus. The highly conserved VP6 capsid protein sequences from group B and C rotaviruses were similarly analyzed and predicted 3 and 2 CTL epitopes, respectively (Table 6.6a and Table 6.6b). We used NetMHCpan 3.1, ProPred and RankPep tools for prediction of HTL epitopes based on high affinity score. We have predicted and found total of 36 HTL epitopes (13-mer) for all proteins analyzed including one and three epitopes for VP6 of group B and C rotaviruses, respectively (Table 6.6a and Table 6.6b). Herein we reported prediction of CTL and HTL epitopes of rotavirus proteins using a total of 27 alleles of major HLA-I and HLA-II supertypes. Immunogenicity of CTL epitopes was predicted using IEDB method and epitopes that were assigned a higher score were selected indicating a greater probability to induce an immune response. Similarly, using IEDB tool we have predicted the immunogenicity of MHC class II epitopes and the results generated peptides of 15-mer amino acid residues with immunogenicity score ranging from 73-99 indicating non-immunogenic peptides (Table 6.6b). The observed poor predicted immunogenicity of CD4 epitopes could be due to the availability of only seven number of HLA alleles in the

database tool [41, 53]. The probable cross-reactive allergenic peptides were predicted by online server AllerTOP v2.0. IEDB tool was used to analyze epitope conservancy with sequence identity threshold less than or equal to 100% and avoiding duplicated protein sequences. We have applied four criteria such as immunogenicity, non-allergenicity, conservancy and the same epitopes is being predicted by two of the three methods used to qualify the selection of predicted CTL and HTL epitopes for docking with MHC molecules (Table 6.5a & 6.5b).

Table 6.4a. List of HLA class I supertype alleles used in this study

Sl. No.	HLA Class I Supertype Alleles	PDB ID/Model	NetMHCpan	nHLAPred	Rankpep
1	HLA-A*02:01	1duz	Yes	Yes	Yes
2	HLA-A*02:03	3ox8	Yes	Yes	Yes
3	HLA-A*02:06	3oxr	Yes	Yes	Yes
4	HLA-A*03:01	2xpg	Yes	Yes	Yes
5	HLA-A*11:01	Model	Yes	Yes	Yes
6	HLA-A*24:02	3i6l	Yes	Yes	Yes
7	HLA-A*31:01	Model	Yes	Yes	Yes
8	HLA-A*68:01	4hwz	Yes	Yes	Yes
9	HLA-A*68:02	4i48	Yes	Yes	Yes
10	HLA-B*07:02	3vcl	Yes	Yes	Yes
11	HLA-B*35:01	4prn	Yes	Yes	Yes
12	HLA-B*44:03	Model	Yes	Yes	Yes
13	HLA-B*51:01	1e27	Yes	Yes	Yes
14	HLA-B*53:01	1a1m	Yes	Yes	Yes
15	HLA-B*58:01	Model	Yes	Yes	Yes
16	HLA-A*01:01	4nqv	Yes	No	Yes
17	HLA-A*33:01	Model	Yes	No	Yes
18	HLA-B*15:01	Model	Yes	No	Yes
19	HLA-B*44:02	Model	Yes	No	Yes
20	HLA-B*57:01	3x12	Yes	No	Yes
21	HLA-A*23:01	Model	Yes	No	No
22	HLA-A*26:01	Model	Yes	No	No
23	HLA-A*30:01	Model	Yes	No	No
24	HLA-A*30:02	Model	Yes	No	No
25	HLA-A*32:01	Model	Yes	No	No
26	HLA-B*08:01	1m05	Yes	No	No
27	HLA-B*40:01	Model	Yes	No	No
Total			**27**	**15**	**20**

Table 6.4b. List of HLA class II supertype alleles used in this study

Sl. No.	HLA Class II Supertype Alleles	PDB ID/Reference PDB ID	NetMHCIIpan	Propred	Rankpep
1	HLA-DRB1*01:01	1aqd	Yes	Yes	Yes
2	HLA-DRB1*03:01	1a6a	Yes	Yes	Yes
3	HLA-DRB1*04:01	1d5z	Yes	Yes	Yes
4	HLA-DRB1*04:05	6bin	Yes	Yes	Yes
5	HLA-DRB1*07:01	1aqd (Ref)	Yes	Yes	Yes
6	HLA-DRB1*11:01	1aqd (Ref)	Yes	Yes	Yes
7	HLA-DRB1*13:02	1aqd (Ref)	Yes	Yes	Yes
8	HLA-DRB1*15:01	1bx2	Yes	Yes	Yes
9	HLA-DRB5*01:01	1hqr	Yes	Yes	Yes
10	HLA-DRB1*08:02	1aqd (Ref)	Yes	Yes	No
11	HLA-DRB1*09:01	1aqd (Ref)	Yes	No	Yes
12	HLA-DRB1*12:01	1aqd (Ref)	Yes	No	Yes
13	HLA-DRB4*01:01	1aqd (Ref)	Yes	No	Yes
14	HLA-DQA1*05:01/DQB1*02:01	5ksu	Yes	No	Yes
15	HLA-DQA1*03:01/DQB1*03:02	5ujt	Yes	No	Yes
16	HLA-DQA1*01:01/DQB1*05:01	4grl	Yes	No	Yes
17	HLA-DQA1*01:02/DQB1*06:02	1uvq	Yes	No	Yes
18	HLA-DRB3*01:01	2q6w	Yes	No	No
19	HLA-DRB3*02:02	4h25	Yes	No	No
20	HLA-DQA1*05:01/DQB1*03:01	5ksu (Ref)	Yes	No	No
21	HLA-DQA1*04:01/DQB1*04:02	4grl (Ref)	Yes	No	No
22	HLA-DPA1*02:01/DPB1*01:01	3lqz (Ref)	Yes	No	No
23	HLA-DPA1*01:03/DPB1*02:01	3lqz	Yes	No	No
24	HLA-DPA1*01/DPB1*04:01	3lqz (Ref)	Yes	No	No
25	HLA-DPA1*03:01/DPB1*04:02	3lqz (Ref)	Yes	No	No
26	HLA-DPA1*02:01/DPB1*05:01	3wex	Yes	No	No
27	HLA-DPA1*02:01/DPB1*14:01	3lqz (Ref)	Yes	No	No
Total			**27**	**10**	**16**

Table 6.5a. Summary of predicted MHC I binding epitopes. Three different tools were used and servers that predicted the corresponding epitope are numbered as IEDB Proteasomal cleavage/TAP transport/MHC class I combined predictor (1), nHLAPred (2) and RankPep (3). The selected epitopes used for designing multi-epitope vaccine constructs are highlighted in bold

Protein	Position	Length	MHC I Epitope (9 mer)	No. of alleles	Server	Immunogenicity by IEDB tool	Allergeicity by AllerTope v. 2.0	Conservancy analysis IEDB tool
VP2	757-765	9	QPVALVGAL	2	1,2&3	0.13229	Non-allergen	97.06%
	760-768	9	ALVGALPFI	12	1,2&3	0.1342	Allergen	35.29
	845-853	9	TSNLTFTVY	6	1,2&3	0.19162	Non-allergen	93.53%
	311-319	9	NLHDNFESL	12	1&2	0.12456	Allergen	97.65%
	777-785	9	IAKLDATVF	4	1&2	0.03415	Non-allergen	99.41%
	95-103	9	KTIPTFEPK	5	1&3	0.25806	Allergen	96.47%
	123-131	9	KLFRIFEPK	5	1&3	0.4079	Allergen	36.47%
	544-552	**9**	**QLVDLTRLL**	**3**	**1&3**	**0.09866**	**Non-allergen**	**95.88%**
	588-596	9	MLIGNATVI	3	1&3	0.16471	Non-allergen	37.65%
	598-606	9	SPQTLFHYY	2	1&3	0.126	Non-allergen	98.24%
	619-627	9	RINDAVAII	2	1&3	0.20796	Non-allergen	97.06%
	666-674	9	RLRDRLRLL	4	1&3	0.11628	Non-allergen	98.24%
	782-790	9	ATVFAQIVK	1	1&3	0.1967	Allergen	87.65%
	625-633	9	AIITAANRL	10	2&3	0.18197	Allergen	97.06%
VP3	**72-80**	**9**	**LFTLIRCNF**	**2**	**1&3**	**0.13048**	**Non-allergen**	**68.66%**
	252-260	9	SQFDIGQYK	2	1&3	0.1219	Non-allergen	98.62%
	397-405	9	LLHHPTTEI	2	1&3	0.16005	Allergen	56.22%
	612-620	9	HVYNALIYY	9	1&3	0.13011	Allergen	97.24%
VP4	**288-296**	**9**	**GYKWSEISF**	**2**	**1&3**	**0.1017**	**Non-allergen**	**25.93%**
	460-468	9	EYYEIAGRF	2	1&3	0.32482	Allergen	22.22%
	720-728	9	AIIDFKTLK	3	1&3	0.0028	Non-allergen	95.68%
VP6	218-226	9	LTTATITLL	13	1&2	0.24133	Allergen	91.80%
	314-322	9	FEHHATVGL	11	1&2	0.17233	Non-allergen	49.18%
	226-234	**9**	**LPDAERFSF**	**3**	**1&3**	**0.19493**	**Non-allergen**	**95.08%**
	253-261	9	ILRPNNVEV	2	1&3	0.08659	Non-allergen	83.61%
VP7	**15-23**	**9**	**SIILLNYIL**	**12**	**1&2**	**0.08979**	**Non-allergen**	**67.91%**
	166-174	9	NPMDITLYY	2	1&3	0.11994	Non-allergen	70.90%
	225-233	9	VITDVVDGV	3	1&3	0.1525	Allergen	40.30%
	253-261	9	GPRENVAVI	1	1&3	0.20725	Allergen	51.49%
	316-324	9	SLNSAAFYY	6	1&3	0.003	Allergen	79.10%

Table 6.5a. contd….

Protein	Position	Length	MHC I Epitope (9 mer)	No. of alleles	Server	Immunogenicity by IEDB tool	Allergeicity by AllerTope v. 2.0	Conservancy analysis IEDB tool
NSP2	234-242	9	VANHADRVY	4	1&2	0.15723	Allergen	50.00%
	9-18	**9**	**YPHLENDSY**	**2**	**1&3**	**0.01281**	**Allergen**	**94.68%**
	177-185	9	MPILDQNFI	3	1&3	0.00754	Allergen	79.79%
	179-187	9	ILDQNFIEY	3	1&3	0.16536	Allergen	76.60%
NSP3	16-24	9	NSSFEAAVV	2	1&2	0.25557	Allergen	42.39%
	66-74	9	KAITIDQAL	1	1&2	0.15784	Allergen	51.09%
	58-66	**9**	**GVKNNLIGK**	**5**	**1&3**	**0.03887**	**Non-allergen**	**28.26%**
NSP4	32-40	9	YFPYIASVL	9	1&2	0.04361	Allergen	94.64%
	36-44	**9**	**IASVLTVLF**	**8**	**1&2**	**0.04194**	**Non-allergen**	**91.07%**
NSP5	**2-10**	**9**	**SLSIDVTSL**	**2**	**1&3**	**0.07678**	**Allergen**	**92.55%**
VP6_Group B	62-70	9	TINAPIISL	12	1,2&3	0.16741	Non-allergen	45.24%
	89-97	**9**	**ILDVLAAAI**	**3**	**1&3**	**0.13065**	**Non-allergen**	**64.29%**
	200-208	9	SEHRFTVEL	13	1&2	0.30646	Non-allergen	45.24%
VP6_Group C	33-41	9	QTNELIRTL	2	1&2	0.27949	Allergen	93.62%
	325-233	**9**	**ILDATTESV**	**3**	**1&3**	**0.10875**	**Non-allergen**	**69.57%**

Table 6.5b. Summary of predicted MHC II binding epitopes. Three different tools were used and servers that predicted the corresponding epitope are numbered as NetMHCpan 3.1 (1), ProPred (2) and RankPep (3). The selected epitopes used for designing multi-epitope vaccine constructs are highlighted in bold

RV Protein	Position	Length	Core	MHC II epitope (13 mer)	No. of alleles	Server	Antigenicity by Vexigen (T=0.4)	Immunogenicity score by IEDB tool	Allergeicity by AllerTope v. 2.0	Conservancy by IEDB conservancy tool
VP2	386-398	13	388-MLSQRTMSL-396	AAMLSQRTMSLDF	2	1&3	1.4669	97.3031	Non-allergen	92.35%
	439-451	13	442-FGMQRMHYR-450	YPAFGMQRMHYRN	2	1&2	1.2356	-	Non-allergen	98.24%
	464-476	13	468-FQVANWLHF-478	QIQNFQVANWLHF	7	1,2&3	0.9045	-	Non-allergen	98.24%
	534-546	**13**	**535-ILLLSNRLG-543**	**GILLLSNRLGQLV**	**7**	**1,2&3**	**0.7962**	**-**	**Non-allergen**	**97.65%**
	578-590	13	580-LTSVTSLCM-588	LQLTSVTSLCMLI	2	1&2	0.8829	99.1627	Non-allergen	98.82%
	624-636	13	627-ITAANRLNL-635	VAIITAANRLNLY	8	1,2&3	0.6395	-	Non-allergen	97.06%
	664-676	13	665-YRLRDRLRL-673	MYRLRDRLRLLPV	11	1,2&3	1.6025	-	Non-allergen	95.29%
	752-764	13	754-LNNQPVALV-761	MLLNNQPVALVGA	4	1&2	0.7018	91.7816	Non-allergen	97.06%
	771-783	13	774-ISLIAKLDA-782	SSVISLIAKLDAT	3	1&2	0.7733	94.5674	Non-allergen	97.65%
	663-675	13	664-MYRLRDRLR-672	QMYRLRDRLRLLP	2	2&3	1.1862	89.2404	Non-allergen	95.29%
VP3	**612-624**	**13**	**614-YNALIYYRY-622**	**HVYNALIYYRYNY**	**3**	**1,2&3**	**0.6634**	92.1476	**Non-allergen**	**97.24%**
	614-626	13	617-LIYYRYNYS-625	YNALIYYRYNYSF	2	1&2	0.9969	-	Non-allergen	41.01%
	617-629	13	620-YRYNYSFDL-628	LIYYRYNYSFDLK	11	1,2&3	1.6711	82.1585	Non-allergen	41.01%
	622-634	13	624-YSFDLKRWI-632	YNYSFDLKRWIYL	3	1,2&3	0.4882	-	Non-allergen	41.47%
	651-663	13	653-IELIYACRS-661	APIELIYACRSAK	4	2&3	0.8995	86.3254	Non-allergen	55.76%
VP4	225-237	13	227-IQNTRNVVP-235	PPIQNTRNVVPLS	2	2&3	1.4020	-	Non-allergen	77.33%
	416-428	**13**	**418-FVSLNSLRF-426**	**TDFVSLNSLRFRF**	**15**	**1,2&3**	**1.3966**	**87.3103**	**Non-allergen**	**94.67%**
	721-733	13	724-FKTLKNLND-732	IIDFKTLKNLNDN	3	1,2&3	1.0048	77.3647	Non-allergen	97.33%
VP6	384-396	13	386-FTVASIRSM-394	RVFTVASIRSMLI	5	1&2	0.4871	89.6841	Non-allergen	68.42%
	284-296	**13**	**288-IRLSFQLMR-296**	**NFDTIRLSFQLMR**	**10**	**1,2&3**	**0.5044**		**Non-allergen**	**91.87%**
	68-81	13	71-LNLDANYVE-79	TLLNLDANYVETA	3	1&2	0.7215	-	Non-allergen	91.39%
	382-394	13	385-VFTVASIRS-393	LQRVFTVASIRSM	5	1&2	0.4609	93.7747	Non-allergen	97.13%

Table 6.5b. contd…..

RV Protein	Position	Length	Core	MHC II epitope (13 mer)	No. of alleles	Server	Antigenicity by Vexigen (T=0.4)	Immunogenicity score by IEDB tool	Allergeicity by AllerTope v. 2.0	Conservancy by IEDB conservancy tool
NSP2	**46-58**	13	**48-YGIAPPPQF-57**	**SIIYGIAPPPQFK**	**6**	**1&2**	**0.6568**	**94.6673**	**Non-allergen**	**41.49%**
	268-280	13	268-WYAFTSSMK-276	NWYAFTSSMKQGN	4	1&2	0.7185	92.8977	Non-allergen	94.68%
	300-312	13	300-FKGLSTDRK-308	FKGLSTDRKMDEV	4	2&3	1.0314	-	Non-allergen	92.55%
NSP3	48-60	13	51-FVMDDSGVK-59	KFDFVMDDSGVKN	5	1&2	0.4569	-	Non-allergen	33.70%
	101-113	13	**103-LRMMLSSKG-111**	**NKLRMMLSSKGID**	**11**	**1,2&3**	**0.8777**	**75.525**	**Non-allergen**	**22.83%**
NSP4	6-18	13	9-YTLSVITLM-17	DLNYTLSVITLMN	2	2&3	1.0054	89.6726	Non-allergen	87.50%
	29-41	13	**32-YFPYIASVL-40**	**GMAYFPYIASVLT**	**5**	**2&3**	**0.7181**	**-**	**Non-allergen**	**92.86%**
	84-96	13	85-YKEQITTKD-93	GYKEQITTKDEIE	4	2&3	0.5294	-	Non-allergen	42.86%
NSP5	179-191	13	181-FALRMRMKQ-189	KYFALRMRMKQVA	8	1,2&3	1.6515	-	Non-allergen	35.11%
	181-193	13	182-LRMRMKQVA-190	FALRMRMKQVAMQ	5	1&2	1.3291	89.8373	Non-allergen	35.11%
	176-188	13	**180-YFALRMRMK-188**	**YKKKYFALRMRMK**	**14**	**1,2&3**	**1.5785**	**85.7915**	**Non-allergen**	**47.87%**
	175-187	13	176-YKKKYFALR-184	KYKKKYFALRMRM	4	1,2&3	1.19	-	Non-allergen	47.87%
VP6_Group B	**315-327**	13	**318-FMFETRRTF-326**	**AISFMFETRRTFT**	**2**	**1&2**	**1.2887**	**-**	**Non-allergen**	**50.00%**
VP6_Group C	339-351	13	342-YSIVANVRR-350	SVDYSIVANVRRD	2	1,2&3	0.9904	-	Non-allergen	38.30%
	344-358	13	348-VRRDSAMPA-356	ANVRRDSAMPAGT	5	1&2	0.4822	88.3861	Non-allergen	80.85%
	381-393	13	**384-LLLVASVKR-392**	**LERLLLVASVKRM**	**9**	**1&2**	**0.415**	**73.2227**	**Non-allergen**	**44.68%**

6.3.4. Docking of predicted T-cell epitope

The structure of peptide was generated by PEP-FOLD 2.0 and capping was performed. The PDB files of MHC I and MHC II molecules were retrieved from the Protein Data Bank and 27 HLA supertypes were used in the prediction of epitopes (Table 6.6a and 6.6b). MHC I alleles lacking crystal structure was modelled using I- TASSER. Some of the MHC II alleles were used as reference crystallographic structures for docking with predicted T-cell epitopes. All MHC structures were energy minimized and MHC-peptide docking simulation was performed using ClusPro v.2.0 [56]. Interaction energy was analyzed by prodigy. CTL and HTL epitopes predicted as immunogenic/antigenic, non-allergenic and conserved across the antigens have been selected for designing multi-epitope vaccine based on docking score or free energy (Table 6.6a and 6.6b). We have selected the docking models of MHC-I/II and T-cell epitope complexes having the lowest binding energies. Conserved peptides with their interaction energies for structural and non-structural proteins in kcal mol^{-1} are given in Table 6.6a and 6.6b. Binding studies have shown that nonameric peptide is the most compatible length and binds MHC I molecules with the closed-ended peptide-binding cleft than peptides longer or shorter than nonameric peptide [69]. Anchor residues are generally hydrophobic in nature and found one at carboxyl terminus and second and third in amino-terminal end of the peptide (Table 6.5a). MHC II binding peptides has specific motif with a central core of 13 amino acid residues. Internal sequence stretches of 7–10 residues form the contact points with an N-terminal aromatic or hydrophobic residue, three hydrophobic residues at the centre and carboxyl end of the peptide (Table 6.5b). This criterion was considered for the selection of final potent T-cell epitopes.

Table 6.6a. Molecular docking of predicted CTL epitopes with MHC I complexes. The selected epitopes used for designing multi-epitope vaccine constructs are highlighted in bold

Rota Protein	Epitope	MHC I allele	Binding energy in ΔG (kcal mol1)
VP2	QPVALVGAL	HLA-B*07:02	-7.9
		HLA-B*35:01	-8.9
	ALVGALPFI	HLA-A*02:01	-7.7
		HLA-B*53:01	-9.2
		HLA-B*51:01	-8.4
		HLA-A*03:01	-8.7
		HLA-A*24:02	-8.6
		HLA-A*02:03	-9.6
		HLA-A*02:06	-8.3
		HLA-B*07:02	-8.2
		HLA-A*68:01	-9
		HLA-A*68:02	-9.6
		HLA-B*35:01	-9.4
		HLA-A*11:01	-8.2
	TSNLTFTVY	HLA-A*01:01	-9.3
		HLA-A*15:01	-8.8
		HLA-A*30:02	-12.2
		HLA-B*44:03	-14.1
		HLA-B*58:01	-12.1
		HLA-B*35:01	-13.8
	NLHDNFESL	HLA-A*02:01	-9.4
		HLA-B*53:01	-8.3
		HLA-B*51:01	-9.3
		HLA-A*03:01	-8.5
		HLA-A*24:02	-9.2
		HLA-A*02:03	-9.4
		HLA-A*02:06	-8.5
		HLA-B*07:02	-8.2
		HLA-A*68:01	-8.8
		HLA-A*68:02	-7.6
		HLA-B*35:01	-8.3
		HLA-A*11:01	-9
	IAKLDATVF	HLA-B*35:01	-8.8
		HLA-B*44:03	-11.1
		HLA-A*58:01	-10.1
		HLA-B*15:01	-7.9
	KTIPTFEPK	HLA-A*03:01	-10.3
		HLA-A*68:01	-8.3
		HLA-A*11:01	-9
		HLA-A*30:01	-10.4

Table 6.6a. contd…

Rota Protein	Epitope	MHC I allele	Binding energy in ΔG (kcal mol1)
VP2	KTIPTFEPK	HLA-A*33:01	-10.3
	KLFRIFEPK	HLA-A*03:01	-9.5
		HLA-A*68:01	-9.5
		HLA_A*33:01	-8.5
		HLA-A*11:01	-8.6
		HLA-A*30:01	-9.2
	QLVDLTRLL	**HLA-A*02:01**	**-9**
		HLA-A*02:03	**-7.8**
		HLA-A*02:06	**-9**
	MLIGNATVI	HLA-A*02:01	-8.1
		HLA-A*02:03	-8.4
		HLA-A*02:06	-8.4
	SPQTLFHYY	HLA-B*53:01	-10.4
		HLA-B*35:01	-9.7
	RINDAVAII	HLA-A*02:01	-8.8
		HLA-A*02:03	-8.8
	RLRDRLRLL	HLA-A*02:03	-8.9
		HLA-B*08:01	-10.3
		HLA-B*07:02	-8.3
	ATVFAQIVK	HLA-A*11:01	-7.9
	AIITAANRL	HLA-A*02:01	-8.3
		HLA-B*53:01	-9
		HLA-B*51:01	-8.8
		HLA-A*03:01	-9.7
		HLA-A*24:02	-8.4
		HLA-B*07:02	-9.1
		HLA-A*68:01	-9.3
		HLA-A*68:02	-9.5
		HLA-B*35:01	-9.7
		HLA-A*11:01	-8.8
VP3	**LFTLIRCNF**	**HLA-A*24:02**	**-9.3**
		HLA-A,2301	**-11.6**
	SQFDIGQYK	HLA-A*03:01	-9
		HLA-A,1101	-8.3

Table 6.6a. contd…

Rota Protein	Epitope	MHC I allele	Binding energy in ΔG (kcal mol1)
VP3	LFTLIRCNF	HLA-A*24:02	-9.3
		HLA-A,2301	-11.6
	SQFDIGQYK	HLA-A*03:01	-9
		HLA-A,1101	-8.3
	LLHHPTTEI	HLA-A*02:01	-9
		HLA-A*02:03	-9.5
	HVYNALIYY	HLA-A*03:01	-10.3
		HLA-A*68:01	-9.7
		HLA-B*35:01	-9.2
		HLA-A*26:01	-10.1
		HLA-A*30:01	-9.6
		HLA-A*30:02	-10.1
		HLA-A*32:01	-9.5
		HLA-A*11:01	-8.6
		HLA-B*15:01	-9.5
VP4	**GYKWSEISF**	**HLA-A*24:02**	**-10.5**
		HLA-A*23:01	**-9.9**
	EYYEIAGRF	HLA-A*24:02	-9.1
		HLA-A*23:01	-8.7
	AIIDFKTLK	HLA-A*03:01	-10.2
		HLA-A*68:01	-8.2
		HLA-A*11:01	-8.6
VP6	LTTATITLL	HLA-A*02:01	-8.9
		HLA-B*53:01	-9
		HLA-B*51:01	-10.4
		HLA-A*03:01	-9.2
		HLA-A*02:03	-7.5
		HLA-A*02:06	-7.1
		HLA-B*07:02	-8.6
		HLA-A*68:01	-8
		HLA-A*68:02	-10.4

Table 6.6a. contd…

Rota Protein	Epitope	MHC I allele	Binding energy in ΔG (kcal mol1)
	LTTATITLL	HLA-B*35:01	-8.2
		HLA-A*11:01	-8.2
		HLA-B*58:01	-10.6
		HLA-A*03:01	-9.2
		HLA-B*53:01	-7.7
		HLA-B*51:01	-8.3
		HLA-A*24:02	-8.9
		HLA-B*07:02	-8.7
		HLA-A*68:01	-9.5
		HLA-A*68:02	-9
		HLA-B*35:01	-8.9
		HLA-A*11:01	-8.6
		HLA-B*40:01	-10.6
	FEHHATVGL	HLA-B*44:03	-10.6
	LPDAERFSF	**HLA-B*07:02**	**-7.8**
		HLA-B*53:01	**-9.3**
		HLA-B*35:01	**-8.9**
	ILRPNNVEV	HLA-A*02:01	-8.7
VP6		HLA-A*02:03	-8.5
VP7	**SIILLNYIL**	**HLA-A*02:01**	**-8.2**
		HLA-B*53:01	**-7.6**
		HLA-B*51:01	**-8.7**
		HLA-A*03:01	**-8.1**
		HLA-A*24:02	**-10.2**
		HLA-B*07:02	**-7.2**
		HLA-A*68:01	**-9.1**
		HLA-A*68:02	**-8.7**
		HLA-B*35:01	**-9.1**
		HLA-A*11:01	**-8.9**
		HLA-A*31:01	**-9.2**
		HLA-A*32:01	**-9.8**

Table 6.6a. contd…

Rota Protein	Epitope	MHC I allele	Binding energy in ΔG (kcal mol1)
NSP2	VANHADRVY	HLA-B*35:01	-8.4
		HLA-B*15:01	-8.1
		HLA-B*44:03	-8.1
		HLA-B*58:01	-11
	YPHLENDSY	**HLA-B*53:01**	**-8.6**
		HLA-B*35:01	**-8.5**
	MPILDQNFI	HLA-B*53:01	-8.1
		HLA-B*51:01	-9.2
		HLA-B*35:01	-8.4
	ILDQNFIEY	HLA-A*01:01	-8.1
		HLA-B*35:01	-7.8
		HLA-A*11:01	-8.1
NSP3	NSSFEAAVV	HLA-A*68:02	-8.8
		HLA-B*58:01	-9.4
	GVKNNLIGK	**HLA-A*03:01**	**-8.5**
		HLA-A*68:01	**-8.1**
		HLA-A*11:01	**-8.4**
		HLA-A*30:01	**-9.2**
		HLA-A*33:01	**-10.2**
NSP4	YFPYIASVL	HLA-B*53:01	-7.6
		HLA-B*51:01	-8.8
		HLA-A*24:02	-10.3
		HLA-B*07:02	-8.6
		HLA-A*68:01	-9.9
		HLA-A*68:02	-10.9
		HLA-A*11:01	-8.2

Table 6.6a. contd…

Rota Protein	Epitope	MHC I allele	Binding energy in ΔG (kcal mol1)
NSP4	**IASVLTVLF**	**HLA-B*57:01**	**-7.9**
		HLA-B*35:01	**-9.8**
		HLA-A*23:01	**-9**
		HLA-A*32:01	**-8.4**
		HLA-B*15:01	**-11.7**
		HLA-B*44:03	**-9.9**
		HLA-B*58:01	**-8.7**
NSP5	**SLSIDVTSL**	**HLA-A*02:01**	**-10.9**
		HLA-A*02:03	**-11.9**
VP6_Group B	TINAPIISL	HLA-B*53:01	-8.5
		HLA-A*02:01	-9.1
		HLA-B*51:01	-8
		HLA-A*03:01	-9.4
		HLA-A*24:02	-9.1
		HLA-A*02:03	-8.4
		HLA-B*07:02	-10.1
		HLA-A*68:01	-8.4
		HLA-A*68:02	-10.8
		HLA-B*35:01	-8.6
		HLA-A*11:01	-9.1
		HLA-A*32:01	-10.2
	ILDVLAAAI	**HLA-A*02:01**	**-9.7**
		HLA-A*02:03	**-9**
		HLA-A*01:01	**-9.9**

Table 6.6a. contd…

Rota Protein	Epitope	MHC I allele	Binding energy in ΔG (kcal mol1)
VP6_Group B	SEHRFTVEL	HLA-B*53:01	-10.5
		HLA-A*02:01	-10.3
		HLA-B*51:01	-11.3
		HLA-A*03:01	-10.2
		HLA-A*24:02	-8.3
		HLA-B*07:02	-10.3
		HLA-A*68:01	-10.5
		HLA-A*68:02	-9.4
		HLA-B*35:01	-10.7
		HLA-A*11:01	-8.4
		HLA-B*40:01	-11.9
		HLA-B*44:02	-8.9
		HLA-B*44:03	-11.1
VP6_Group C	QTNELIRTL	HLA-A*68:02	-9.8
		HLA-B*58:01	-8.5
	ILDATTESV	**HLA-A*02:01**	**-8.9**
		HLA-A*02:03	**-7.6**
		HLA-A*02:06	**-8.8**

Table 6.6b. Molecular docking of predicted HTL epitopes with MHC II complexes. The selected epitopes used for designing multi-epitope vaccine constructs are highlighted in bold

RV protein	Epitope	MHC II allele	Binding energy in ΔG (kcal mol^{-1})
VP2	AAMLSQRTMSLDF	HLA-DRB4*01:01	-6.1
		HLA-DRB1*04:01	-5.3
	YPAFGMQRMHYRN	HLA-DRB1*13:02	-5.5
		HLA-DRB5*01:01	-11.5
	QIQNFQVANWLHF	HLA-DRB1*07:01	-7.1
		HLA-DRB1*04:01	-6
		HLA-DPA1*02:01/DPB1*01:01	-5.2
		HLA-DPA1*02:01/DPB1*05:01	-6.4
	GILLLSNRLGQLV	**HLA-DRB1*01:01**	**-5.7**
		HLA-DRB1*15:01	**-6.6**
		HLA-DRB1*04:05	**-5.2**
	LQLTSVTSLCMLI	HLA-DRB1*07:01	-5.7
		HLA-DRB1*04:05	-6.7
	VAIITAANRLNLY	HLA-DRB1*03:01	-5.4
		HLA-DRB1*08:02	-5.7
		HLA-DRB1*15:01	-6.4
		HLA-DRB3*02:02	-5.4
		HLA-DRB1*04:01	-6.5
	MYRLRDRLRLLPV	HLA-DRB1*03:01	-5.6
		HLA-DRB4*01:01	-5.6
		HLA-DRB1*15:01	-5.4
		HLA-DRB1*04:01	-6.1
		HLA-DPA1*02:01/DPB1*05:01	-6.2
	MLLNNQPVALVGA	HLA-DRB1*13:02	-6
		HLA-DQA1*01:02/DQB1*06:02	-7.5
		HLA-DRB3*02:02	-6.3
	SSVISLIAKLDAT	HLA-DRB1*11:01	-5.5
	QMYRLRDRLRLLP	HLA-DRB4*01:01	-5.7
		HLA-DRB5*01:01	-9.7
VP3	**HVYNALIYYRYNY**	**HLA-DRB1*01:01**	**-5.2**
		HLA-DRB5*01:01	**-8.9**
		HLA-DRB1*15:01	**-6.2**
	YNALIYYRYNYSF	HLA-DRB1*08:02	-7.5
		HLA-DRB1*15:01	-5.6
	LIYYRYNYSFDLK	HLA-DRB1*01:01	-6.6
		HLA-DRB1*15:01	-6.1
		HLA-DRB1*04:01	-5
		HLA-DRB5*01:01	-9.4
		HLA-DRB3*01:01	-6.3
		HLA-DRB3*02:02	-7.3
		HLA-DRB1*04:05	-6.3
	YNYSFDLKRWIYL	HLA-DRB1*13:02	-6.1
		HLA-DRB3*01:01	-5.8
	APIELIYACRSAK	HLA-DRB1*01:01	-6.5
		HLA-DRB1*04:01	-5.7

Table 6.6b. contd….

RV protein	Epitope	MHC II allele	Binding energy in ΔG (kcal mol^{-1})
VP4	PPIQNTRNVVPLS	HLA-DRB1*15:01	-5.9
		HLA-DRB1*04:01	-7.1
	TDFVSLNSLRFRF	**HLA-DRB1*03:01**	**-6.3**
		HLA-DRB1*01:01	**-5**
		HLA-DRB1*15:01	**-5.6**
		HLA-DRB1*04:01	**-5.7**
		HLA-DRB5*01:01	**-9.2**
		HLA-DPA1*02:01/DPB1*01:01	**-7.7**
		HLA-DPA1*02:01/DPB1*05:01	**-6.4**
		HLA-DPA1*02:01/DPB1*05:01	**-6.3**
		HLA-DRB1*04:05	**-5.5**
	IIDFKTLKNLNDN	HLA-DRB1*01:01	-5.8
		HLA-DRB1*04:01	-5.7
		HLA-DRB1*04:05	-4.8
VP6	RVFTVASIRSMLI	HLA-DRB1*09:01	-6.4
		HLA-DRB1*04:01	-5.8
		HLA-DPA1*02:01/DPB1*14:01	-5.8
		HLA-DRB3*02:02	-6.2
	NFDTIRLSFQLMR	**HLA-DRB1*03:01**	**-6.8**
		HLA-DRB1*11:01	**-5.8**
		HLA-DRB1*04:01	**-5.9**
		HLA-DRB5*01:01	**-9.6**
		HLA-DPA1*02:01/DPB1*01:01	**-6.9**
		HLA-DPA1*02:01/DPB1*05:01	**-7**
	TLLNLDANYVETA	HLA-DRB1*03:01	-5.8
		HLA-DRB3*01:01	-5.6
		HLA-DRB1*04:05	-5.4
	LQRVFTVASIRSM	HLA-DRB1*07:01	-5.3
		HLA-DRB5*01:01	-7.3
		HLA-DRB1*04:05	-6
VP7	**LISIILLNYILKS**	**HLA-DRB1*03:01**	**-5.4**
		HLA-DRB1*08:02	**-5.7**
		HLA-DRB1*15:01	**-5**
		HLA-DRB1*04:01	**-5.5**
		HLA-DPA1*03:01/DPB1*04:02	**-5.5**
	PMDITLYYYQQTD	HLA-DRB1*15:01	-5.6
		HLA-DQA1*01:01/DQB1*05:01	-8.2

Table 6.6b. contd…..

RV protein	Epitope	MHC II allele	Binding energy in ΔG (kcal mol⁻¹)
NSP2	**SIIYGIAPPPQFK**	**HLA-DRB1*03:01**	**-5**
		HLA-DRB1*09:01	**-6.1**
		HLA-DRB5*01:01	**-10.4**
	NWYAFTSSMKQGN	HLA-DRB1*09:01	-6.1
		HLA-DRB1*04:01	-6.8
		HLA-DRB5*01:01	-9.5
		HLA-DRB1*04:05	-5.8
	FKGLSTDRKMDEV	HLA-DRB1*01:01	-5.3
		HLA-DRB1*04:01	-5.6
		HLA-DRB5*01:01	-9.5
		HLA-DRB1*04:05	-5.8
NSP3	KFDFVMDDSGVKN	HLA-DRB1*03:01	-5.8
		HLA-DRB1*08:02	-6.6
		HLA-DRB1*04:01	-5.1
		HLA-DRB5*01:01	-8.3
		HLA-DRB3*01:01	-6.8
	NKLRMMLSSKGID	**HLA-DRB1*03:01**	**-5.7**
		HLA-DRB1*01:01	**-5.8**
		HLA-DRB1*15:01	**-4.4**
		HLA-DRB1*04:01	**-6.8**
		HLA-DRB5*01:01	**-7.5**
		HLA-DRB3*02:02	**-5**
		HLA-DRB1*04:05	**-4.7**
NSP4	DLNYTLSVITLMN	HLA-DRB1*07:01	-7
		HLA-DRB1*04:01	-5.5
	GMAYFPYIASVLT	**HLA-DRB1*01:01**	**-5.1**
		HLA-DRB1*15:01	**-5.7**
	GYKEQITTKDEIE	HLA-DRB1*01:01	-5.2
		HLA-DRB1*04:01	-5.9
		HLA-DRB1*04:05	-5.1

Table 6.6b. contd…..

RV protein	Epitope	MHC II allele	Binding energy in ΔG (kcal mol^{-1})
NSP5	KYFALRMRMKQVA	HLA-DRB1*12:01	-6.3
		HLA-DRB1*04:01	-6.1
		HLA-DPA1*02:01/DPB1*01:01	-6.2
		HLA-DPA1*02:01/DPB1*05:01	-7.3
	FALRMRMKQVAMQ	HLA-DRB1*03:01	-5
		HLA-DRB1*12:01	-5.8
	YKKKYFALRMRMK	**HLA-DRB1*01:01**	**-7.4**
		HLA-DRB1*15:01	**-6.8**
		HLA-DRB5*01:01	**-9.3**
		HLA-DPA1*02:01/DPB1*01:01	**-6.8**
		HLA-DPA1*02:01/DPB1*05:01	**-7**
		HLA-DRB3*02:02	**-7.3**
		HLA-DRB1*04:05	**-6.1**
	KYKKKYFALRMRM	HLA-DRB1*08:02	-5.7
		HLA-DRB5*01:01	-10.4
		HLA-DPA1*01/DPB1*04:01	-6.7
VP6_B	**AISFMFETRRTFT**	**HLA-DPA1*02:01/DPB1*05:01**	**-7.3**
		HLA-DRB1*13:02	**-5.8**
VP6_C	SVDYSIVANVRRD	HLA-DRB1*01:01	-6.5
		HLA-DRB5*01:01	-11.1
	ANVRRDSAMPAGT	HLA-DRB1*03:01	-5.3
		HLA-DRB1*13:02	-6.5
		HLA-DRB1*15:01	-6.3
		HLA-DRB1*04:01	-6.5
	LERLLLVASVKRM	**HLA-DRB1*03:01**	**-6.2**
		HLA-DRB1*01:01	**-5.4**
		HLA-DRB1*15:01	**-5.6**
		HLA-DRB5*01:01	**-8**
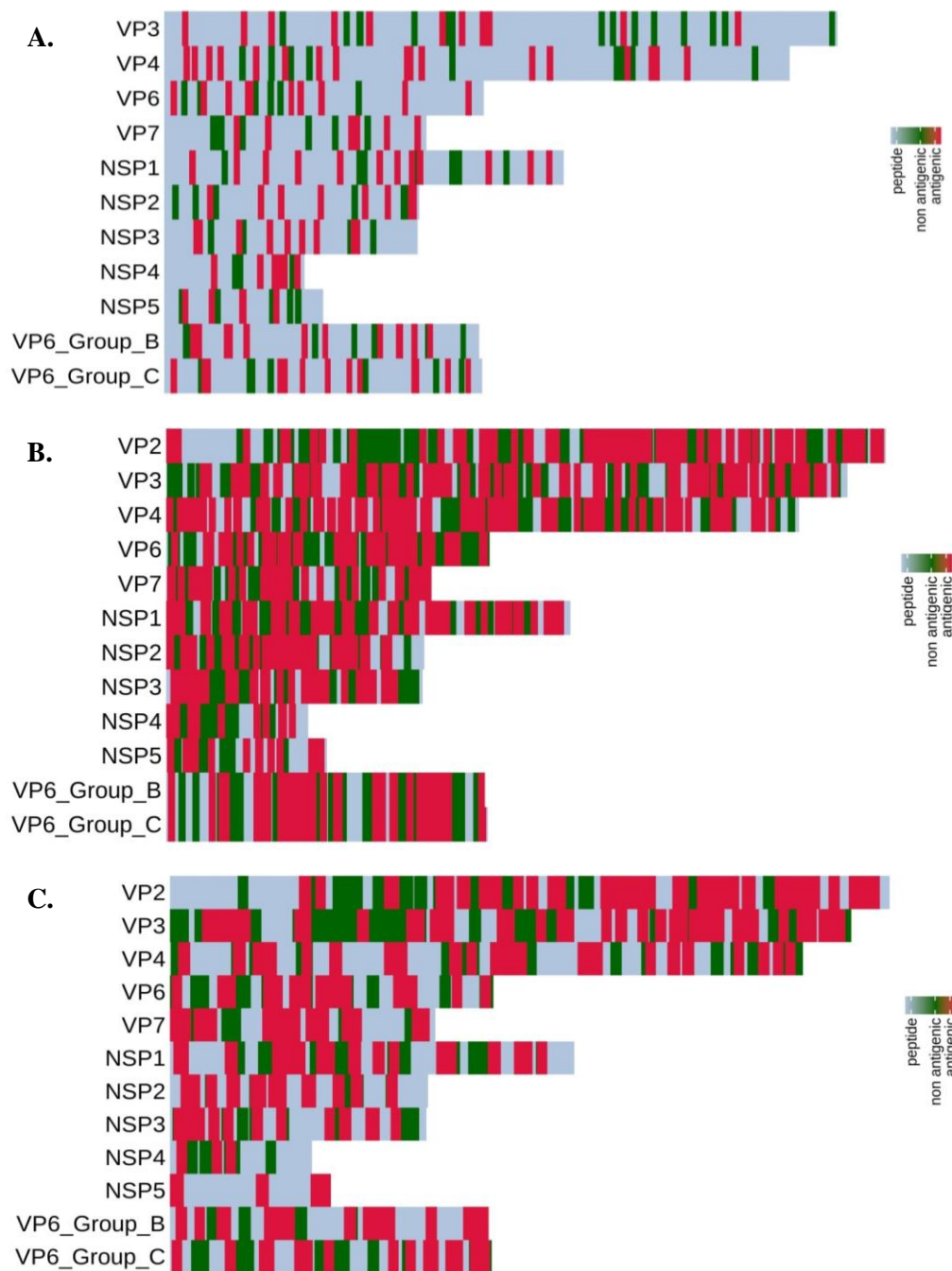
Figure 6.4. Summary of rotavirus protein-derived B- and T-cell epitopes. Heat map showing the distribution of (A) linear (continuous) B-cell epitopes, (B) HLA-class I and (C) II epitopes across the structural and non-structural protein sequences of rotavirus. Strong binding affinity epitopes with <0.5% rank and 2% rank, to HLA class I and class II, respectively, for each HLA molecule are represented here. Red color represents likely antigenic epitopes that were predicted using the methods described in Figure 6.1.

Table 6.7. Rotavirus proteins, total number of epitopes predicted and the immunogenicity/antigenicity/allergenicity as obtained from immune epitope database

Sl No.	RV protein	B-/T-cell epitope	Types	Total no. of epitopes	Selected Epitope for vaccine construct	Length	Immunogenicity	Antigenicity	Allergenicity	Agadir Score	Conservancy
1	VP2	B-cell epitope	Linear	5	189-AVENKNSRDAGK-200	12	-	-	-	0.33	98.82%
			Confo	4	K339,E340,L341,V342,S343,T344, E345,A346,Q347,I348,Q349,K350, M351	13	-	-	-	0.41	97.65%
		T-cell epitope	MHC I	14	544-QLVDLTRLL-552	9	0.09866	-	Non-allergen	-	95.88%
			MHC II	10	534-GILLLSNRLGQLV-546	13	-	0.7962	Non-allergen	-	97.65%
2	VP3	B-cell epitope	Linear	3	238-TIKLKQERWLGK-249	12	-	-	-	0.36	46.08%
			Confo	3	R176,M177,T178,T179,S180,L181, P182,I183,A184,R185,L186,S187, N188,R189,V190,F191,R192	17	-	-	-	0.53	98.16%
		T-cell epitope	MHC I	4	72-LFTLIRCNF-80	9	0.13048	-	Non-allergen	-	68.66%
			MHC II	5	612-HVYNALIYYRYNY-624	13	-	0.6634	Non-allergen	-	97.24%
3	VP4	B-cell epitope	Linear	6	241-RDVIHYRAQANED-253	13	-	-	-	0.29	4.00%
					208-IPRSEESKCTEYI-220	14	-	-	-	0.41	4.67%
					262-WKEMQYNRDI-271	10	-	-	-	0.48	97.33%
					657-PDIVTEASEKF-667	11	-	-	-	0.4	76.67%
			Confo	1	T413,Q414,F415,T416,D417,F418, V419,S420,L421,N422,S423,L424	12	-	-	-	0.27	93.33%
		T-cell epitope	MHC I	3	288-GYKWSEISF-296	9	0.1017	-	Non-allergen	-	25.93%
			MHC II	3	416-TDFVSLNSLRFRF-428	13	-	1.3966	Non-allergen	-	94.67%

Table 6.7. contd….

Sl No.	RV protein	B-/T-cell epitope	Types	Total no. of epitopes	Selected Epitope for vaccine construct	Length	Immunogenicity	Antigenicity	Allergenicity	Agadir Score	Conservancy
4	VP6	B-cell epitope	Linear	5	9-KTLKDARDKIVEG-21	13	-	-	-	0.63	88.52%
					139-WNLQNRRQRTG-149	11	-	-	-	0.69	98.36%
					373-NYSPSREDNLQR-384	12	-	-	-	0.3	96.72%
			Confo	3	Y24,S25,N26,V27,S28,D29,L30,I31,Q32,Q33,F34,N35,Q36	13	-	-	-	0.57	90.16%
					D74,A75,N76,Y77,V78,E79,T80,A81,R82,N83,T84,I85,D86,Y87	14	-	-	-	0.58	44.26%
		T-cell epitope	MHC I	4	226-LPDAERFSF-234	9	0.19493	-	Non-allergen	-	95.08%
			MHC II	4	284-NFDTIRLSFQLMR-296	13	-	0.5044	Non-allergen	-	91.87%
5	VP7	B-cell epitope	Linear	2	308-QVMSKRSRSLNSA-320	13	-	-	-	0.28	73.88%
			Confo	4	R286,I287,N288,W289,K290,K291,W292,W293,Q294,V295	10	-	-	-	0.61	26.87%
					D169,I170,T171,L172,Y173,Y174,Y175,Q176,Q177,T178,D179,E180,A181,N182,K183,W184	16	-	-	-	0.32	29.10%
		T-cell epitope	MHC I	5	15-SIILLNYIL-23	9	0.08979	-	Non-allergen	-	67.91%
			MHC II	2	13-LISIILLNYILKS-25	13	-	0.5661	Non-allergen	-	57.46%

Table 6.7. contd….

Sl No.	RV protein	B-/T-cell epitope	Types	Total no. of epitopes	Selected Epitope for vaccine construct	Length	Immunogenicity	Antigenicity	Allergenicity	Agadir Score	Conservancy
6	NSP2	B-cell epitope	Linear	2	267-QNWYAFTSSMKQGNT-281	15	-	-	-	0.32	72.34%
			Confo	1	N298,P299,F300,K301,G302,L303,S304,T305,D306,R307,K308,M309,D310,E311,V312,S313	16	-	-	-	0.39	89.36%
		T-cell epitope	MHC I	3	9-YPHLENDSY-18	9	0.01281	-	Allergen	-	94.68%
			MHC II	3	46-SIIYGIAPPPQFK-58	13	-	0.6568	Non-allergen	-	41.49%
7	NSP3	B-cell epitope	Linear	3	108-LSSKGIDQKMRVL-120	13	-	-	-	0.48	96.74%
			Confo	3	K77,F78,G79,S80,A81,I82,R83,N84,R85,N86	10	-	-	-	0.36	45.65%
		T-cell epitope	MHC I	3	58-GVKNNLIGK-66	9	0.03887	-	Non-allergen	-	28.26%
			MHC II	2	101-NKLRMMLSSKGID-113	13	-	0.8777	Non-allergen	-	22.83%
8	NSP4	B-cell epitope	Linear	4	117-TTREIEQVELLK-128	13	-	-	-	0.48	96.74%
			Confo	2	I51,P52,T53,M54,K55,I56,A57,L58,K59	9	-	-	-	0.36	91.74%
		T-cell epitope	MHC I	2	36-IASVLTVLF-44	9	0.04194		Non-allergen		91.07%
			MHC II	3	29-GMAYFPYIASVLT-41	13		0.7181	Non-allergen		92.86%
9	NSP5	B-cell epitope	Linear	1	170-KCKNCKYKKKYFAL-183	14	-	-	-	0.55	74.47%
			Confo	3	A66,S67,N68,D69,P70,L71,T72,S73,F74,S75,I76,R77,S78,N79,A80,V81,K82,T83,N84,A85	20	-	-	-	0.5	89.36%
		T-cell epitope	MHC I	1	2-SLSIDVTSL-10	9	0.07678		Allergen		92.55%
			MHC II	4	176-YKKKYFALRMRMK-188	13		1.5785	Non-allergen		47.87%

Table 6.7. contd….

Sl No.	RV protein	B-/T-cell epitope	Types	Total no. of epitopes	Selected Epitope for vaccine construct	Length	Immunogenicity	Antigenicity	Allergenicity	Agadir Score	Conservancy
10	VP6 Group B	B-cell epitope	Linear	3	74-ISTDDYDDMRSGI-86	13	-	-	-	0.28	76.19%
					197-GMDSEHRFTVELKTR-211	15	-	-	-	0.57	34.38%
			Confo	1	E154,N155,P156,L157,Y158,A159,D160,I161,I162,E163,Q164,I165,V166,H167,R168	15		-	-	-	0.59	35.71%
		T-cell epitope	MHC I	3	89-ILDVLAAAI-97	9	0.13065	-	Non-allergen	-	64.29%
			MHC II	1	315-AISFMFETRRTFT-327	13	-	1.2887	Non-allergen	-	50.00%
11	VP6 Group C	B-cell epitope	Linear	4	93-EAVCDDEIVREA-104	12	-	-	-	0.48	86.96%
					143-SRRENPVYEYKNPM-156	14	-	-	-	0.3	60.87%
			Confo	1	F364,P365,W366,E367,Q368,T369,L370,S371,N372,Y373,T374,V375,A376,Q377,E378	15		-	-	-	0.32	59.57%
		T-cell epitope	MHC I	2	325-ILDATTESV-233	9	0.10875	-	Non-allergen	-	69.57%
			MHC II	3	381-LERLLLVASVKRM-393	13	-	0.415	Non-allergen	-	44.68%

6.3.5. Designing of multi-epitope subunit vaccine

A total of 10 multi-epitope vaccine constructs comprising of 69 amino acids (aa) through 576 aa consisting of 11 CTL, 11 HTL, 18 linear and 14 conformational B-cell epitopes have been described (Table 6.7 and 6.8). These predicted epitopes were derived from 5 structural (VP2, VP3, VP4, VP6 and VP7) and 4 non-structural proteins (NSP2, NSP3, NSP4 and NSP5). Linear B-cell epitopes were selected and included in the vaccine constructs based on (i) Agadir score (the helical content of peptide), (ii) conservancy (Table 6.2), (iii) surface localization of epitopes on the native protein of rotavirus (Figure 6.2). Conformational B cell epitopes were selected based on prediction of the same epitope by (i) two prediction tools used, (ii) Agadir score and (iii) conservancy (Table 6.3). Similarly, T cell epitopes were included in the multi-subunit vaccine constructs based on prediction of the same epitope by (i) three prediction tools used, (ii) antigenicity/immunogenicity, (iii) non-allergenicity, (iv) conservancy (Table 6.5a & 6.5b), and best docking score (Table 6.6a and 6.6b). Each epitope in the vaccine construct was occupied by the appropriate linkers, adjuvant and CTL epitopes were combined by EAAAK rigid linker, intra-CTL and intra-HTL epitopes joint by AAY and KK cleavable linker, respectively, and B- cell epitopes were linked together by GGGGS flexible linker [32,33,34,70,21,22,23,60]. Poly-Gly-rich flexible linkers are well characterized and generally do not affect the folding and function of fusion proteins [71]. Finally, vaccine construct was made containing N-terminal integrin binding motif (RGD) as adjuvant, CTL, HTL and B-cell epitopes (Figure 6.5). Rotavirus entry into the cell involves a multi-step process with sialic acid and integrins as viral receptors. The arginine-glycine-aspartate (RGD) motif has been shown to enhance immunogenicity and adjuvanicity in peptide antigens [72]. Since integrins are used as one of the receptors by rotavirus, RGD motif was selected as biological adjuvant to improve the immunogenicity of vaccine constructs. The rationale for a non-live subunit RV vaccine has no competition of uptake with enteric viruses in the gut, live-attenuated oral RV vaccines have lower rate of efficacies in developing countries and genetic background of the population is not critical (e.g. secretors/non-secretors) [7,8]. We have designed a total of 10 possible multi-subunit vaccine constructs using the predicted B and T cell epitopes of RV proteins. Construct 1 (VP6A/B/C) has a combination of B and T cell epitope predicted using the VP6 protein of group A, B and C rotaviruses, Construct 2 (VP4/6/7) has B and T cell epitope of VP4, VP6 and VP7 proteins, Construct 3 (VP2/3/4/6/7) has B

and T cell epitope of VP2, VP3, VP4, VP6 and VP7 proteins, Construct 4 (NSP2/3/4/5) has B and T cell epitope of NSP2, NSP3, NSP4 and NSP5 proteins, Construct 5 (VP2/3/4/6/7-NSP2/3/4/5) has B and T cell epitope of VP2, VP3, VP4, VP6, VP7, NSP2, NSP3, NSP4, and NSP5 proteins, Construct 6 (VP6A/B/C–B) has B-cell epitope predicted using the VP6 protein of group A, B and C rotaviruses, Construct 7 (VP4/6/7-B) has B cell epitope of VP4, VP6 and VP7 proteins, Construct 8 (VP4/A) has B and T cell epitope of VP4 protein of group A rotavirus, Construct 9 (VP6/A) has B and T cell epitope of VP6 protein of group A rotavirus, and Construct 10 (VP7/A) has B and T cell epitope of VP7 protein of group A rotavirus (Table 6.7 and 6.8). Some of the constructs were designed with predicted B-cell epitope with a long-term goal to express chimeric antigen to possibly develop rapid detection of rotavirus antigen in stool specimens. Intestinal mucosal immunity mediated mainly by IgA antibodies is often associated with protective immunity during rotavirus reinfection. The outer capsid layer of RV is composed of VP4 and VP7 proteins that are mainly responsible for viral attachment and entry are often targeted for protective neutralizing antibodies during rotavirus infections [73,74]. However, a non-neutralizing IgA monoclonal antibody directed against the VP6 protein has been shown to protect mice from rotavirus infection [75]. Studies on several non-replicating RV vaccines are being performed and assessed in various animal models. The expressed truncated VP6 and VP8 protein sub-units, bivalent vaccine (NSP4 & VP6) and ''virus-like particles" (VP2, VP4, VP6, and VP7) are being investigated as potential vaccine for rotavirus [76]. The results of preclinical studies have shown that majority of these potential vaccine candidates for rotavirus induces a strong immune responses and provides a protection against oral challenge with rotavirus strains in mice model [77,78,79]. VP6-specific polyclonal IgA inhibits RV replication at the transcription level by blocking channels on RV particles and preventing RV mRNA release [80]. The recent findings of an efficient intracellular neutralization mediated mainly by VP6-specific IgG and subsequent protection of mice against the challenge of rotavirus might have implications in developing next generation vaccine for rotavirus [81].

Table 6.8. Predicted B- and T-cell epitopes obtained from the immune epitope database. The amino acid sequence of selected epitopes used for design of final multi-subunit chimeric antigen constructs

Multi-epitope antigen construct		RV Protein	Linear B-cell epitope	Conformational B-cell epitope	CTL epitope	HTL epitope
VP6A/B/C (Construct 1)		VP6 GroupA	9-KTLKDARDKIVEG-21, 139-WNLQNRRQRTG-149, 373-NYSPSREDNLQR-384	Y24,S25,N26,V27,S28,D29,L30,I31,Q32,Q33,F34,N35,Q36	226-LPDAERFSF-234	284-NFDTIRLSFQLMR-296
				D74,A75,N76,Y77,V78,E79,T80,A81,R82,N83,T84,I85,D86,Y87		
		VP6 Group B	74-ISTDDYDDMRSGI-86, 197-GMDSEHRFTVELKTR-211	E154,N155,P156,L157,Y158,A159,D160,I161,I162,E163,Q164,I165,V166,H167,R168	89-TINAPIISL-97	315-AISFMFETRRTFT-327
		VP6 Group C	93-TVSDLKKKV-104, 143-EAVCDDEIVREA-156	F364,P365,W366,E367,Q368,T369,L370,S371,N372,Y373,T374,V375,A376,Q377,E378	325-ILDATTESV-334	381-LERLLLVASVKRM-393
VP4/6/7 (Construct 2)	VP4/A (Construct 8)	VP4	241-RDVIHYRAQANED-253, 208-IPRSEESKCTEYI-220, 262-WKEMQYNRDI-271, 657-PDIVTEASEKF-667	T413,Q414,F415,T416,D417,F418,V419,S420,L421,N422,S423,L424	288-GYKWSEISF-296	416-TDFVSLNSLRFRF-428
	VP6/A (Construct 9)	VP6	9-KTLKDARDKIVEG-21, 373-NYSPSREDNLQR-384	Y24,S25,N26,V27,S28,D29,L30,I31,Q32,Q33,F34,N35,Q36	226-LPDAERFSF-234	284-NFDTIRLSFQLMR-296
				D74,A75,N76,Y77,V78,E79,T80,A81,R82,N83,T84,I85,D86,Y87		
	VP7/A (Construct 10)	VP7	308-QVMSKRSRSLNSA-320	D169,I170,T171,L172,Y173,Y174,Y175,Q176,Q177,T178,D179,E180,A181,N182,K183,W184	15-SIILLNYIL-23	13-LISIILLNYILKS-25

Table 6.8 contd….

Multi-epitope antigen construct		RV Protein	Linear B-cell epitope	Conformational B-cell epitope	CTL epitope	HTL epitope
VP2/3/4/6/7-NSP2/3/4/5 (Construct 5)	VP2/3/4/6/7 (Construct 3)	VP2	189-AVENKNSRDAGK-200	K339,E340,L341,V342,S343,T344,E345,A346,Q347,I348,Q349,K350,M351	544-QLVDLTRLL-552	534-GILLLSNRLGQLV-546
		VP3	238-TIKLKQERWLGK-249	R176,M177,T178,T179,S180,L181,P182,I183,A184,R185,L186,S187,N188,R189,V190,F191,R192	72-LFTLIRCNF-80	612-HVYNALIYYRYNY-624
		VP4	657-PDIVTEASEKF-667	T413,Q414,F415,T416,D417,F418,V419,S420,L421,N422,S423,L424	288-GYKWSEISF-296	416-TDFVSLNSLRFRF-428
		VP6	373-NYSPSREDNLQR-384	Y24,S25,N26,V27,S28,D29,L30,I31,Q32,Q33,F34,N35,Q36	226-LPDAERFSF-234	284-NFDTIRLSFQLMR-296
		VP7	308-QVMSKRSRSLNSA-320	D169,I170,T171,L172,Y173,Y174,Y175,Q176,Q177,T178,D179,E180,A181,N182,K183,W184	15-SIILLNYIL-23	13-LISIILLNYILKS-25
	NSP2/3/4/5 (Construct 4)	NSP2	267-QNWYAFTSSMKQGNT-281	N298,P299,F300,K301,G302,L303,S304,T305,D306,R307,K308,M309,D310,E311,V312,S313	9-YPHLENDSY-18	46-SIIYGIAPPPQFK-58
		NSP3	108-LSSKGIDQKMRVL-120	K77,F78,G79,S80,A81,I82,R83,N84,R85,N86	58-GVKNNLIGK-66	101-NKLRMMLSSKGID-113
		NSP4	117-TTREIEQVELLK-128	I51,P52,T53,M54,K55,I56,A57,L58,K59	36-IASVLTVLF-44	29-GMAYFPYIASVLT-41
		NSP5	170-KCKNCKYKKKYFAL-183	A66,S67,N68,D69,P70,L71,T72,S73,F74,S75,I76,R77,S78,N79,A80,V81,K82,T83,N84,A85	2-SLSIDVTSL-10	176-YKKKYFALRMRMK-188

Table 6.8 contd….

Multi-epitope antigen construct	RV Protein	Linear B-cell epitope	Conformational B-cell epitope	CTL epitope	HTL epitope
VP6A/B/C-B (Construct 6)	VP6 GroupA	9-KTLKDARDKIVEG-21, 139-WNLQNRRQRTG-149, 373-NYSPSREDNLQR-384	Y24,S25,N26,V27,S28,D29,L30,I31,Q32,Q33,F34,N35,Q36	-	-
			D74,A75,N76,Y77,V78,E79,T80,A81,R82,N83,T84,I85,D86,Y87	-	-
	VP6 Group B	74-ISTDDYDDMRSGI-86, 197-GMDSEHRFTVELKTR-211	E154,N155,P156,L157,Y158,A159,D160,I161,I162,E163,Q164,I165,V166,H167,R168	-	-
	VP6 Group C	93-TVSDLKKKV-104, 143-EAVCDDEIVREA-156	F364,P365,W366,E367,Q368,T369,L370,S371,N372,Y373,T374,V375,A376,Q377,E378	-	-
VP4/6/7-B (Construct 7)	VP4	241-RDVIHYRAQANED-253, 208-IPRSEESKCTEYI-220, 262-WKEMQYNRDI-271, 657-PDIVTEASEKF-667	T413,Q414,F415,T416,D417,F418,V419,S420,L421,N422,S423,L424	-	-
	VP6	9-KTLKDARDKIVEG-21, 139-WNLQNRRQRTG-149, 373-NYSPSREDNLQR-384	Y24,S25,N26,V27,S28,D29,L30,I31,Q32,Q33,F34,N35,Q36	-	-
			D74,A75,N76,Y77,V78,E79,T80,A81,R82,N83,T84,I85,D86,Y87	-	-
	VP7	308-QVMSKRSRSLNSA-320	D169,I170,T171,L172,Y173,Y174,Y175,Q176,Q177,T178,D179,E180,A181,N182,K183,W184	-	-
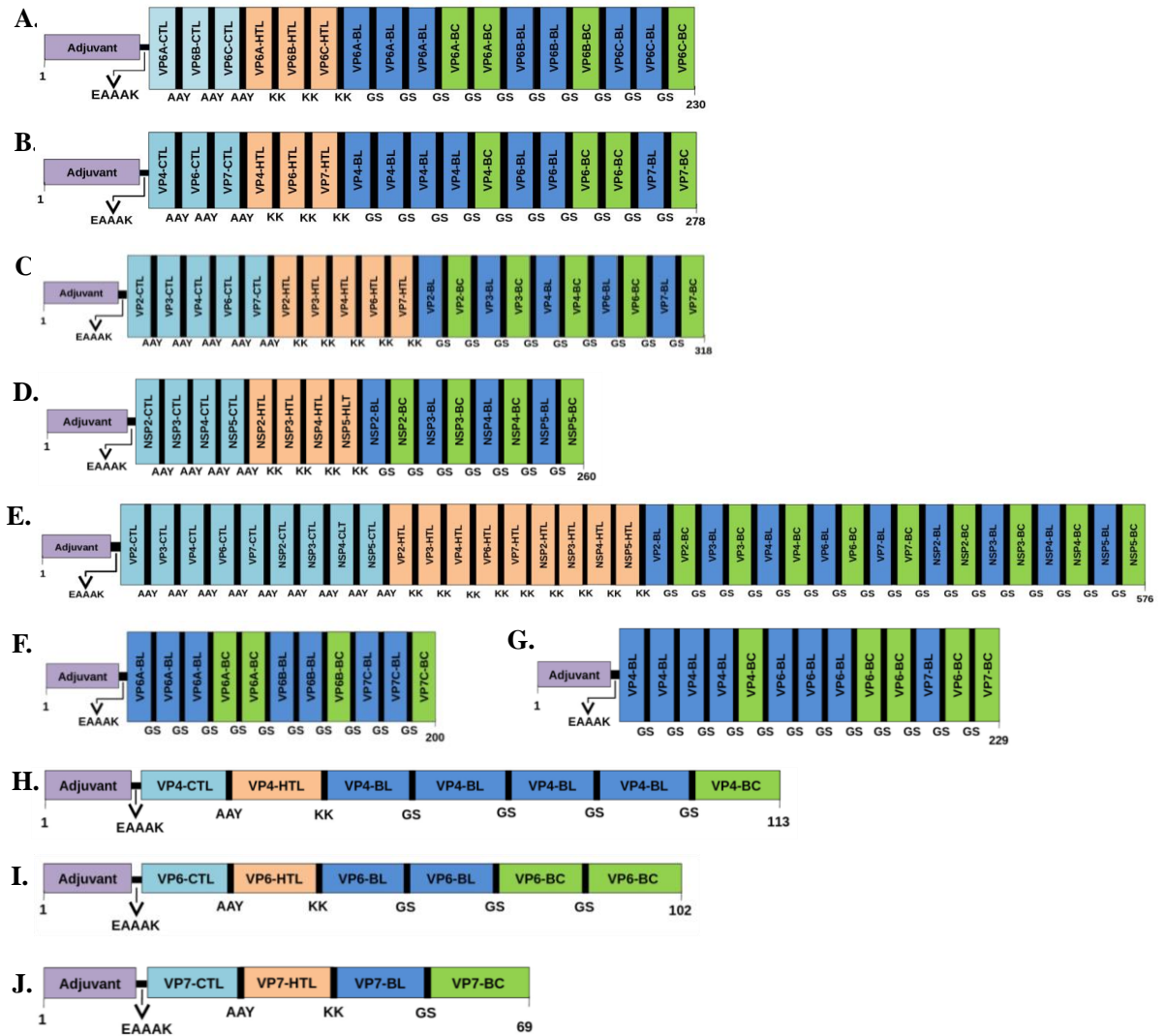
Figure 6.5. Schematic diagram of multi-epitope chimeric constructs. The multi-epitope constructs sequence consisting adjuvant followed by T- and B-cell epitope. Adjuvant and CTL epitope has been joined by EAAAK linker, whereas the AAY, KK and GGGGS linkers were used to join the CTL, HTL and linear/conformational B-cell epitopes, respectively. A. Construct 1 (VP6A/B/C), B. Construct 2 (VP6/4/7), C. Construct 3 (VP2/3/4/6/7), D. Construct 4 (NSP2/3/4/5) and E. Construct 5 (VP2/3/4/6/7-NSP2/3/4/5), F. Construct 6 (VP6A/B/C–B), G. Construct 7 (VP4/6/7-B), H. Construct 8 (VP4/A), I. Construct 9 (VP6/A) and J. Construct 10 (VP7/A); (BL-Linear B-cell epitope, BC- Conformational B-cell epitope). A/B/C: VP6 sequence of group A, B and C rotaviruses; A: group A rotavirus; B: B-cell epitopes (Both linear and conformational).

6.3.6. Allergenicity, antigenicity and physicochemical parameters of the vaccine constructs

All vaccine constructs were predicted as non-allergenic by Allertop v.2. Construct 1 was predicted as non-antigenic by Vexijen v.2.0 with a score (3.888) close to default threshold value of 4.0. Of 10 vaccine constructs, the antigenicity of construct 4 (NSP2/3/4/5), construct 5 (VP2/3/4/6/7- NSP2/3/4/5) and construct 8 (VP4/A) were predicted to be 0.7059, 0.6263, 0.7943, respectively, using the VaxiJen server indicating the probable antigenic properties of vaccine constructs (Table 6.9). Various physicochemical parameters of vaccine constructs were analyzed by ProtParam. The final vaccine constructs were found moderately thermostable based on the aliphatic index scores. We found negative value of gravy scores suggesting the likelihood of multi-epitope vaccine being globular and hydrophilic in nature (Table 6.9).

Table 6.9. Physico-chemical parameter of final multi-epitope constructs. Number of residues, theoretical pI, molecular weight, aliphatic index, and grand average of hydrophobicity (GRAVY) by ProtParam

Multi-epitope antigen	No. of residues	Isoelectric Point	Mol Wt. in KDa	Aliphatic Index	GRAVY Score	Secondary structure by PSIPRED	Allergenicity by Allertop v.2.0	Antigenicity by Vexijen v2.0 (T=0.4)
VP6A/B/C (Construct 1)	230	5.24	24.77	70.04	-0.532	52.2% Helix, 3.0% Sheet and 44.8% Coil	Non-allergen	Non-antigen (0.3888)
VP4/6/7 (Construct 2)	278	8.91	30.10	66.01	-0.613	10.43% Helix, 9.71% Sheet and 79.86% Coil	Non-allergen	Antigen (0.5901)
VP2/3/4/6/7 (Construct 3)	318	9.96	34.87	81.32	-0.375	36.2% Helix,11.0% Sheet and 52.8% Coil	Non-allergen	Antigen (0.5537)
NSP2/3/4/5 (Construct 4)	260	10.11	27.63	66.88	-0.428	25.39% Helix, 11.92% Sheet and 62.69% Coil	Non-allergen	Antigen (0.7059)
VP2/3/4/6/7-NSP2/3/4/5 (Construct 5)	576	10.04	62.05	74.91	-0.369	34.0% Helix, 3.7% Sheet and 62.3% Coil	Non-allergen	Antigen (0.6263)
VP6A/B/C-B (Construct 6)	200	4.83	20.64	52.65	-0.872	28.5% Helix, 4.0% Sheet and 67.5% Coil	Non-allergen	Antigen (0.5319)
VP4/6/7-B (Construct 7)	229	6.83	24.04	45.59	-0.976	19.2% Helix, 4.8% Sheet and 76.0% Coil	Non-allergen	Antigen (0.5374)
VP4/A (Construct 8)	113	6.80	12.31	50.09	-0.777	11.5% Helix, 32.7% Sheet and 55.8% Coil	Non-allergen	Antigen (0.7943)
VP6/A (Construct 9)	102	6.45	11.09	55.59	-0.884	40.2% Helix, 2% Sheet and 57.8% Coil	Non-allergen	Antigen (0.4670)
VP7/A (Construct 10)	69	9.52	7.7	110.43	-0.123	59.4% Helix, 11.6% Sheet and 29% Coil	Non-allergen	Antigen (0.4165)

6.3.7. Prediction of secondary and tertiary structure

We used online server PSIPRED to predict the secondary structure of the final vaccine constructs. The predicted α-helix, β-sheets and random coil of vaccine constructs have been provided in Table 6.9 and Figure 6.6. Tertiary structure of the final vaccine constructs was modeled using ITASSER, RaptorX and Phyre (Figure 6.7). All the modeled structures were analyzed, and the common predicted structure was selected for further molecular simulation. I-TASSER modeled structures were found satisfactory for vaccine constructs (1, 2, 3, 4, 5, 7, 8, 9, & 10) with c-values of the best models -3.19, -2.68, 3.84, -2.84, -1.99, -1.69, -2.42, -2.59 and -2.51, respectively, while for construct 6, RaptorX modeled structure was chosen with a P-value of 2.78e-03, a lower p-value is indicative of best modelled structure [82].
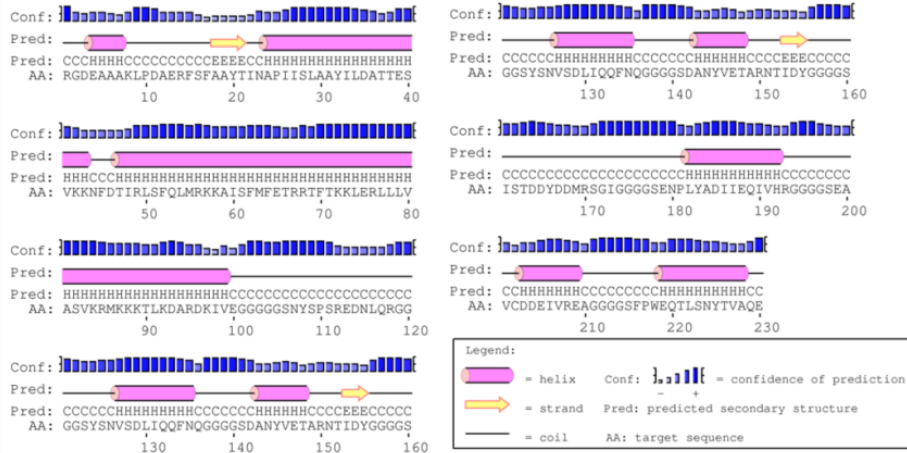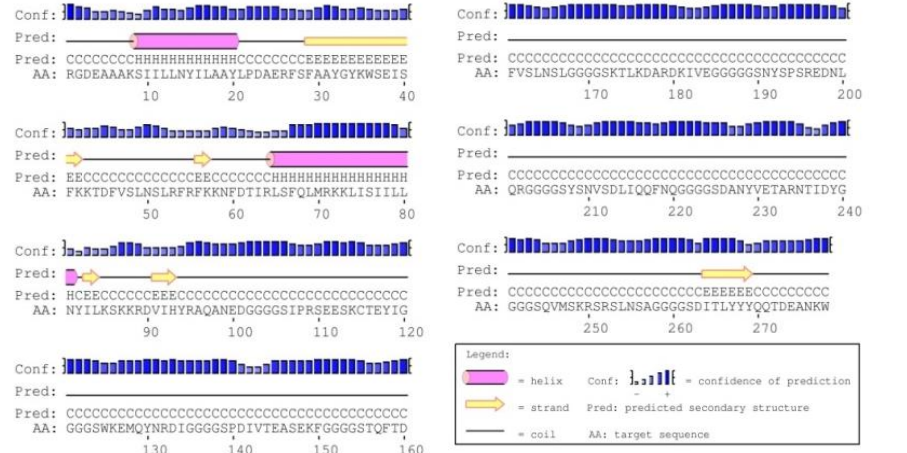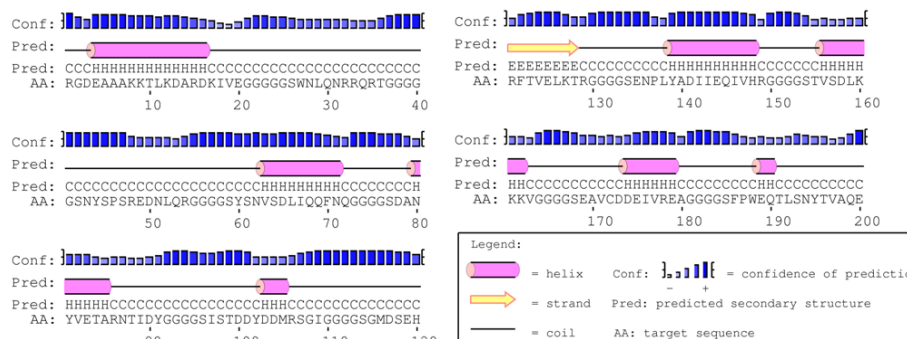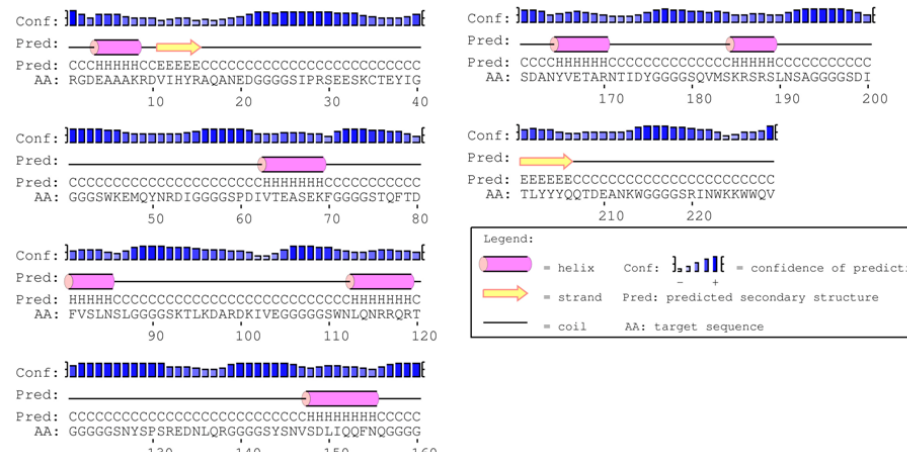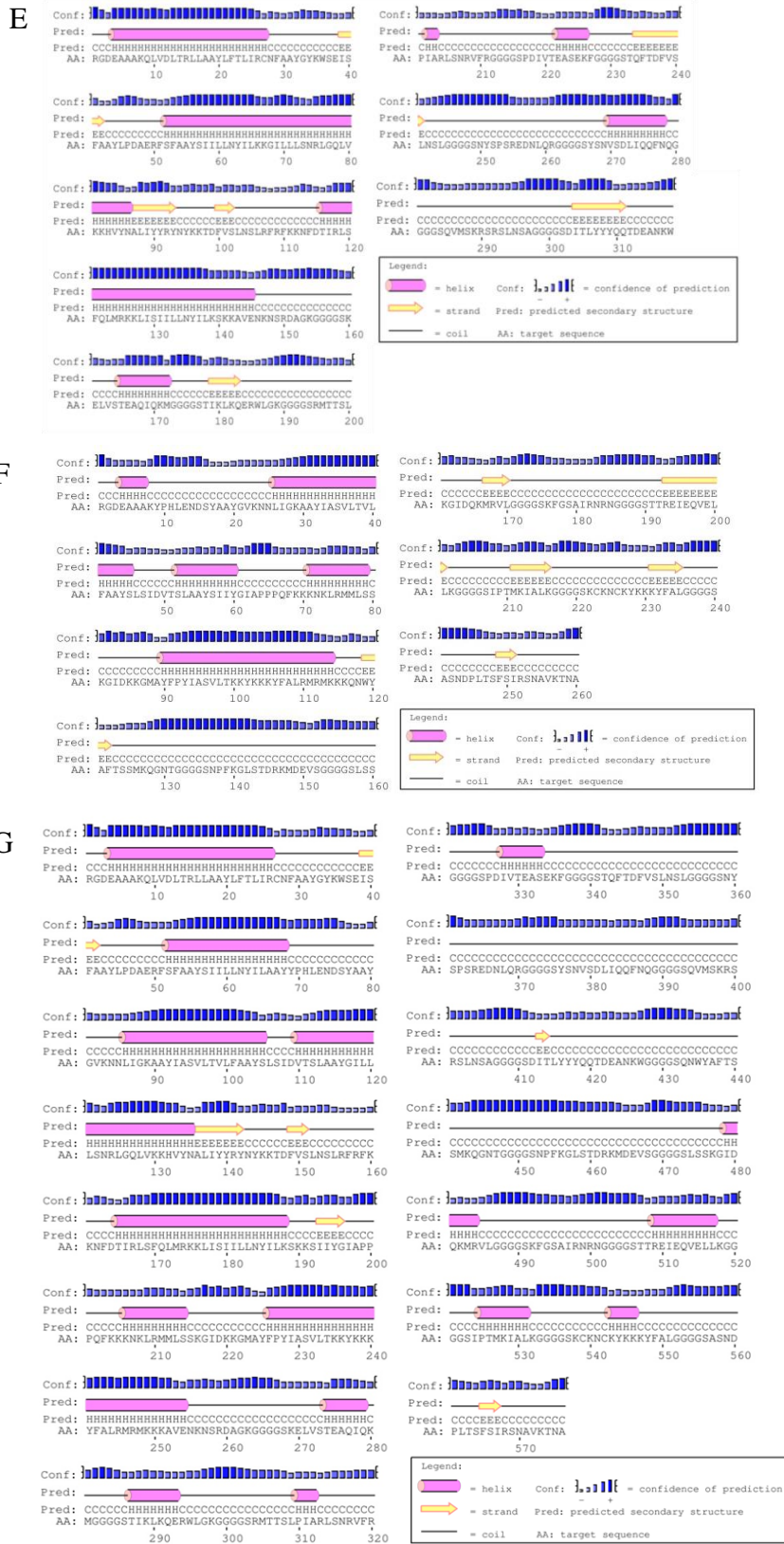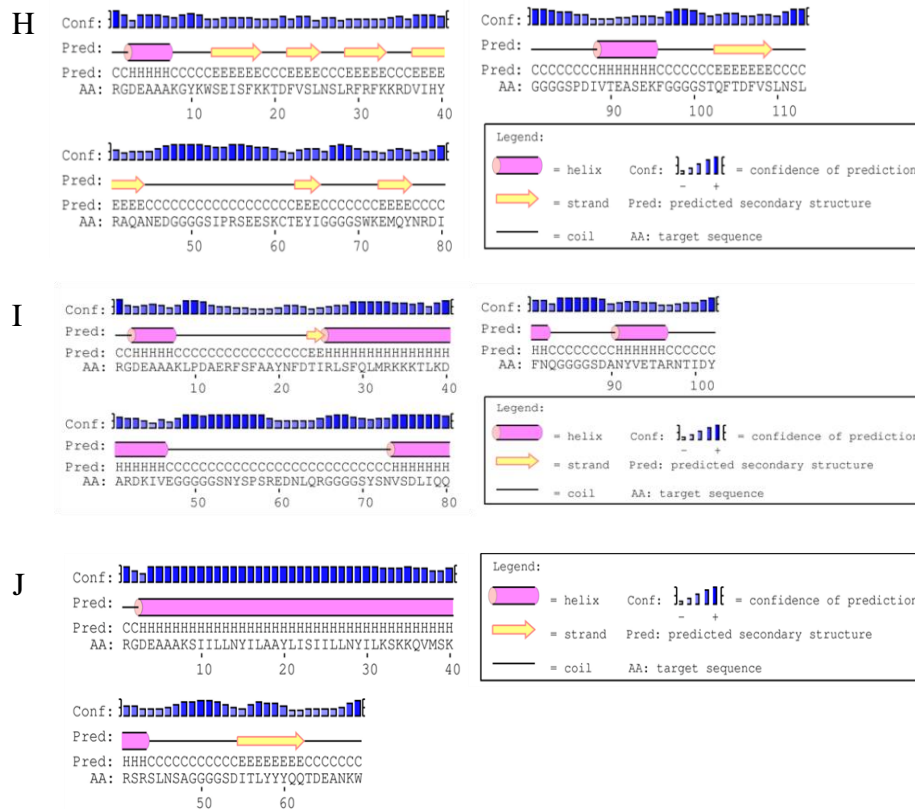
Figure 6.6. Graphical representation of secondary structure obtained for the multi-epitope constructs using PSIPRED server. A. Construct 1, 52.2% helix, 3.0% sheet and 44.8% coil, B. Construct 2, 10.43% helix, 9.71% sheet and 79.86% coil, C. Construct 6, 28.5% helix, 4.0% sheet and 67.5% coil and D. Construct 7, 19.2% helix, 4.8% sheet and 76.0% coil, E. Construct 3, 36.2% helix,11.0% sheet and 52.8% coil, F. Construct 4, 25.39% helix, 11.92% sheet and 62.69% coil, G. Construct 5, 34.0% Helix, 3.7% Sheet and 62.3% Coil, H. Construct 8, 11.5% helix, 32.7% sheet and 55.8% coil, I. Construct 9, 40.2 % helix, 2 % sheet and 57.8 % coil and J. Construct 10, 59.4 % helix, 11.6 % sheet and 29 % coil.
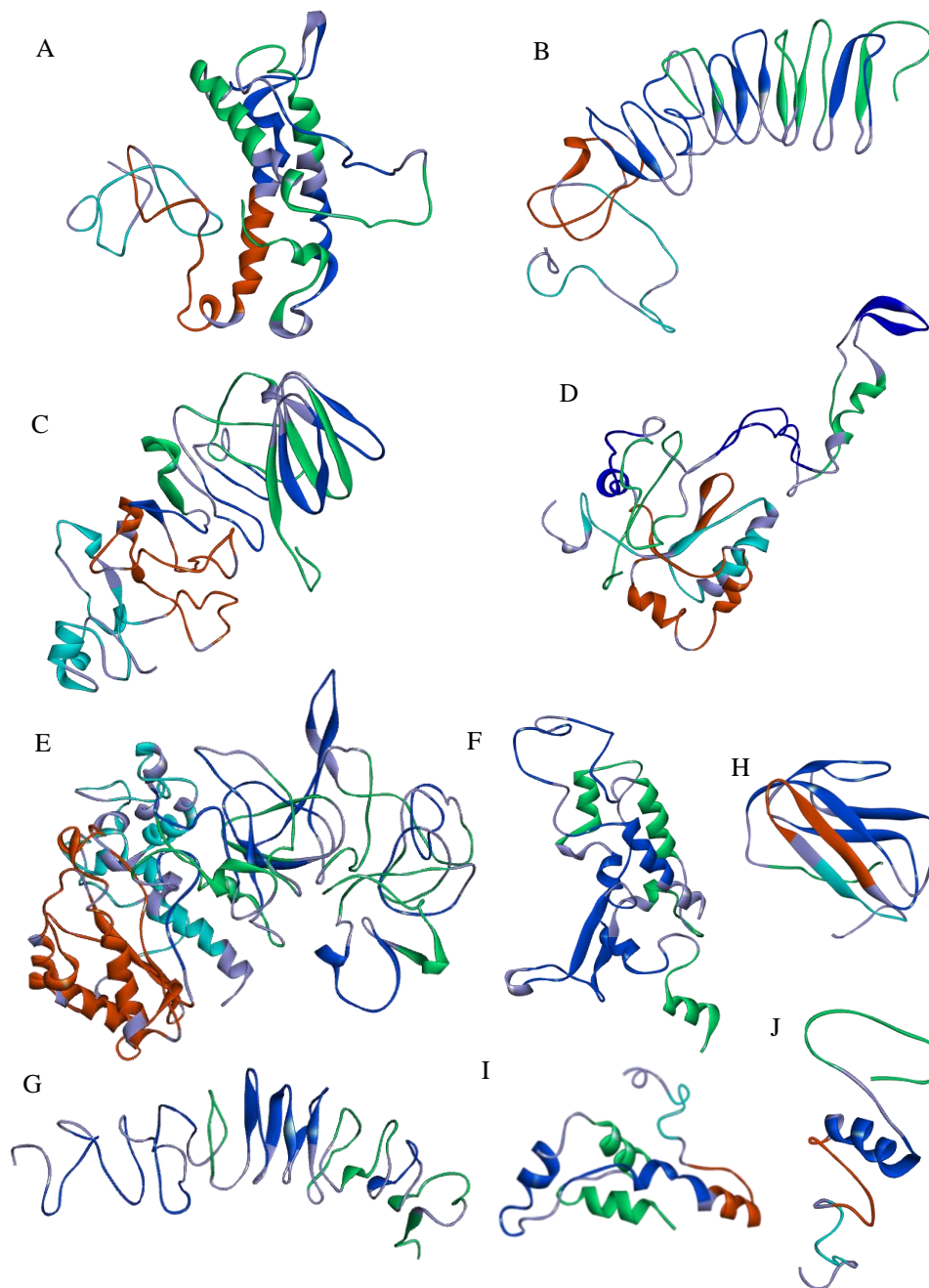
Figure 6.7. Tertiary structure modeling of multi-epitope constructs. Cyan color represents CTL epitopes, orange represents HTL epitopes, blue represents linear B- cell epitopes and conformational B-cell epitope is highlighted with green. A. Construct 1; B. Construct 2; C. Construct 3; D. Construct 4; E. Construct 5; F. Construct 6; G. Construct 7; H. Construct 8; I. Construct 9; and J. Construct 10.

6.3.8. Molecular dynamics simulation and tertiary structure validation

Further refinement and overall stability of multi-epitope subunit vaccine constructs were performed using molecular dynamics simulation in GROMACS, CHARMM27 force

field and SPC/E water model as described previously. A plot of root square deviation (RMSD) against time reflects fluctuations generated within a time interval of 20 ns for all constructs and 40 ns for construct 5 having a predicted molecular weight of 62 kDa (Table 6.9). RMSD value of multi-subunit vaccine backbone was predicted to be 0.2–0.7 nm (Figure 6.8) and the structure validation of final vaccine was carried out using RAMPAGE server (Figure 6.9). Table 6.9 provides the summary of distribution of amino acid residues in energetically favored area, allowed part and outlier region of vaccine constructs. The results of Ramachandran plots are suggestive of high structural quality due to the presence of minimum steric atomic clashes between the residues in the refined vaccine constructs (Figure 6.9 and Table 6.10).
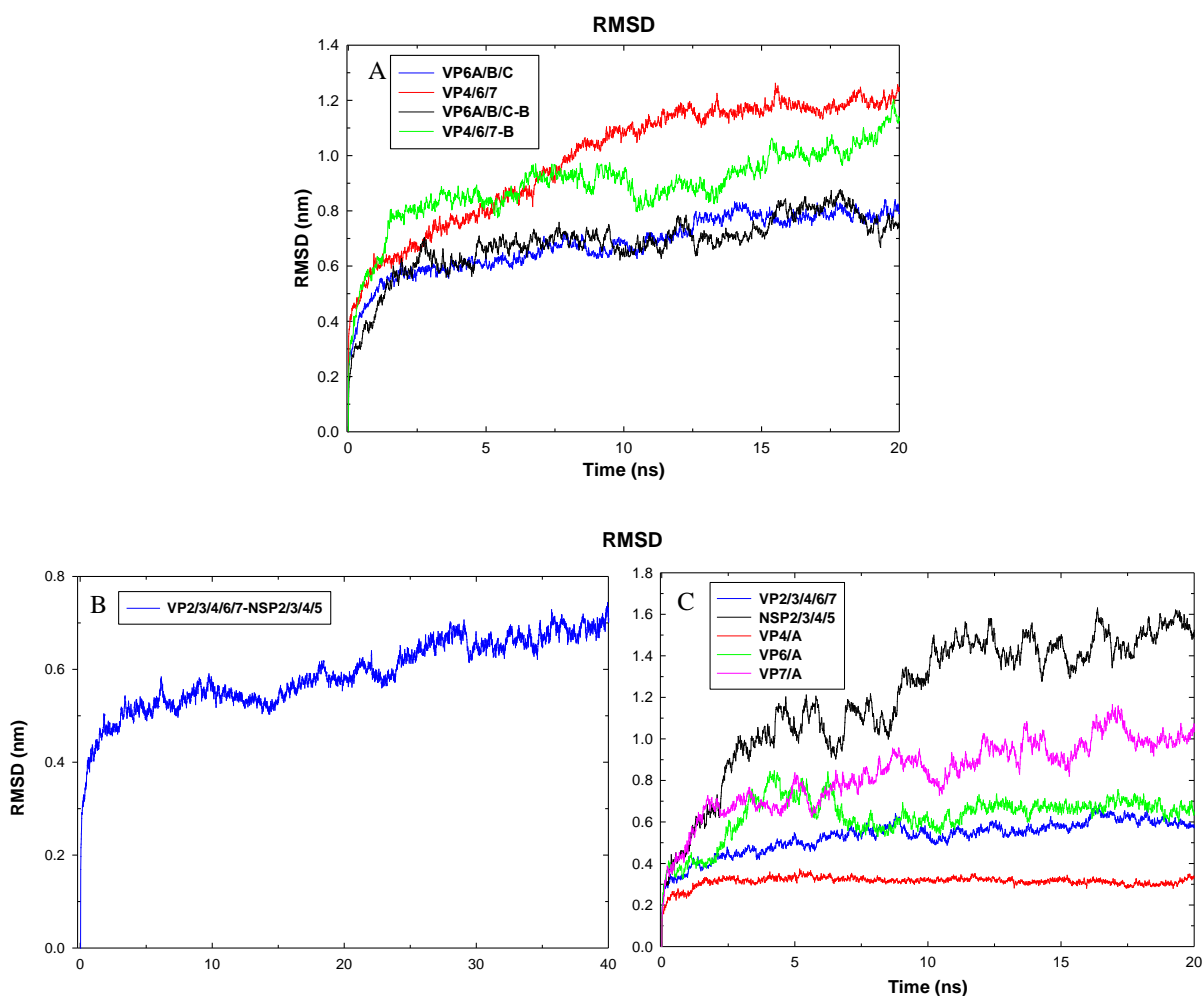
Figure 6.8. Molecular dynamics simulation study of final multi-epitope constructs representing root mean square deviation. A. Simulation was carried out for time duration of 20 ns for construct 1, 2, 6 and 7, B. Simulation for construct 5 was performed for the time duration of 40 ns, C. Simulation for 20ns for constructs 3,4,8,9 and 10.
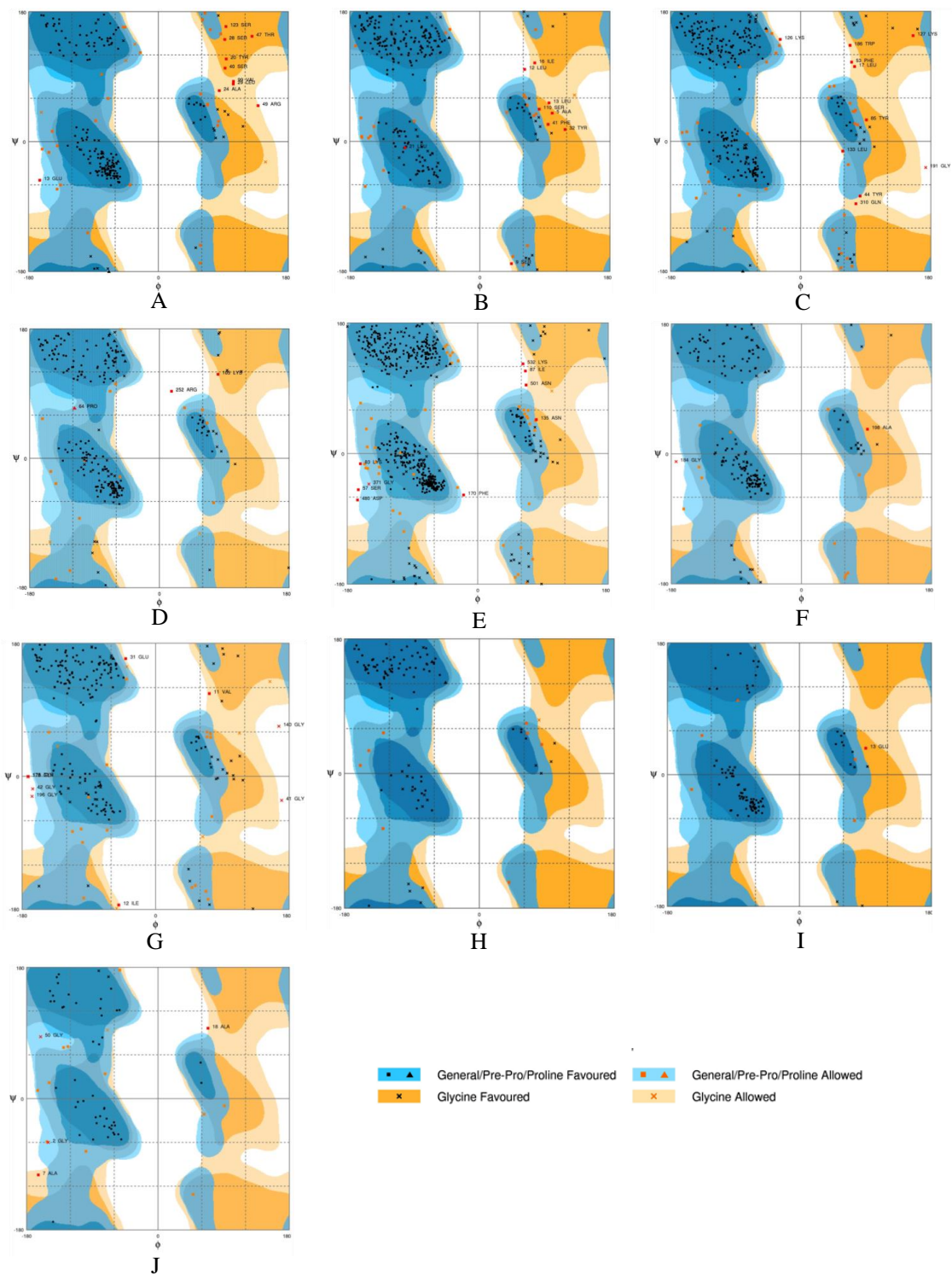
Figure 6.9. Structure prediction and validation of final multi-epitope constructs.
Ramachandran plot analysis of the simulated structures. Summary of residues in favored, allowed and in outlier part is provided in Table 6.10.

Table 6.10. Summary of amino acid residues of vaccine constructs in the energetically favored, allowed and residues in the outlier region as analyzed by physico-chemical parameter of final multi-epitope constructs

Multi-epitope antigen	No. of residues in the favored region	No. of residues in the allowed region	No. of residues in the outlier region
VP6A/B/C (Construct 1)	188 (82.8%)	29 (12.8%)	10 (4.4%)
VP4/6/7 (Construct 2)	242 (88.0%)	24 (8.7%)	9 (3.3%)
VP2/3/4/6/7 (Construct 3)	270 (85.7%)	35 (11.1%)	10 (3.2%)
NSP2/3/4/5 (Construct 4)	237 (92.2%)	17 (6.6%)	3 (1.2%)
VP2/3/4/6/7-NSP2/3/4/5 (Construct 5)	522 (91%)	42 (7.3%)	9 (1.6%)
VP6A/B/C-B (Construct 6)	184 (93.4%)	11 (5.6%)	2 (1.0%)
VP4/6/7-B (Construct 7)	193 (85.4%)	24 (10.6%)	9 (4.0%)
VP4/A (Construct 8)	101 (91.8%)	9 (8.2%)	0 (0.0%)
VP6/A (Construct 9)	93 (93.9%)	5 (5.1%)	1 (1.0%)
VP7/A (Construct 10)	50 (75.8%)	12 (18.2%)	4 (6.1%)

6.3.9. Surface accessibility of linkers and verification of conformational B-cell epitopes in the vaccine construct

Cathepsin and carboxypeptidase are involved in MHC class II antigen presentation pathway through proteolytic cleavage of dibasic (RR, KK, KR or RK) sites present in the endocytosed proteins [83]. MHC class II molecules expressed by antigen presenting cells are associated with presentation of processed peptides to CD4+ T cells. Proteases that are involved in MHC class II antigen presentation pathway exhibits preferential cleavage of substrates containing hydrophobic motifs (AAY). We found that the cleavable linker residues (AAY and KK) in the multi-epitope subunit vaccines were accessible suggesting

that the probability of T-cell epitopes presentation by MHC molecules as predicted by discovery studio (Figure 6.10). Conformational B-cell epitopes that were included in the final vaccine construct was further verified with the help of four prediction servers - CBTOPE, Ellipro, Discotope and EPSVR. The results showed that the conformation epitopes were similarly predicted by CBTOPE, Ellipro, Discotope and EPSVR (Table 6.11). We have predicted an additional discontinuous B-cell epitopes with the help of Ellipro (Figure 6.11 and Table 6.12). ElliPro is a web-based server commonly used for prediction of an antibody epitopes in protein antigens [39,84].
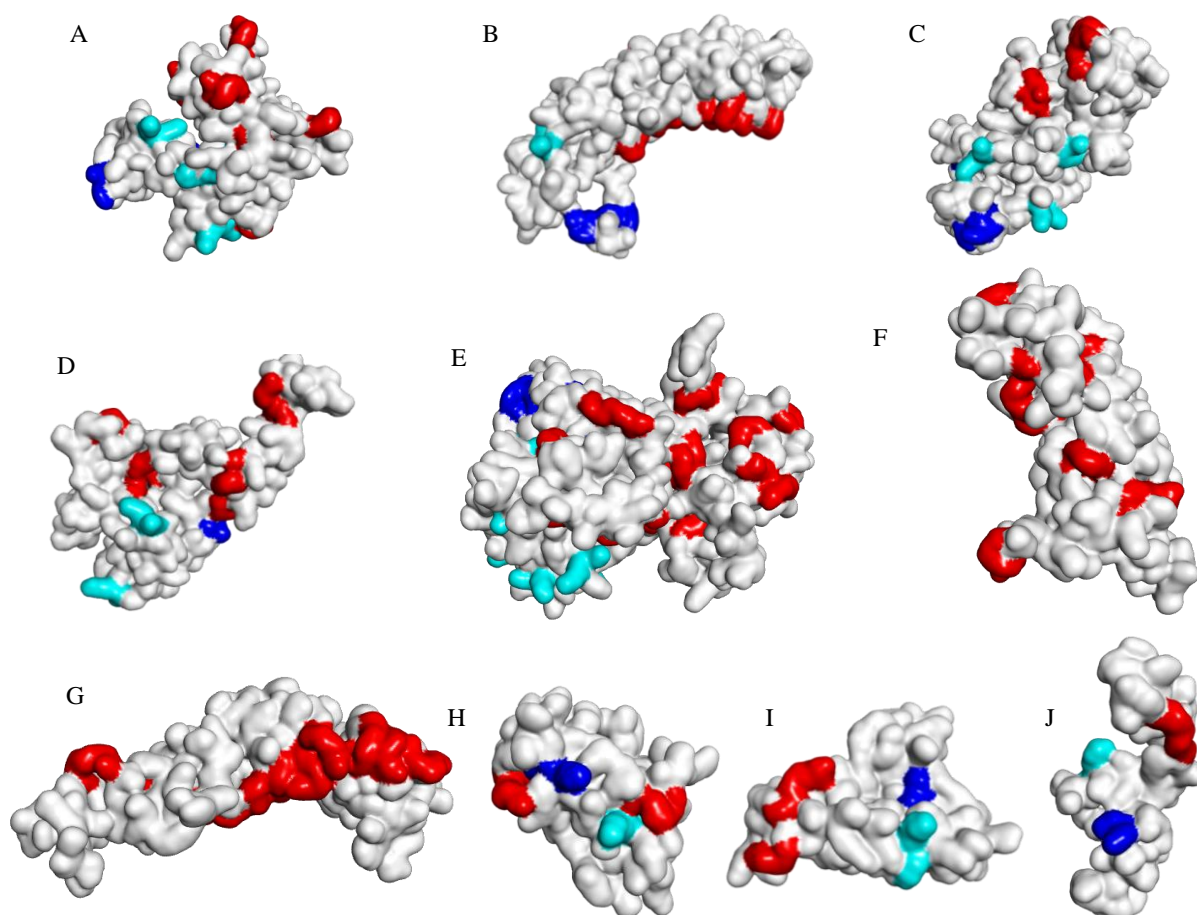
Figure 6.10. Surface accessibility of linkers in the final multi-epitope constructs. A. Construct 1; B. Construct 2; C. Construct 3; D. Construct 4; E. Construct 5; F. Construct 6; G. Construct 7; H. Construct 8; I. Construct 9; and J. Construct 10. Blue color represents AAY linker, cyan represents KK linker and GGGGS is represented by red color.
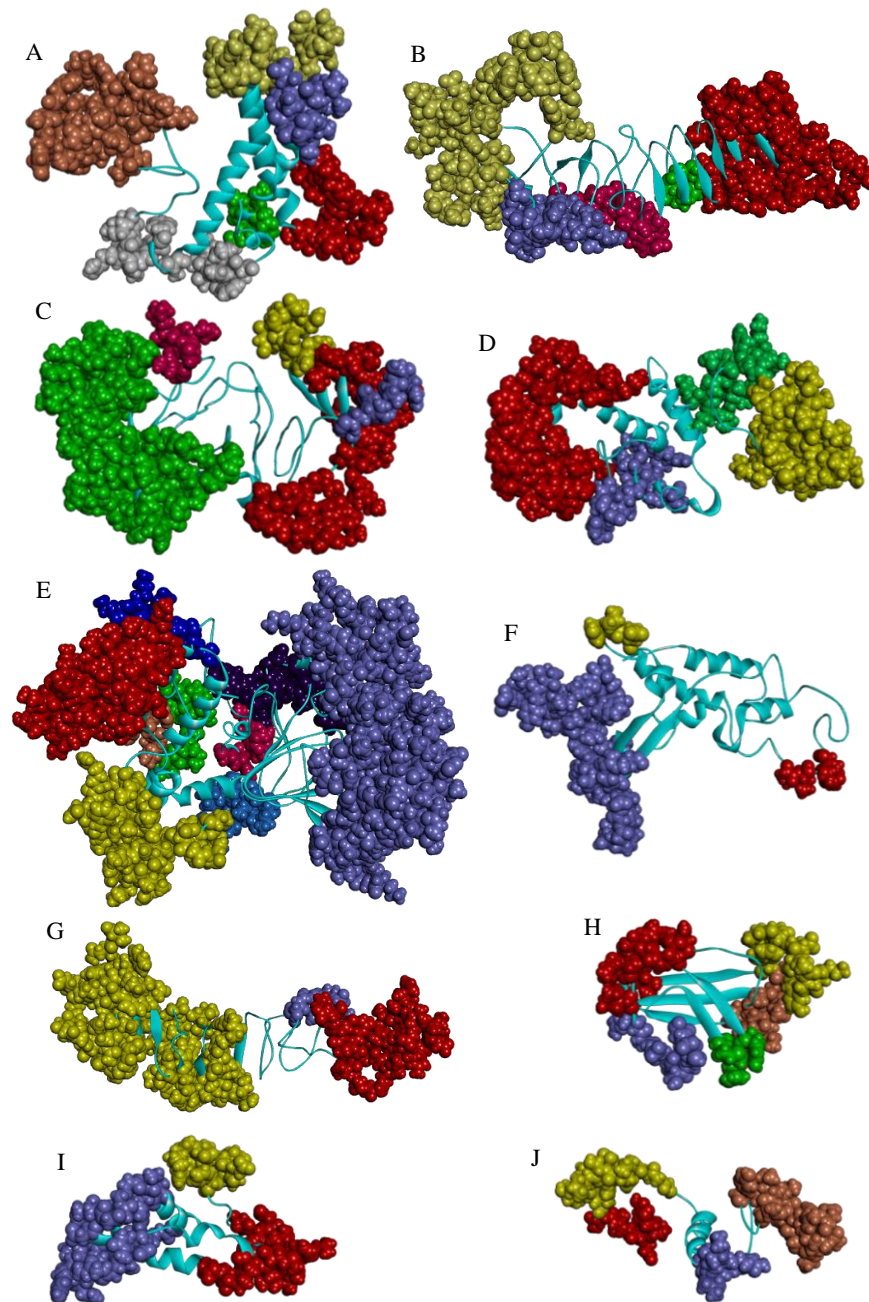
Figure 6.11. Conformational B-cell epitopes prediction for the final multi-epitope constructs by Ellipro. A. Construct 1, B. Construct 2, C. Construct 3, D. Construct 4, E. Construct 5, F. Construct 6, G. Construct 7, H. Construct 8, I. Construct 9 and J. Construct 10. The epitopes are represented as colored spheres in the final vaccine model where each color represents one epitope.

Table 6.11. Verification of conformational B-cell epitopes. The epitopes in the final vaccine constructs were superimposed with their native structure by Phymol and Yale alignment server. The corresponding B-cell epitopes or part of the epitope predicted using four servers are numbered as CBTOPE (1), Ellipro (2), Discotope (3) and EPSVR (4).

Multi-epitope construct	RV Protein	Conformational B-cell epitope	RMSD of superimposition		server
			Pymol	Yale Alignment Server	
VP6A/B/C	VP6 GroupA	Y24,S25,N26,V27,S28,D29,L30,I31,Q32,Q33,F34,N35,Q36	1.236	1.235635	1,3&4
		D74,A75,N76,Y77,V78,E79,T80,A81,R82,N83,T84,I85,D86,Y87	4.523	4.522595	1,2,3&4
	VP6 Group B	E154,N155,P156,L157,Y158,A159,D160,I161,I162,E163,Q164,I165,V166,H167,R168	5.448	5.448080	1,2,3&4
	VP6 Group C	F364,P365,W366,E367,Q368,T369,L370,S371,N372,Y373,T374,V375,A376,Q377,E378	4.662	4.662487	2&3
VP4/6/7	VP4	T413,Q414,F415,T416,D417,F418,V419,S420,L421,N422,S423,L424	4.112	4.112052	1,2,3&4
	VP6-	Y24,S25,N26,V27,S28,D29,L30,I31,Q32,Q33,F34,N35,Q36	5.166	5.165656	1,2,3&4
		D74,A75,N76,Y77,V78,E79,T80,A81,R82,N83,T84,I85,D86,Y87	6.584	6.584060	1,2,3&4
	VP7	D169,I170,T171,L172,Y173,Y174,Y175,Q176,Q177,T178,D179,E180,A181,N182,K183,W184	5.543	5.559023	1,2&3
VP2/3/4/6/7	VP2	K339,E340,L341,V342,S343,T344,E345,A346,Q347,I348,Q349,K350,M351	2.253	3.176211	2,3&4
	VP3	R176,M177,T178,T179,S180,L181,P182,I183,A184,R185,L186,S187,N188,R189,V190,F191,R192	6.117	7.039348	2,3&4
	VP4	T413,Q414,F415,T416,D417,F418,V419,S420,L421,N422,S423,L424	4.123	4.123033	2,3&4
	VP6	Y24,S25,N26,V27,S28,D29,L30,I31,Q32,Q33,F34,N35,Q36	5.641	5.640909	2,3&4
	VP7	D169,I170,T171,L172,Y173,Y174,Y175,Q176,Q177,T178,D179,E180,A181,N182,K183,W184	5.559	5.559023	2,3&4

Table 6.11. contd….

Multi-epitope construct	RV Protein	Conformational B-cell epitope	RMSD of superimposition		server
			Pymol	Yale Alignment Server	
NSP2/3/4/5	NSP2	N298,P299,F300,K301,G302,L303,S304,T305,D306,R307,K308,M309,D310,E311,V312,S313	4.682	4.740787	1,2,3&4
	NSP3	K77,F78,G79,S80,A81,I82,R83,N84,R85,N86	0.372	1.361094	1,2,3&4
	NSP4	I51,P52,T53,M54,K55,I56,A57,L58,K59	4.195	4.195239	1,2&3
	NSP5	A66,S67,N68,D69,P70,L71,T72,S73,F74,S75,I76,R77,S78,N79,A80,V81,K82,T83,N84,A85	6.172	6.171581	1,2,3&4
VP2/3/4/6/7-NSP2/3/4/5	VP2	K339,E340,L341,V342,S343,T344,E345,A346,Q347,I348,Q349,K350,M351	3.743	3.743109	1,2,3&4
	VP3	R176,M177,T178,T179,S180,L181,P182,I183,A184,R185,L186,S187,N188,R189,V190,F191,R192	3.855	4.518686	1,3&4
	VP4	T413,Q414,F415,T416,D417,F418,V419,S420,L421,N422,S423,L424	7.294	7.321160	1,2,3&4
	VP6	Y24,S25,N26,V27,S28,D29,L30,I31,Q32,Q33,F34,N35,Q36	5.437	5.436957	1,3&4
	VP7	D169,I170,T171,L172,Y173,Y174,Y175,Q176,Q177,T178,D179,E180,A181,N182,K183,W184	5.201	5.212638	1,2,3&4
	NSP2	N298,P299,F300,K301,G302,L303,S304,T305,D306,R307,K308,M309,D310,E311,V312,S313	5.200	5.200160	1,2,3&4
	NSP3	K77,F78,G79,S80,A81,I82,R83,N84,R85,N86	4.638	4.638486	1,2,3&4
	NSP4	I51,P52,T53,M54,K55,I56,A57,L58,K59	3.804	3.803996	1,2,3&4
	NSP5	A66,S67,N68,D69,P70,L71,T72,S73,F74,S75,I76,R77,S78,N79,A80,V81,K82,T83,N84,A85	6.331	5.959602	1,2&3

Table 6.11. contd….

Multi-epitope construct	RV Protein	Conformational B-cell epitope	RMSD of superimposition Pymol	Yale Alignment Server	server
VP6A/B/C-B	VP6 GroupA	Y24,S25,N26,V27,S28,D29,L30,I31,Q32,Q33,F34,N35,Q36	1.035	1.034830	1,2,3&4
		D74,A75,N76,Y77,V78,E79,T80,A81,R82,N83,T84,I85,D86,Y87	4.878	4.877540	1,2,3&4
	VP6 Group B	E154,N155,P156,L157,Y158,A159,D160,I161,I162,E163,Q164,I165,V166,H167,R168	5.056	5.056235	1,2,3&4
	VP6 Group C	F364,P365,W366,E367,Q368,T369,L370,S371,N372,Y373,T374,V375,A376,Q377,E378	4.353	4.352642	1,2&3
VP4/6/7-B	VP4	T413,Q414,F415,T416,D417,F418,V419,S420,L421,N422,S423,L424	4.003	4.024564	1,3&4
	VP6	Y24,S25,N26,V27,S28,D29,L30,I31,Q32,Q33,F34,N35,Q36	5.214	5.213927	1,2,3&4
		D74,A75,N76,Y77,V78,E79,T80,A81,R82,N83,T84,I85,D86,Y87	6.058	6.057730	1,2,3&4
	VP7	D169,I170,T171,L172,Y173,Y174,Y175,Q176,Q177,T178,D179,E180,A181,N182,K183,W184	5.341	3.793345	1,2,3&4
		R286,I287,N288,W289,K290,K291,W292,W293,Q294,V295	3.541	4.642401	1,2&3
VP4/A	VP4	T413,Q414,F415,T416,D417,F418,V419,S420,L421,N422,S423,L424	4.237	6.780728	1,2&3
VP6/A	VP6	Y24,S25,N26,V27,S28,D29,L30,I31,Q32,Q33,F34,N35,Q36	1.560	1.560356	1,3&4
		D74,A75,N76,Y77,V78,E79,T80,A81,R82,N83,T84,I85,D86,Y87	1.638	1.638197	1,2,3&4
VP7/A	VP7	D169,I170,T171,L172,Y173,Y174,Y175,Q176,Q177,T178,D179,E180,A181,N182,K183,W184	0.954	1.304295	1,2,3&4

Table 6.12. Conformational B-cell epitopes prediction for the final multi-epitope vaccine construct by Ellipro

Multi-epitope construct	Epitope No.	Conformational B-cell epitope	No. of residues
VP6A/B/C	1	F64, E65,T66,R67,R68,T69,F70,K73,L74,E209,A210,G211,G212,G213,G214,S215,F216,P217,W218	19
	2	R1,G2,D3,E4,A5,A6,A7,K8,L9,P10,D11,A12,E13,R14,F15,S16,F17,A18,A19,Y20,T21,I22,N23,A24,P25,I26,I27,S40,K42,K43,N44,F45,D46,T47,I48,R49,L50,S51	38
	3	V99,E100,G101,G102,G103,G104,G105,S106,N107,Y108,S109,P110,S111,R112,E113,D114,N115,L116,Q117,R118,G119,G120,G121,G122,S123,Y124,S125	27
	4	V146,E147,T148,A149,R150,N151,T152,I153,D154,Y155,G156,G157,G158,G159,S160,I161,S162,T163,D164,D165,D167,D168,M169,R170	24
	5	G172,I173,G174,G175,G176,G177,S178,E179,N180,P181,L182,Y183,A184,D185,I186	15
	6	D203,D204,I206,V207,R208	5
VP4/6/7	1	R1,G2,D3,E4,A5,A6,A7,K8,S9,I10,I11,L12,L13,N14,Y15,I16,L17,A18,A19,Y20,L21,P22,D23,A24,E25,R26,F27,S28,F29,A30,A31,Y32,G33,Y34,K35,K42,K43,L44,I45,S46,I47,I48,L49,L50,N51,Y52,I53,L54,K72,K73,T74,D75,F76,V77	54
	2	S195,R196,E197,R202,S212,D213,L214,I215,Q216,Q217,F218,N219,Q220,G221,G222,G223,G224,S225,D226,Y229,V230,E231,T232,A233,R234,N235,T236,I237,D238,Y239,G240,G241,G242,G243,S244,S248,K249,R250,S253,L254,N255,S256,A257,G258,G259,G260,G261,S262,D263,I264,T265,L266,Y267,Y268,Y269,Q270,Q271,T272,D273,E274,A275,N276,K277,W278	64
	3	S56,N59,F60,D61,T62,I63,R64,L65,S66,F67,F86,K87,K88,D90,V91,I92,H93,Y94,I107,R109,S110,E111,E112,S113	24
	4	R179,D180,D198,N199	4
	5	R95,K114,C115,G135,G136,G137,G138,S139,P140,D141,I142,T159,D160,F161,V162,S163,L164	17
VP2/3/4/6/7	1	Y309,Q310,Q311,T312,D313,E314,A315,N316,K317,W318	10
	2	T198,S199,P201,K226,G228,G229,G230,G231,S232,T233,Q234,F235,T236,D237,F238,V239,S240,L241,N242,S243,L244,G245,G247,G248,S249,N250,D257,N258,L259,Q260,R261,G262,G263,G264,G265,S271,D272,L273,I274,Q275,Q276,F277,N278,Q279,G280,G281,G282,G283,S284,K289,R290,S291,R292,S293,L294,N295,S296,A297,G298,G299,G300,G301,S302	63
	3	A203,R204,Y251,S252,P253,S254,R255	7
	4	R1,G2,D3,E4,A5,A6,A7,K8,Q9,L10,V11,D12,L13,T14,R15,L16,L17,A18,A19,Y20,L21,F22,T23,L24,I25,R26,C27,N28,F29,A30,A31,Y32,G33,Y34,K35,W36,S37,E38,I39,A43,Y44,L45,A48,E49,R50,F51,S52,F53,A54,A55,Y56,S57,I58,I59,L60,L61,N62,Y63,I64,L65,K66,K67,R92,Y93,N94,Y95,K96,K97,T98,D99,F100,V101,S102,L103,L138,K139,S140,K141,G157,G158,S159,K160	82
	5	L72,R75,Q78,L79,V80,K81,K82,H83	

Table 6.12. contd….

Multi-epitope construct	Epitope No.	Conformational B-cell epitope	No. of residues
NSP2/3/4/5	1	K199,G200,G201,G202,G203,S204,I205,A211,L212,K213,G214,G215,G216,G217,S218,K219,C220,K221,N222,C223,K224,Y225,K226,K227,K228,F230,G233,G234,G235,G236,S237,A238,S239,N240,D241,P242,L243,T244,S245,F246,S247,I248,R249,S250,N251,A252,V253,K254,T255,N256,A257	51
	2	A19,G21,V22,K23,N24,N25,L26,I27,G28,K29,A30,A31,Y32,I33,A34,S35,V36,L37,T38,V39,L40,F41,A42,A43,Y44,S45,L46,S47,I48,D49,V50,T51,S52,K54,S56,I57,I58,Y59,G60,P64,Q66,K69,K72,L73,R74,M75,M76,L77,S78,S79,K80,G81,I82,D83,K84,K85,G86,A88,Y89	59
	3	H11,L12,E13,N14,D15,S16,Y17,A18,R111,M112,K113,Q114,N115,W116,Y117,F119,S121,K124	18
	4	K163,M164,R165,V166,L167,G168,G169,G170,G171,S172,K173,F174,G175,S176,A177,I178,R179,N180,R181,N182,G183,G184,G186	23
VP2/3/4/6/7-NSP2/3/4/5	1	L24,I25,R26,C27,N28,F29,A30,A31,Y32,G33,Y34,K35,W36,Y68,Y69,P70,L72,E73,N74,D75,S76,Y77,A78,A79,Y80,G81,V82,K83,N84,N85,L86,I87,G88,K89,A90,A91,Y92,I93,A94,S95,L97,T98	42
	2	T111,S112,L113,A114,A115,Y116,G117,I118,L119,L120,L121,S122,N123,R124,L125,G126,Q127,L128,V129,K130,K131,H132,A136,L137,Y142,N143,Y144,K145,K146,T147,D148,F149,V150,L168,S169,Q171,L172,M173,R174,K175,K176,L177,I178,S179,I180,I181,L182,L183,N184,Y185,I186,L187,K188,S189,K190,K191,S192,I193,Y241	59
	3	G407,G408,G409,G410,S411,D412,I413,T414,L415,Y416,Y417,Y418,Q420,T421,D422,Y436,A437,F438,T439,S440,S441,M442,K443,Q444,G445,N446,T447,G448,G449,G450,G451,S452,N453,P454,F455,K456,G457,L458,S459,T460,D461,R462,K463,M464,D465,E466,V467,S468,G469,G470,G471,G472,S473,L474,S475,S476,K477,G478,I479,D480,Q481,K482,M483,R484,V485,L486,G487,G488,G489,G490,S491,K492,F493,G494,S495,A496,I497,R498,N499,R500,N501,G502,G503,G504,G505,S506,T507,T508,Q513,V514,E515,L516,L517,K518,G519,G520,G521,G522,S523,I524,P525,T526,M527,K528,G536,S537,K538,C542,K543,Y544,K545,K546,K547,Y548,F549,A550,G553,G554,G555,S556,A557,S558,N559,D560,P561,L562,T563,S564,F565,S566,I567,R568,S569,N570,A571,V572	136
	4	K205,K206,N207,K208,M211,M212,L213,S214,S215,K216,G217,I218,D219,K220,K221	15
	5	S231,V232,L233,T234,K235,K236,Y237,K238,K239,K240,F242,A243,R247,A252	14
	6	S258,G264,G265,G266,G267,S268,K269,E270,L271,V272,S273,T274,E275,A276,Q277,I278,Q279,K280,M281,G282,G284,S286,R294,D346,V348,S349,L350,N351,S352	29
	7	E293,W295,L296,G297,K298,G299,G300,R304	8
	8	K160,K161,N162,F163,D164,T165,I166,R167	8
	9	S57,I58,I59,L60,L61,N62,Y63,I64,L65,A66,K335,F336	12

Table 6.12. contd….

Multi-epitope construct	Epitope No.	Conformational B-cell epitope	No. of residues
VP6A/B/C-B	1	Y81,V82,E83	3
	2	N28,L29,N31,R32	4
	3	D100,D101,Y102,D103,D104,M105,R106,S107,G108,I109,G110,G111,G112,G113,S114,G115,M116,D117,S118,E119,R121,I176,V177,R178,E179,A180,G181,G182,G183,G184,S185,F186,P187,W188,E189,Q190,T191,L192,S193,N194,Y195,T196,V197,A198,Q199,E200	46
	4	G24,G25,S26,W27,Q30,R33,Q34,R35,T36,G37,G38,G39,G40,G41,S42,N43,Y44,S45,P46,S47,R48,E49,D50,N51,L52,Q53,R54,S59,Y60,S61,G131,G132,G133,S134,E135,N136,P137,L138,Y139	39
	5	G2,D3,Q68,Q72,G73,G74,G75,G76,S77,D78,A79,N80,T84,A85,R86,N87,D90,T128	18
VP4/6/7-B	1	R1,G2,D3,E4,A5,A6,A7,K8,R9,D10,V11,I12,H13,Y14,R15,A16,Q17,A18,N19,E20,D21,G22,G23,G24,G25,S26,I27,P28,R29,S30,E31,E32,S33,K34,E37,Y38,I39,G40	38
	2	D97,A98,R99,D100,K101,I102,L113,Q114,N115,R116,R117,Q118,S129,P130,S131,R132,E133,D134,N135,L136,Q137,R138,D149,L150,I151,Q152,Q153,F154,N155,Q156,G157,E167,T168,A169,R170,N171,T172,I173,D174,Y175,G176,G177,G178,G179,S180,K185,R186,S187,R188,S189,L190,N191,A193,G194,G195,G196,G197,S198,D199,I200,L202,Y204,Y205,Q206,Q207,T208,D209,E210,A211,N212,K213,W214,G215,G216,G217,G218,S219,R220,I221,N222,W223,K224,K225,W226,W227,Q228,V229	87
	3	T36,G55,G56,G57,G58,S59,P60,D61,I62,G73	10
VP4/A	1	R1,G2,D3,E4,A5,A6,A7,K8,G9,Y10,W12	11
	2	T20,D21,F22,V23,S24,L25,D47,G48,G49,G50,G51,I53,K95,F96,G97,G98,G99,G100,S101,T102,Q103	21
	3	R55,S56,E57,E58,S59,K60,C61,T62,E63	9
	4	Y40,M74,Q75,Y76	4
	5	K11,K34,R35,D36,V37,I38,H39,D79,I80,G81,G82,G83,G84,S85	14
VP6/A	1	R1,G2,D3,E4,A5,A6,A7,K8,L9,P10,D11,A12,E13,F15	14
	2	N21,F22,D23,T24,I25,R26,L27,S28,F29,Q30,L31,M32,K34,K35,D101,Y102	16
	3	E47,G48,G49,G50,G51,G52,S53,N54,Y55,S56,P57,S58,R59,E60,D61,Q64,R65,G66,G67,G68,G69,S70,Y71,S72,G84,G85,G86,G87,S88,D89,A90	31
VP7/A	1	G49,G50,G51,G52,S53,D54,I55,T56,L57,Y58,Y59,Y60	12
	2	Q61,Q62,T63,D64,E65,A66,N67,K68	8
	3	N28,I30,L31,K32,S33,K34	6
	4	R1,G2,D3,E4,A5,A6,A7,K8,S9,I10,I11,L12,L13,N14,Y15,Y20	16

6.3.10. Docking of vaccine constructs with receptor

Rotavirus entry is a multistep process involving the proteolytic cleavage of spike protein VP4 into two fragments VP5 and VP8, the interaction of these polypeptides and VP7 with integrins (αvβ3) and sialic acid including heat shock cognate protein [43,85]. Modeled and refined structures of vaccine constructs was used for molecular docking with integrin receptors using ClusPro v.2.0 docking program (www.cluspro.bu.edu) with default settings [53]. The interacting residues of four vaccine constructs with integrin receptor chain A and B is summarized in Table 6.13. All the four vaccine models have shown interactions with chain A of integrin subunit (αIIbβ3 and αVβ3) receptors (Figure 6.12) that are well known to mediate the entry of rotavirus involving VP4 and VP7 surface proteins [43,85].
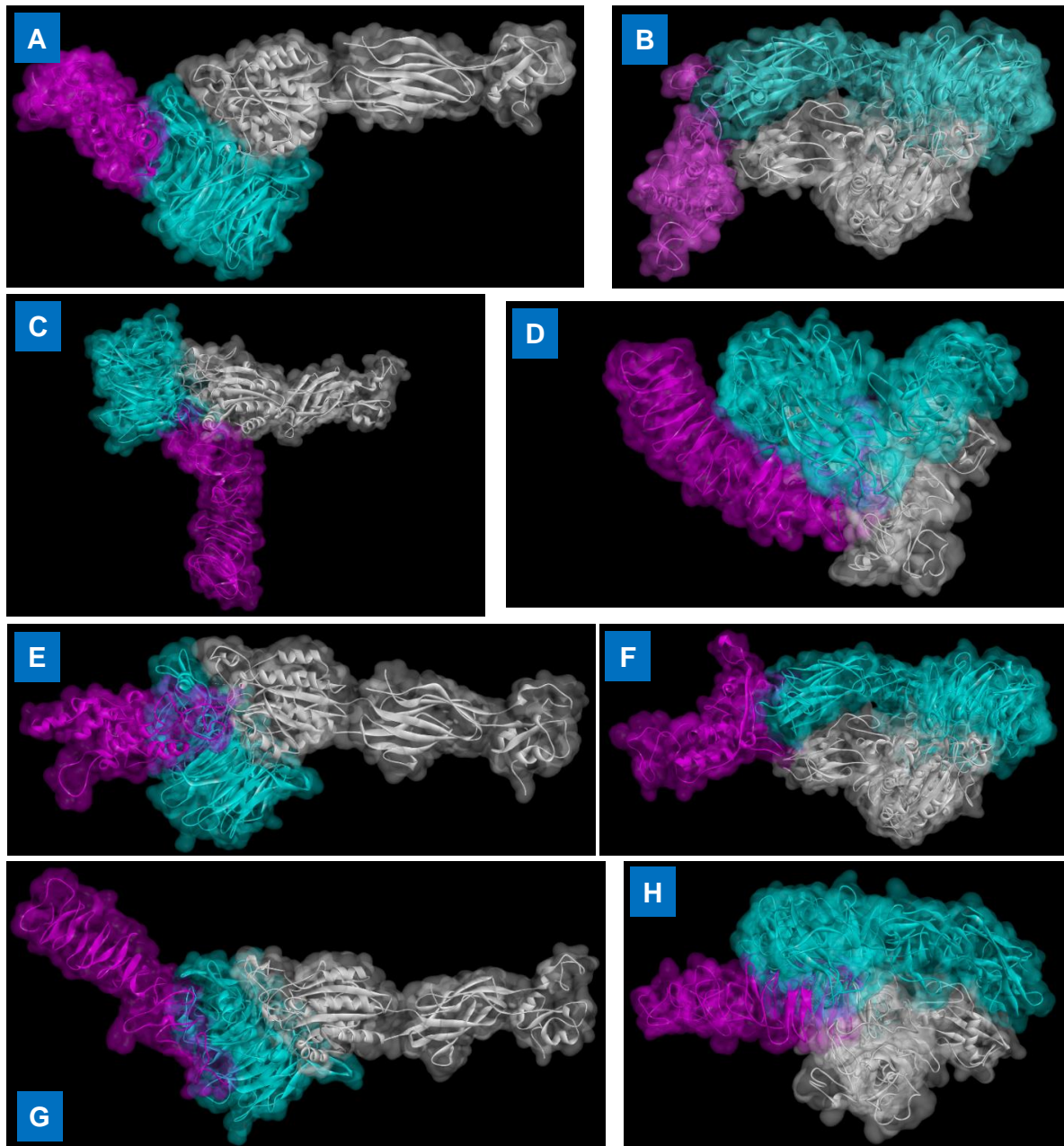
Figure 6.12. Docked complex of multi-subunit vaccine constructs with integrin receptor. A. Construct1 interaction with αIIbβ3 B. Construct 1 with αVβ3 C. Construct 2 with αIIbβ3 D. Construct 2 with αVβ3 E. Construct 6 with αIIbβ3 F. Construct 6 with αVβ3 G. Construct 7 with αIIbβ3 H. Construct 7 with αVβ3. Integrin receptor chain A and B has been shown in cyan and silver color, respectively, whereas magenta color represents the multi-epitope vaccine constructs in the docked complex.

Table 6.13. A list of interacting residues of docked multi-subunit vaccine constructs with integrin receptor complex

Vaccine constructs	Integrin receptor	Binding energy (kcal mol⁻¹)		Interacting residues of vaccine constructs	
		Integrin receptor chain A	Integrin receptor chain B	A	B
Construct 1	αIIbβ3 (PDB ID: 2vdp)	-10.8	0	GLU75, ARG76, TYR145, VAL146, GLU147, THR148, ALA149,THR152, GLN220, PHE216, TRP218, GLU219, THR221, VAL227, ALA228,	-
Construct 1	αVβ3 (PDB ID: 4O02)	-8.5	-6.0	LEU9, GLU13, TYR20, THR21, ILE22, ASN23, THR38, ARG49, LEU50, SER51, ARG67	GLN53, MET55, ARG56, LYS58, ALA228
Construct 2	αIIbβ3 (PDB ID: 2vdp)	-9.4	-8.1	GLU4, ALA5, LYS8, SER9, ILE10, LEU12, LEU17, ALA18, TYR20, GLU25	LEU12, LEU13, TYR15, LEU17, ARG26, PHE27, SER28, TYR34, ASN59,
Construct 2	αVβ3 (PDB ID: 4O02)	-14.7	-10.4	ASP3, ALA31, TYR32, LYS35, LYS57, LYS58, ILE119, GLY120, GLY121, TRP125, GLY153, GLY171	LYS8, SER9, ILE11, ILE12, TYR20, GLU25, ARG26, LYS42
Construct 6	αIIbβ3 (PDB ID: 2vdp)	-11.1	-6.7	GLY23, GLY24, GLY25, SER26, TRP27, LEU29, ARG33, ARG35, ASN51, GLN53, GLY115, ASP141, GLU144, GLN145, HIS148, ARG149	LEU29, ASN31, ARG32
Construct 6	αVβ3 (PDB ID: 4O02)	-10.5	-7.1	ARG1, TYR81, TYR91, GLY148, LYS162, PHE186, PRO187, TRP188, LEU192, TYR195, ALA198, GLU200,	ASN80, TYR81, GLU83, ARG86
Construct 7	αIIbβ3 (PDB ID: 2vdp)	-20.1	0	GLY2, GLU4, ALA6, ALA7, ARG9, ARG15, ALA16, ALA18, ASN19, ASP21, GLY22, GLY25, TYR38, ILE39, GLY40, GLY41, SER44, TRP45, SER59, PRO60, ILE62, VAL63, THR64, GLU65, ALA66, GLN77, THR79,	-
Construct 7	αVβ3 (PDB ID: 4O02)	-14.4	-7.4	ARG132, ASP134, SER148, ASP149, GLN152, GLU167, ARG170, LYS185, ARG186, GLN206, LYS225, TRP226, TRP227, VAL229,	SER198, GLU210, LYS224, GLN228

6.3.11. Functional validations of predicted B- and T-cell epitopes based on published literature

Immunoinformatic approaches have commonly been used to identify potential B and T-cell epitopes that can help to induce humoral and cell-mediated immune responses. Neutralizing antibodies to VP4 and VP7 proteins are known to induce immunity against RV in natural infection in humans [8,86], anti-VP6 antibodies and CD4+ T cells have also been implicated in immune protection [87,88]. In this work we have identified a total of 4 linear B-cell epitopes, of which two linear epitopes (aa117-128 and aa144-155) and 2 conformational B-cell epitopes (aa151-159, aa157-167) forms a part of secreted soluble form of NSP4 (Table 6.2 and 6.4, Table 6.3a and 6.3b). It was previously shown that the secreted form of NSP4 (aa112–175) during rotavirus- infected cells was characterized as an enterotoxin of rotavirus protein. In a previous study, an antibody to NSP4 aa112-175 was found to reduce the occurrence and severity of rotavirus-induced diarrhoea in suckling mice pups [89]. It has been previously shown that a peptide (aa266-326) derived from VP7 can permeabilize artificial membranes leading to subsequent replication in virus-infected cells [90]. In silico analysis of rotavirus VP7 revealed the presence of potential linear (aa308-320), conformational B-cell (aa286-295) and CTL (aa316-324) epitopes in the membrane permeabilization domain (Table 6.3a and 6.3b). Antibody to such peptides might block membrane crossing by non-enveloped rotavirus during infection. Rotavirus VP7 protein has well defined antigenic epitopes namely 7-1 and 7-2. 7-1 epitope is subdivided into 7-1a and 7-1b [91]. Region 7-1 that spans the inter-subunit boundary is reported as an immunodominant epitope. Antibodies that target region 7-1 of VP7 probably neutralized entry of rotavirus through stabilization of VP7 trimer and inhibition of uncoating signal required for VP4 structural rearrangement [91]. Cytotoxic T lymphocytes specific to rotavirus is reported to play an important role in the clearance of rotavirus infection. Rotavirus VP7 protein was shown to induce a class I MHC-restricted CTL response and the CTL epitopes (aa5-13, aa8-16 and aa31-40) were mapped to H1 and H2 signal sequence of protein [92]. Using immunoinformatic tools we have identified and mapped CTL (aa15-23) and HTL (aa13-25) epitopes that were previously characterized as MHC class I epitopes of VP7 (Table 6.4). It has been shown that a synthetic peptide containing aa642 to 658 of VP5 can compete with the binding of the RRV to the heat shock cognate protein, HSC70 [93]. The VP5* subunit (aa308-310) of cleaved fragment of VP4 spike protein contains the α2β1 integrin (Asp-Gly-Glu)

binding motif [94]. Synthetic peptides or antibodies to the regions spanning the predicted conformational (aa413-424) and linear B-cell epitope (aa657-667) of VP5 might provide a steric hindrance to rotavirus particle that uses α2β1 integrin as a receptor during entry (Table 6.4). VP6 protein is the most abundant and highly conserved group specific antigen of rotavirus. The sequence between amino acid residues 48 to 75 of VP6 has previously been characterized as immunodominant based on reactivity of monoclonal antibodies [95]. In the present study, we have identified aa68-81 as potential HTL epitope spanning the previously predicted antibody binding epitope of VP6 protein (Table 6.6a). In a previous study a synthetic peptide comprising of 14-amino acid spanning the region aa289-302 (RLSFQLVRPPNMTP) of VP6 protein was found to provide complete protection of mice against oral challenge of rotavirus [95]. Intriguingly, we predicted a 13-mer peptide (aa284-296) as potential HTL epitope of VP6 with a high conservancy (92%) among different rotavirus strains (Table 6.4).

VP4 and VP7 proteins are the primary targets of vaccine development and neutralizing antibodies against VP4 and VP7 proteins do not prevent rotavirus reinfection suggesting the possible role of other structural and nonstructural proteins. Previous literature has observed the presence of NSP2-specific IgA and IgG antibodies in more than 75% of naturally rotavirus infected children [96]. The region of NSP2 that interacts with NSP5 protein include the C-terminal α-helix, the loop between aa 291 and 302, the loops between aa 64 to 68 and aa 179 to 183 and the helix between residues 232 and 251 [97]. Using phage display, antibody-binding epitope aa244-252 has been mapped to the region on NSP2 protein known to interact with NSP5 during viroplasm formation in virus-infected cells [98]. NSP2 aa298–312 (linear epitope) and aa298-313 (conformational B-cell epitope) predicted as B-cell epitope with a conservancy of around 89% (Table 6.2, Table 6.3a and 6.3b) might be useful for further experimental validations. The highly conserved C-terminal domain of rotavirus phosphoprotein NSP5 is required for viroplasm-like structure formation and is important for insolubility and hyperphosphorylation during rotavirus replication [99]. The findings of present in silico analysis revealed the presence of four overlapping HTL epitopes corresponding to NSP5 amino acid positions, aa175-193 using three independent prediction tools (Table 6.6b). NSP5 aa170-183 and aa173-184 that have been found to contain predicted linear and conformational B-cell epitope, respectively, this region of NSP5 is also predicted as HTL epitopes (Table 6.3a and 6.3b). Similarly, NSP5 aa2-10 (9-mer peptide) was predicted as

CTL epitope, while the aa19-36 and aa66-85 of N-terminal region of NSP5 protein was predicted as conformational B-cell epitopes (Table 6.3b). Interestingly, N- (aa1–33) and C-terminal region (aa 131–198) of NSP5 was previously shown to involved in interaction with NSP2 during rotavirus infection [100]. Rotavirus NSP2 and NSP5 are required for viroplasm formation and targeting both proteins may provide therapeutic implications during rotavirus-infected cells.

6.3.12. Codon optimization, synthesis, expression, and affinity purification of chimeric constructs in *E. coli*

The vaccine construct was codon optimized as per E. coli (Strain ATCC 27325/DSM 5911/W3110/K12K12) strain using JCAT server and we found GC content of vaccine constructs 1 to 10 as 45.87%, 48.93%, 48.38%, 45.98%, 47.57%, 52.24%, 51.45, 47.67, 50.49 and 46.19%, respectively. GC content observed was in the range of 30–70% suggesting a minimal impact on transcriptional and translational efficiency. The value of codon adaptive index (CAI) for all vaccine constructs was 1 which is considered as good and satisfactory.

Of the 10 multi-subunit vaccines chimeric antigens designed, four constructs namely, construct 1, construct 2, construct 6 and construct 7 (Table 6.9) have been synthesized and cloned into champion pET directional TOPO expression system (pET100/D-TOPO) (Figure 6.13B) using manufacturer instructions (Thermofischer Scientific). The recombinant clones were verified by PCR using gene specific primers (Figure 6.13A). We found optimum expression and solubility of N-terminal 6xHis-tagged multisubunit chimeric antigens induced with 200 µM concentration of IPTG at 25°C temperature for 16 h (Figure 6.13C). Silver stained-SDS-PAGE gel electrophoresis confirmed the homogeneity of affinity purified chimeric proteins (Figure 6.14A-C) and different concentrations of BSA was loaded to determine the approximate concentration of purified proteins estimated using Bradford assay (Figure 6.15). The yield for 100 ml culture of construct 1, 2, 6 and 7 were 2.59 mg, 5.93 mg, 2.75 mg and 3.1 mg, respectively.
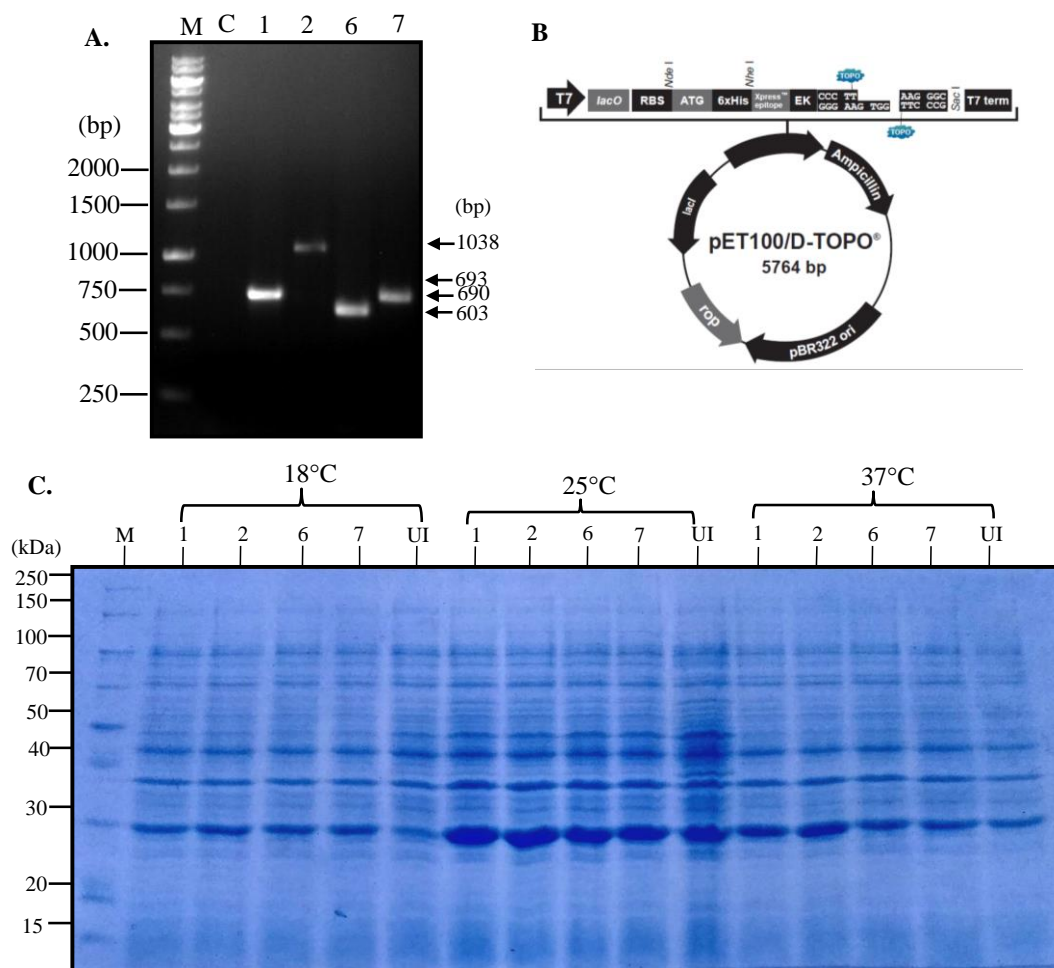
Figure 6.13. Cloning, expression, and affinity purification of four chimeric constructs in E. coli. A) Confirmation of recombinant clones using PCR. Construct 1 (expected gene size 693 bp); Construct 2 (expected gene size 837 bp with 201 bp from vector sequence due to use of T7 forward primer), Construct 6 (expected gene size 603 bp) and Construct 7 (expected gene size 690 bp) were synthesized and cloned into champion pET directional TOPO expression vector (pET100/D-TOPO). C: Negative control without template DNA; M: GeneRuler 1 kb DNA ladder (SM0311, Thermo Scientific). B) pET100/D-TOPO vector map, C) SDS-PAGE analysis showing the expression of recombinant chimeric proteins induced with IPTG (200 µM) at 18ºC, 25ºC and 37ºC induction temperature. Construct 1 (expected size 28.9 kDa including tag); Construct 2 (expected size 34 kDa including tag); Construct 6 (expected size 28.9 kDa including tag); Construct 7 (expected size 34 kDa including tag); UI: uninduced E. coli whole cell lysates.

A.

M : Protein Marker
UI : Uninduced
SO : Soluble Fraction
IN/S : Insoluble Supernatant
IN/P : Insoluble Pellet
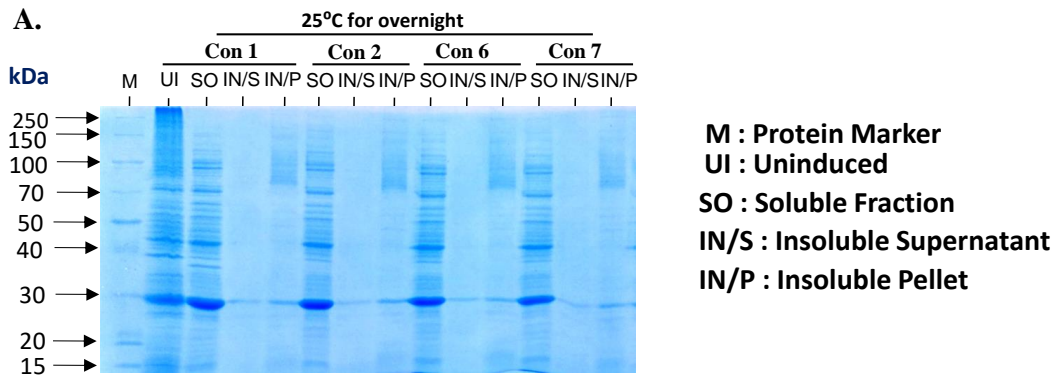
B.

Recombinant antigens	Size (kDa)	Size of extra length (kDa)	Total size (kDa)	Conc. of protein estimated (ng/µl) for 100 µl elution		
				Elute 1	Elute 2	Elute 3
Construct 1	24.77	4.143	28.913	70.08	64.60	60.00
Construct 2	30.10		34.243	60.00	95.6	36.6

Con 1 (28.913 KDa)   Con 2 (34.243 KDa)
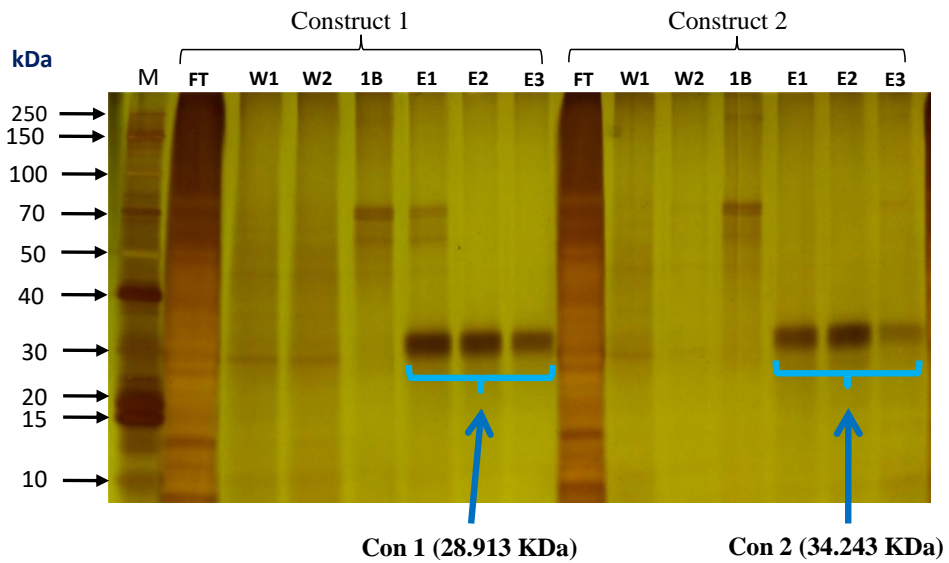
C.

Recombinant antigens	Size (kDa)	Size of extra length (kDa)	Total Size (kDa)	Conc. of protein estimated (ng/µl) for 100 µl elution		
				Elute 1	Elute 2	Elute 3
Construct 6	20.64	4.143	24.783	63.00	86.40	41.20
Construct 7	24.04		28.183	49.00	111.2	16.4

Con 6 (24.783 kDa)   **Con 7 (28.183 kDa)**
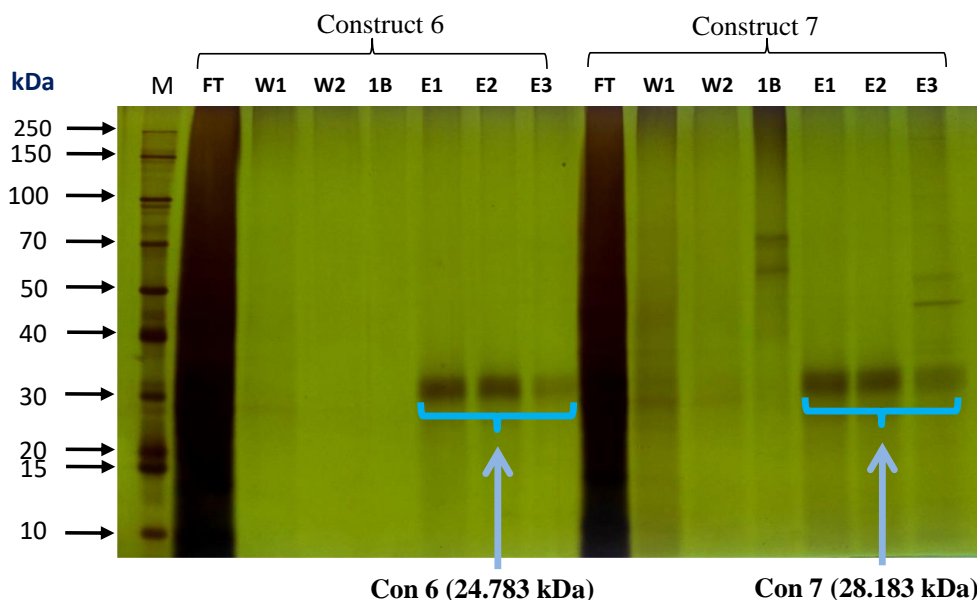
Figure 6.14. A. Analysis of recombinant protein in soluble and insoluble fractions of bacterial whole cell lysate. SDS-PAGE analysis showing the expressed recombinant chimeric proteins induced with IPTG (200 µM) at 25ºC in soluble fraction. Construct 1 (expected size 28.9 kDa including tag); Construct 2 (expected size 34 kDa including tag); Construct 6 (expected size 28.9 kDa including tag); Construct 7 (expected size 34 kDa including tag); M: Protein Marker, UI: uninduced E. coli whole cell lysates, SO: Soluble fraction, IN/S: Insoluble Supernatant, IN/P: Insoluble Pellet, **B. Purification of soluble protein by Ni-NTA affinity chromatography and confirmation by SDS-PAGE followed by silver staining**. Construct 1 (expected size 28.9 kDa including tag); Construct 2 (expected size 34 kDa including tag); Construct 6 (expected size 28.9 kDa including tag); Construct 7 (expected size 34 kDa including tag); M: Protein Marker, FT: Flow Through, W1: First Wash, W2: Second Wash, E1, E2 and E3: First, second and third elute. Inset table: Expected size of construct 1 & 2 and concentration of protein estimated (ng/µl) for 100 µl elution, C**. Purification of soluble protein by Ni-NTA affinity chromatography and confirmation by SDS-PAGE followed by silver staining.** Construct 1 (expected size 28.9 kDa including tag); Construct 2 (expected size 34 kDa including tag); Construct 6 (expected size 28.9 kDa including tag); Construct 7 (expected size 34 kDa including tag); M: Protein Marker, FT: Flow Through, W1: First Wash, W2: Second Wash, E1, E2 and E3: First, second and third elute. Inset table: Expected size of construct 6 & 7 and concentration of protein estimated (ng/µl) for 100 µl elution.
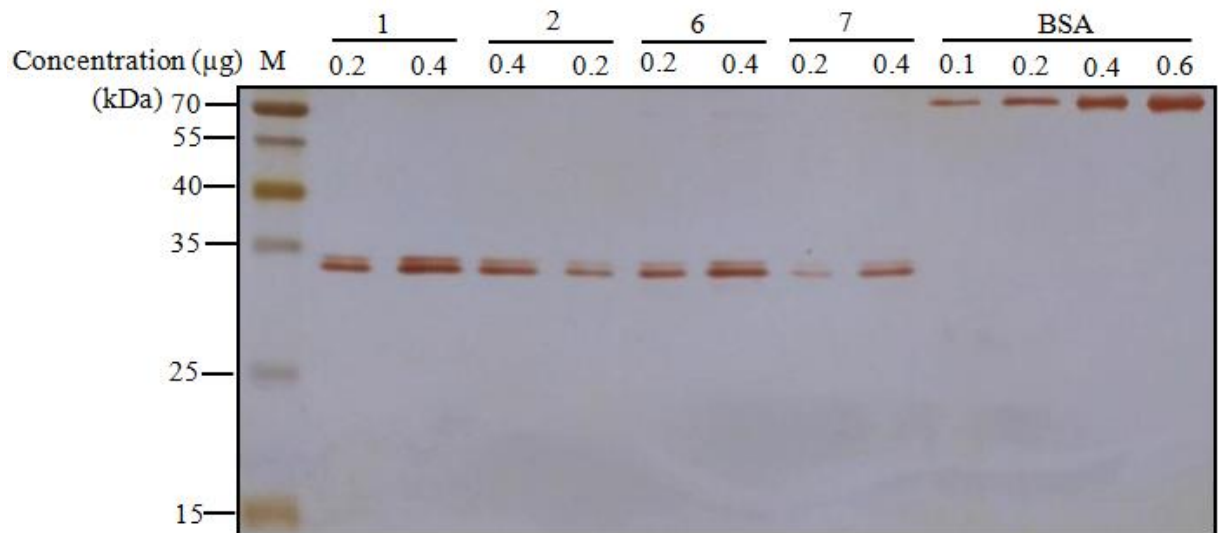
Figure 6.15. Silver stained-SDS-PAGE gel electrophoresis showing the purity of multi-epitope antigens. Different concentrations of BSA were loaded to determine the approximate concentration of purified proteins estimated using Bradford assay. M: Prestained protein ladder (Cat. 26616, ThermoScientific).

6.4. Conclusions

In this study, we have predicted and identified immuno-dominant antigenic fragments derived from 9 protein sequences of rotavirus structural (VP2, VP3, VP4, VP6 and VP7) and non-structural proteins (NSP2, NSP3, NSP4 and NSP5) that might have the abilities to induce immunity against rotavirus infection. As a part of our thesis work we have cloned and expressed the multi-epitope vaccine prototype constructs in *E. coli* and need to be experimentally validated for further use. Although the findings of present study are mainly based on computational prediction algorithms, but the immune epitopes presented herein will provide a platform for future experimental validations that may help to design peptide-based vaccine and diagnostic assay against rotavirus.

6.5. Bibliography

[1] Tate, J. E., Burton, A. H., Boschi-Pinto, C., Parashar, U. D., & World Health Organization–Coordinated Global Rotavirus Surveillance Network (2016). Global, Regional, and National Estimates of Rotavirus Mortality in Children <5 Years of Age, 2000-2013. *Clinical infectious diseases*, 62(2):S96–S105. https://doi.org/10.1093/cid/civ1013.

[2] Ruiz-Palacios, G. M., Pérez-Schael, I., Velázquez, F. R., Abate, H., Breuer, T., Clemens, S. C., Cheuvart, B., Espinoza, F., Gillard, P., Innis, B. L., Cervantes, Y., Linhares, A. C., López, P., Macías-Parra, M., Ortega-Barría, E., Richardson, V., Rivera-Medina, D. M., Rivera, L., Salinas, B., Pavía-Ruz, N., … Human Rotavirus Vaccine Study Group (2006). Safety and efficacy of an attenuated vaccine against severe rotavirus gastroenteritis. *The New England journal of medicine*, 354(1):11–22. https://doi.org/10.1056/NEJMoa052434.

[3] Vesikari, T., Matson, D. O., Dennehy, P., Van Damme, P., Santosham, M., Rodriguez, Z., Dallas, M. J., Heyse, J. F., Goveia, M. G., Black, S. B., Shinefield, H. R., Christie, C. D., Ylitalo, S., Itzler, R. F., Coia, M. L., Onorato, M. T., Adeyi, B. A., Marshall, G. S., Gothefors, L., Campens, D.,Rotavirus Efficacy and Safety Trial (REST) Study Team (2006). Safety and efficacy of a pentavalent human-bovine (WC3) reassortant rotavirus vaccine. *The New England journal of medicine*, 354(1):23–33. https://doi.org/10.1056/NEJMoa052664.Rose, J., Hawthorn, R. L., Watts, B., & Singer, M. E. (2009). Public health impact and cost effectiveness of mass vaccination with live

[4] human rotavirus vaccine (RIX4414) in India: model-based analysis. *BMJ (Clinical research ed.)*, 339:b3653. https://doi.org/10.1136/bmj.b3653.

[5] Rose, J., Homa, L., Meropol, S. B., Debanne, S. M., Bielefeld, R., Hoyen, C., & Singer, M. E. (2017). Health impact and cost-effectiveness of a domestically-produced rotavirus vaccine in India: A model based analysis. *PloS one*, 12(11):e0187446. https://doi.org/10.1371/journal.pone.0187446.

[6] Vesikari, T., Van Damme, P., Giaquinto, C., Dagan, R., Guarino, A., Szajewska, H., & Usonis, V. (2015). European Society for Paediatric Infectious Diseases consensus recommendations for rotavirus vaccination in Europe: update 2014. *The Pediatric infectious disease journal*, 34(6):635–643. https://doi.org/10.1097/INF.0000000000000683.

[7] Madhi SA, Cunliffe NA, Steele D, Witte D, Kirsten M, Louw C, Ngwira B, Victor JC, Gillard PH, Cheuvart BB, Han HH, Neuzil KM (2016). Effect of human rotavirus vaccine on severe diarrhea in African infants. *Malawi Med J*, 28(3):108-114.

[8] Zaman K, Sack DA, Neuzil KM, Yunus M, Moulton LH, Sugimoto JD, Fleming JA, Hossain I, Arifeen SE, Azim T, Rahman M, Lewis KDC, Feller AJ, Qadri F, Halloran ME, Cravioto A, Victor JC (2017). Effectiveness of a live oral human

rotavirus vaccine after programmatic introduction in Bangladesh: A cluster-randomized trial. *PLoS Med*, 14(4):e1002282. https://doi.org/10.1371/journal.pmed.1002282.

[9] Bhandari, N., Rongsen-Chandola, T., Bavdekar, A., John, J., Antony, K., Taneja, S., Goyal, N., Kawade, A., Kang, G., Rathore, S. S., Juvekar, S., Muliyil, J., Arya, A., Shaikh, H., Abraham, V., Vrati, S., Proschan, M., Kohberger, R., Thiry, G., Glass, R., India Rotavirus Vaccine Group (2014). Efficacy of a monovalent human-bovine (116E) rotavirus vaccine in Indian infants: a randomised, double-blind, placebo-controlled trial. *Lancet*, 383(9935):2136–2143. https://doi.org/10.1016/S0140-6736(13)62630-6.

[10] Bhandari N, Rongsen-Chandola T, Bavdekar A, John J, Antony K, Taneja S, Goyal N, Kawade A, Kang G, Rathore SS, Juvekar S, Muliyil J, Arya A, Shaikh H, Abraham V, Vrati S, Proschan M, Kohberger R, Thiry G, Glass R, Greenberg HB, Curlin G, Mohan K, Harshavardhan GV, Prasad S, Rao TS, Boslego J, Bhan MK (2014). India Rotavirus Vaccine Group. Efficacy of a monovalent human-bovine (116E) rotavirus vaccine in Indian infants: a randomised, double-blind, placebo-controlled trial. *Lancet*, 383:2136–2143. https://10.1016/S0140-6736(13)62630-6.

[11] Naik, S. P., Zade, J. K., Sabale, R. N., Pisal, S. S., Menon, R., Bankar, S. G., Gairola, S., & Dhere, R. M. (2017). Stability of heat stable, live attenuated Rotavirus vaccine (ROTASIIL®). Vaccine, 35(22):2962–2969. https://doi.org/10.1016/j.vaccine.2017.04.025.

[12] Kulkarni, P. S., Desai, S., Tewari, T., Kawade, A., Goyal, N., Garg, B. S., Kumar, D., Kanungo, S., Kamat, V., Kang, G., Bavdekar, A., Babji, S., Juvekar, S., Manna, B., Dutta, S., Angurana, R., Dewan, D., Dharmadhikari, A., Zade, J. K., Dhere, R. M., … SII BRV-PV author group (2017). A randomized Phase III clinical trial to assess the efficacy of a bovine-human reassortant pentavalent rotavirus vaccine in Indian infants. *Vaccine*, 35(45):6228–6237. https://doi.org/10.1016/j.vaccine.2017.09.014.

[13] Isanaka, S., Guindo, O., Langendorf, C., Matar Seck, A., Plikaytis, B. D., Sayinzoga-Makombe, N., McNeal, M. M., Meyer, N., Adehossi, E., Djibo, A., Jochum, B., & Grais, R. F. (2017). Efficacy of a Low-Cost, Heat-Stable Oral Rotavirus Vaccine in Niger. The New England Journal of Medicine, 376(12):1121–1130. https://doi.org/10.1056/NEJMoa1609462.

[14] Ogden, K. M., Tan, Y., Akopov, A., Stewart, L. S., McHenry, R., Fonnesbeck, C. J., Piya, B., Carter, M. H., Fedorova, N. B., Halpin, R. A., Shilts, M. H., Edwards, K. M., Payne, D. C., Esona, M. D., Mijatovic-Rustempasic, S., Chappell, J. D., Patton, J. T., Halasa, N. B., & Das, S. R. (2018). Multiple Introductions and Antigenic Mismatch with Vaccines May Contribute to Increased Predominance of G12P[8] Rotaviruses in the United States. Journal of virology, 93(1):e01476-18. https://doi.org/10.1128/JVI.01476-18.

[15] Burnett, E., Parashar, U., & Tate, J. (2018). Rotavirus Vaccines: Effectiveness, Safety, and Future Directions. Paediatric drugs, 20(3):223–233. https://doi.org/10.1007/s40272-018-0283-3.

[16] Kassim, P., & Eslick, G. D. (2017). Risk of intussusception following rotavirus vaccination: An evidence based meta-analysis of cohort and case-control studies. Vaccine, 35(33):4276–4286. https://doi.org/10.1016/j.vaccine.2017.05.064.

[17] Parashar, U. D., Cortese, M. M., Payne, D. C., Lopman, B., Yen, C., & Tate, J. E. (2015). Value of post-licensure data on benefits and risks of vaccination to inform vaccine policy: The example of rotavirus vaccines. Vaccine, 33(4):D55–D59. https://doi.org/10.1016/j.vaccine.2015.05.094.

[18] Simonsen, L., Viboud, C., Elixhauser, A., Taylor, R. J., & Kapikian, A. Z. (2005). More on RotaShield and intussusception: the role of age at the time of vaccination. The Journal of infectious diseases, 192(1):S36–S43. https://doi.org/10.1086/431512.

[19] Nascimento, I. P., & Leite, L. C. (2012). Recombinant vaccines and the development of new vaccine strategies. Brazilian journal of medical and biological research = Revista brasileira de pesquisas medicas e biologicas, 45(12):1102–1111. https://doi.org/10.1590/s0100-879x2012007500142.

[20] Oyarzún, P., & Kobe, B. (2016). Recombinant and epitope-based vaccines on the road to the market and implications for vaccine design and production. Human vaccines & immunotherapeutics, 12(3):763–767. https://doi.org/10.1080/21645515.2015.1094595.

[21] Gouvea, V., Glass, R. I., Woods, P., Taniguchi, K., Clark, H. F., Forrester, B., & Fang, Z. Y. (1990). Polymerase chain reaction amplification and typing of rotavirus nucleic acid from stool specimens. Journal of clinical microbiology, 28(2):276–282. https://doi.org/10.1128/jcm.28.2.276-282.1990.

[22] Taniguchi, K., Wakasugi, F., Pongsuwanna, Y., Urasawa, T., Ukae, S., Chiba, S., &Urasawa, S. (1992). Identification of human and bovine rotavirus serotypes by polymerase chain reaction. *Epidemiology and infection*, 109(2):303–312. https://doi.org/10.1017/s0950268800050263.

[23] Tang, B., Gilbert, J. M., Matsui, S. M., & Greenberg, H. B. (1997). Comparison of the rotavirus gene 6 from different species by sequence analysis and localization of subgroup-specific epitopes using site-directed mutagenesis. *Virology*, 237(1):89–96. https://doi.org/10.1006/viro.1997.8762.

[24] Dyson HJ, Lerner RA, Wright PE (1988). The physical basis for induction of protein-reactive antipeptide antibodies. *Annu Rev BiophysBiophys Chem*, 17:305–324. PMID: 2456075.

[25] Posnett, D. N., McGrath, H., & Tam, J. P. (1988). A novel method for producing anti-peptide antibodies. Production of site-specific antibodies to the T cell antigen receptor beta-chain. *The Journal of biological chemistry*, 263(4):1719–1725.

[26] Simmonds, P., Rose, K. A., Graham, S., Chan, S. W., McOmish, F., Dow, B. C., Follett, E. A., Yap, P. L., & Marsden, H. (1993). Mapping of serotype-specific, immunodominant epitopes in the NS-4 region of hepatitis C virus (HCV): use of type-specific peptides to serologically differentiate infections with HCV types 1, 2, and 3. *Journal of clinical microbiology*, 31(6):1493–1503. https://doi.org/10.1128/jcm.31.6.1493-1503.1993.

[27] Jackwood, M. W., & Hilt, D. A. (1995). Production and immunogenicity of multiple antigenic peptide (MAP) constructs derived from the S1 glycoprotein of infectious bronchitis virus (IBV). *Advances in experimental medicine and biology*, 380:213–219. https://doi.org/10.1007/978-1-4615-1899-0_35.

[28] Saravanan, P., Kumar, S., & Kataria, J. M. (2004). Use of multiple antigenic peptides related to antigenic determinants of infectious bursal disease virus (IBDV) for detection of anti-IBDV-specific antibody in ELISA--quantitative comparison with native antigen for their use in serodiagnosis. *Journal of immunological methods*, 293(1-2):61–70. https://doi.org/10.1016/j.jim.2004.07.001.

[29] Dechamma, H. J., Dighe, V., Kumar, C. A., Singh, R. P., Jagadish, M., & Kumar, S. (2006). Identification of T-helper and linear B epitope in the hypervariable region of nucleocapsid protein of PPRV and its use in the development of specific

antibodies to detect viral antigen. *Veterinary microbiology*, 118(3-4):201–211. https://doi.org/10.1016/j.vetmic.2006.07.023.

[30] Soria-Guerra RE, Nieto-Gomez R, Govea-Alonso DO, Rosales-Mendoza S. An overview of bioinformatics tools for epitope prediction: implications on vaccine development (2015). *J Biomed Inform*, 53:405-14. https://10.1016/j.jbi.2014.11.003.

[31] Schneider FS, Nguyen DL, Castro KL, Cobo S, Machado de Avila RA, Ferreira Nde A, Sanchez EF, Nguyen C, Granier C, Galéa P, Chávez-Olortegui C, Molina F (2014). Use of a synthetic biosensor for neutralizing activity-biased selection of monoclonal antibodies against atroxlysin-I, an hemorrhagic metalloproteinase from Bothropsatrox snake venom. *PLoSNegl Trop Dis*, 8(4):e2826. https://10.1371/journal.pntd.0002826.

[32] Kumar A, Kumar P, Saumya KU, Kapuganti SK, Bhardwaj T, Giri R (2020). Exploring the SARS-CoV-2 structural proteins for multi-epitope vaccine development: an in-silico approach. *Expert Rev Vaccines*, 19(9):887-898. https://10.1080/14760584.2020.1813576.

[33] Kumar Pandey R, Ojha R, Mishra A, Kumar Prajapati V (2018). Designing B- and T-cell multi-epitope based subunit vaccine using immunoinformatics approach to control Zika virus infection. *J Cell Biochem*, 119(9):7631-7642. https://10.1002/jcb.27110.

[34] Ojha R, Pareek A, Pandey RK, Prusty D, Prajapati VK (2019). Strategic Development of a Next-Generation Multi-Epitope Vaccine To Prevent Nipah Virus Zoonotic Infection. *ACS Omega*, 4(8):13069-13079. https://10.1021/acsomega.9b00944.

[35] Ansari HR, Raghava GP (2010). Identification of conformational B-cell Epitopes in an antigen from its primary sequence. *Immunome Res*, 6:6. https://10.1186/1745-7580-6-6.

[36] S. Saha, G.P.S. Raghava (2004). BcePred: prediction of continuous B-cell epitopes inantigenic sequences using physico-chemical properties, in: G. Nicosia, V. Cutello,P.J. Bentley, J. Timmis (Eds.), *Artificial Immune Systems. ICARIS, Lecture Notes in Computer Science*, 3239, pages 197–204, Springer, Berlin, Heidelberg.

[37] Kringelum JV, Lundegaard C, Lund O, Nielsen M (2012). Reliable B cell epitope predictions: impacts of method development and improved benchmarking. *PLoSComput Biol*, 8(12):e1002829. https://10.1371/journal.pcbi.1002829.

[38] Liang S, Zheng D, Standley DM, Yao B, Zacharias M, Zhang C (2010). EPSVR and EPMeta: prediction of antigenic epitopes using support vector regression and multiple server results. *BMC Bioinformatics*, 11:381. https://10.1186/1471-2105-11-381.

[39] Khatoon N, Pandey RK, Prajapati VK (2017). Exploring Leishmania secretory proteins to design B and T cell multi-epitope subunit vaccine using immunoinformatics approach. *Sci Rep*, 7(1):8285. https://10.1038/s41598-017-08842-w.

[40] Tenzer S, Peters B, Bulik S, Schoor O, Lemmel C, Schatz MM, Kloetzel PM, Rammensee HG, Schild H, Holzhütter HG (2005). Modeling the MHC class I pathway by combining predictions of proteasomal cleavage, TAP transport and MHC class I binding. *Cell Mol Life Sci*, 62(9):1025-37. https://10.1007/s00018-005-4528-2.

[41] Dhanda SK, Karosiene E, Edwards L, Grifoni A, Paul S, Andreatta M, Weiskopf D, Sidney J, Nielsen M, Peters B, Sette A (2018). Predicting HLA CD4 Immunogenicity in Human Populations. *Front Immunol*, 9:1369. https://10.3389/fimmu.2018.01369.

[42] Dimitrov I, Flower DR, Doytchinova I (2013). AllerTOP--a server for in silico prediction of allergens. *BMC Bioinformatics*, 14(6):S4. https://10.1186/1471-2105-14-S6-S4.

[43] Guerrero CA, Méndez E, Zárate S, Isa P, López S, Arias CF (2000). Integrin alpha(v)beta(3) mediates rotavirus cell entry. *Proc Natl Acad Sci U S A*. 97(26):14644-9. https://10.1073/pnas.250299897.

[44] Bhasin M, Raghava GP (2007). A hybrid approach for predicting promiscuous MHC class I restricted T cell epitopes. *J Biosci*, 32(1):31-42. https://10.1007/s12038-007-0004-5.

[45] Reche PA, Glutting JP, Reinherz EL (2002). Prediction of MHC class I binding peptides using profile motifs. *Hum Immunol*, 63(9):701-9. https://10.1016/s0198-8859(02)00432-9.

[46] Singh H, Raghava GP (2001). ProPred: prediction of HLA-DR binding sites. *Bioinformatics*, 17(12):1236-7. https://10.1093/bioinformatics/17.12.1236.

[47] González-Galarza FF, Takeshita LY, Santos EJ, Kempson F, Maia MH, da Silva AL, Teles e Silva AL, Ghattaoraya GS, Alfirevic A, Jones AR, Middleton D (2015). Allele frequency net 2015 update: new features for HLA epitopes, KIR and disease and HLA adverse drug reaction associations. *Nucleic Acids Res*, 43(Database issue):D784-8. https://10.1093/nar/gku1166.

[48] Cao K, Hollenbach J, Shi X, Shi W, Chopek M, Fernández-Viña MA (2001). Analysis of the frequencies of HLA-A, B, and C alleles and haplotypes in the five major ethnic groups of the United States reveals high levels of diversity in these loci and contrasting distribution patterns in these populations. *Hum Immunol*, 62(9):1009-30. https://10.1016/s0198-8859(01)00298-1.

[49] Schipper RF, van Els CA, D'Amaro J, Oudshoorn M (1996). Minimal phenotype panels. A method for achieving maximum population coverage with a minimum of HLA antigens. *Hum Immunol*, 51(2):95-8. https://10.1016/s0198-8859(96)00138-3.

[50] Andreatta M, Karosiene E, Rasmussen M, Stryhn A, Buus S, Nielsen M (2015). Accurate pan-specific prediction of peptide-MHC class II binding affinity with improved binding core identification. *Immunogenetics*, 67(11-12):641-50. https://10.1007/s00251-015-0873-y.

[51] Weiskopf D, Angelo MA, de Azeredo EL, Sidney J, Greenbaum JA, Fernando AN, Broadwater A, Kolla RV, De Silva AD, de Silva AM, Mattia KA, Doranz BJ, Grey HM, Shresta S, Peters B, Sette A (2013). Comprehensive analysis of dengue virus-specific responses supports an HLA-linked protective role for CD8+ T cells. *Proc Natl Acad Sci U S A*, 110(22):E2046-53. https://10.1073/pnas.1305227110.

[52] Calis JJ, Maybeno M, Greenbaum JA, Weiskopf D, De Silva AD, Sette A, Keşmir C, Peters B (2013). Properties of MHC class I presented peptides that enhance immunogenicity. *PLoSComput Biol*, 9(10):e1003266. https://10.1371/journal.pcbi.1003266.

[53] Paul S, LindestamArlehamn CS, Scriba TJ, Dillon MB, Oseroff C, Hinz D, McKinney DM, Carrasco Pro S, Sidney J, Peters B, Sette A (2015). Development and validation of a broad scheme for prediction of HLA class II restricted T cell epitopes. *J Immunol Methods*, 422:28-34. https://10.1016/j.jim.2015.03.022.

[54] Bui HH, Sidney J, Li W, Fusseder N, Sette A (2007). Development of an epitope conservancy analysis tool to facilitate the design of epitope-based diagnostics and vaccines. *BMC Bioinformatics*, 8:361. https://10.1186/1471-2105-8-361.

[55] Shen Y, Maupetit J, Derreumaux P, Tufféry P (2014). Improved PEP-FOLD Approach for Peptide and Miniprotein Structure Prediction. *J Chem Theory Comput*, 10(10):4745-58. https://10.1021/ct500592m.

[56] Kozakov D, Hall DR, Xia B, Porter KA, Padhorny D, Yueh C, Beglov D, Vajda S (2017). The ClusPro web server for protein-protein docking. *Nat Protoc*, 12(2):255-278. https://10.1038/nprot.2016.169.

[57] Xue LC, Rodrigues JP, Kastritis PL, Bonvin AM, Vangone A (2016). PRODIGY: a web server for predicting the binding affinity of protein-protein complexes. *Bioinformatics*, 32(23):3676-3678. https://10.1093/bioinformatics/btw514.

[58] Muñoz V, Serrano L (1994). Elucidating the folding problem of helical peptides using empirical parameters. *Nat Struct Biol*, 1(6):399-409. https://10.1038/nsb0694-399.

[59] Gasteiger E, Hoogland C, Gattiker A, Duvaud S, Wilkins MR, Appel RD and Bairoch A (2005) Protein Identification and Analysis Tools on the ExPASy Server. In: Walker J.M. (eds) *The Proteomics Protocols Handbook,* pages 571-607. Humana Press. https://doi.org/10.1385/1-59259-890-0:571.

[60] McGuffin LJ, Bryson K, Jones DT (2000). The PSIPRED protein structure prediction server. *Bioinformatics*, 16(4):404-5. https://10.1093/bioinformatics/16.4.404.

[61] Roy A, Kucukural A, Zhang Y (2010). I-TASSER: a unified platform for automated protein structure and function prediction. *Nat Protoc*, 5(4):725-38. https://10.1038/nprot.2010.5.

[62] Kelley LA, Mezulis S, Yates CM, Wass MN, Sternberg MJ (2015). The Phyre2 web portal for protein modeling, prediction and analysis. *Nat Protoc*, 10(6):845-58. https://10.1038/nprot.2015.053.

[63] Lovell SC, Davis IW, Arendall WB 3rd, de Bakker PI, Word JM, Prisant MG, Richardson JS, Richardson DC (2003). Structure validation by Calpha geometry: phi,psi and Cbeta deviation. *Proteins*, 50(3):437-50. https://10.1002/prot.10286.

[64] Pronk S, Páll S, Schulz R, Larsson P, Bjelkmar P, Apostolov R, Shirts MR, Smith JC, Kasson PM, van der Spoel D, Hess B, Lindahl E (2013). GROMACS 4.5: a

high-throughput and highly parallel open source molecular simulation toolkit. *Bioinformatics*, 29(7):845-54. https://10.1093/bioinformatics/btt055.

[65] Dong Y, Zeng CQ, Ball JM, Estes MK, Morris AP (1997). The rotavirus enterotoxin NSP4 mobilizes intracellular calcium in human intestinal cells by stimulating phospholipase C-mediated inositol 1,4,5-trisphosphate production. *Proc Natl Acad Sci U S A*, 94(8):3960-5. https://10.1073/pnas.94.8.3960.

[66] Ousingsawat J, Mirza M, Tian Y, Roussa E, Schreiber R, Cook DI, Kunzelmann K (2011). Rotavirus toxin NSP4 induces diarrhea by activation of TMEM16A and inhibition of Na+ absorption. *Pflugers Arch*, 461(5):579-89. https://10.1007/s00424-011-0947-0.

[67] Shimabukuro-Vornhagen A, Hallek MJ, Storb RF, von Bergwelt-Baildon MS (2009). The role of B cells in the pathogenesis of graft-versus-host disease. *Blood*, 114(24):4919-27. https://10.1182/blood-2008-10-161638.

[68] Haste Andersen P, Nielsen M, Lund O (2006). Prediction of residues in discontinuous B-cell epitopes using protein 3D structures. *Protein Sci*, 15(11):2558-67. https://10.1110/ps.062405906.

[69] Engelhard VH (1994). Structure of peptides associated with MHC class I molecules. *CurrOpin Immunol*, 6(1):13-23. https://10.1016/0952-7915(94)90028-0.

[70] Li M, Jiang Y, Gong T, Zhang Z, Sun X (2016). Intranasal Vaccination against HIV-1 with Adenoviral Vector-Based Nanocomplex Using Synthetic TLR-4 Agonist Peptide as Adjuvant. *Mol Pharm*, 13(3):885-94. https://10.1021/acs.molpharmaceut.5b00802.

[71] Hynes TR, Kautz RA, Goodman MA, Gill JF, Fox RO (1989). Transfer of a beta-turn structure to a new protein context. *Nature*, 339(6219):73-6. https://10.1038/339073a0.

[72] Yano A, Onozuka A, Matin K, Imai S, Hanada N, Nisizawa T (2003). RGD motif enhances immunogenicity and adjuvanicity of peptide antigens following intranasal immunization. *Vaccine*, 22(2):237-43. https://10.1016/s0264-410x(03)00561-9.

[73] N. Nair, N. Feng, L.K. Blum, M. Sanyal, S. Ding, B. Jiang, A. Sen, J.M. Morton, X.S. He, W.H. Robinson and H.B. Greenberg (2017). VP4- and VP7-specific antibodies mediateheterotypic immunity to rotavirus in humans. *9, Sci. Transl. Med.* 21(395):eaam5434. https://doi.org/10.1126/scitranslmed.aam5434.

[74] Ward R (2009). Mechanisms of protection against rotavirus infection and disease. *Pediatr Infect Dis J*, 28(3):S57-9. https://10.1097/INF.0b013e3181967c16.

[75] Feng N, Lawton JA, Gilbert J, Kuklin N, Vo P, Prasad BV, Greenberg HB (2002). Inhibition of rotavirus replication by a non-neutralizing, rotavirus VP6-specific IgA mAb. *J Clin Invest*, 109(9):1203-13. https://10.1172/JCI14397.

[76] Kirkwood CD, Ma LF, Carey ME, Steele AD (2019). The rotavirus vaccine development pipeline. *Vaccine*, 37(50):7328-7335. https://10.1016/j.vaccine.2017.03.076.

[77] Lappalainen S, Pastor AR, Malm M, López-Guerrero V, Esquivel-Guadarrama F, Palomares LA, Vesikari T, Blazevic V (2015). Protection against live rotavirus challenge in mice induced by parenteral and mucosal delivery of VP6 subunit rotavirus vaccine. *Arch Virol*, 160(8):2075-8. https://10.1007/s00705-015-2461-8.

[78] Ward RL, McNeal MM (2010). VP6: A candidate rotavirus vaccine. *J Infect Dis*, 202 Suppl:S101-7. https://10.1086/653556.

[79] Feng H, Li X, Song W, Duan M, Chen H, Wang T, Dong J (2017). Oral Administration of a Seed-based Bivalent Rotavirus Vaccine Containing VP6 and NSP4 Induces Specific Immune Responses in Mice. *Front Plant Sci*, 8:910. https://10.3389/fpls.2017.00910.

[80] Aiyegbo MS, Sapparapu G, Spiller BW, Eli IM, Williams DR, Kim R, Lee DE, Liu T, Li S, Woods VL Jr, Nannemann DP, Meiler J, Stewart PL, Crowe JE Jr (2013). Human rotavirus VP6-specific antibodies mediate intracellular neutralization by binding to a quaternary structure in the transcriptional pore. *PLoS One*, 8(5):e61101. https://10.1371/journal.pone.0061101.

[81] Caddy SL, Vaysburd M, Wing M, Foss S, Andersen JT, O'Connell K, Mayes K, Higginson K, Iturriza-Gómara M, Desselberger U, James LC (2020). Intracellular neutralisation of rotavirus by VP6-specific IgG. *PLoSPathog*, 16(8):e1008732. https://10.1371/journal.ppat.1008732.

[82] Källberg M, Wang H, Wang S, Peng J, Wang Z, Lu H, Xu J (2012). Template-based protein structure modeling using the RaptorX web server. *Nat Protoc*, 7(8):1511-22. https://10.1038/nprot.2012.085.

[83] Moudgil KD, Deng H, Nanda NK, Grewal IS, Ametani A, Sercarz EE (1996). Antigen processing and T cell repertoires as crucial aleatory features in induction of autoimmunity. *J Autoimmun*, 9(2):227-34. https://10.1006/jaut.1996.0028.

[84] Ponomarenko J, Bui HH, Li W, Fusseder N, Bourne PE, Sette A, Peters B (2008). ElliPro: a new structure-based tool for the prediction of antibody epitopes. *BMC Bioinformatics*, 9:514. https://10.1186/1471-2105-9-514.

[85] Zárate S, Romero P, Espinosa R, Arias CF, López S (2004). VP7 mediates the interaction of rotaviruses with integrin alphavbeta3 through a novel integrin-binding site. *J Virol*, 78(20):10839-47. https://10.1128/JVI.78.20.10839-10847.2004.

[86] Choi AH, McNeal MM, Basu M, Flint JA, Stone SC, Clements JD, Bean JA, Poe SA, VanCott JL, Ward RL (2002). Intranasal or oral immunization of inbred and outbred mice with murine or human rotavirus VP6 proteins protects against viral shedding after challenge with murine rotaviruses. *Vaccine*, 20(27-28):3310-21. https://10.1016/s0264-410x(02)00315-8.

[87] McNeal MM, VanCott JL, Choi AH, Basu M, Flint JA, Stone SC, Clements JD, Ward RL (2002). CD4 T cells are the only lymphocytes needed to protect mice against rotavirus shedding after intranasal immunization with a chimeric VP6 protein and the adjuvant LT(R192G). *J Virol*, 76(2):560-8. https://10.1128/jvi.76.2.560-568.2002.

[88] Zhang M, Zeng CQ, Morris AP, Estes MK (2000). A functional NSP4 enterotoxin peptide secreted from rotavirus-infected cells. *J Virol*, 74(24):11663-70. https://10.1128/jvi.74.24.11663-11670.2000.

[89] Elaid S, Libersou S, Ouldali M, Morellet N, Desbat B, Alves ID, Lepault J, Bouaziz S (2014). A peptide derived from the rotavirus outer capsid protein VP7 permeabilizes artificial membranes. *BiochimBiophys Acta*, 1838(8):2026-35. https://10.1016/j.bbamem.2014.04.005.

[90] Aoki ST, Settembre EC, Trask SD, Greenberg HB, Harrison SC, Dormitzer PR (2009). Structure of rotavirus outer-layer protein VP7 bound with a neutralizing Fab. *Science*, 324(5933):1444-7. https://10.1126/science.1170481.

[91] Buesa J, Raga JV, Colomina J, de Souza CO, Muñoz C, Gil MT (1999). Rotavirus-specific cytotoxic T lymphocytes recognize overlapping epitopes in the amino-terminal region of the VP7 glycoprotein. *Virology*, 257(2):424-37. https://10.1006/viro.1999.9646.

[92] Zárate S, Cuadras MA, Espinosa R, Romero P, Juárez KO, Camacho-Nuez M, Arias CF, López S (2003). Interaction of rotaviruses with Hsc70 during cell entry

is mediated by VP5. *J Virol*, 77(13):7254-60. https://10.1128/jvi.77.13.7254-7260.2003.

[93] Graham KL, Takada Y, Coulson BS (2006). Rotavirus spike protein VP5* binds alpha2beta1 integrin on the cell surface and competes with virus for cell binding and infectivity. *J Gen Virol*, 87(Pt 5):1275-1283. https://10.1099/vir.0.81580-0.

[94] Kohli E, Maurice L, Vautherot JF, Bourgeois C, Bour JB, Cohen J, Pothier P (1992). Localization of group-specific epitopes on the major capsid protein of group A rotavirus. *J Gen Virol*, 73 (Pt 4):907-14. https://10.1099/0022-1317-73-4-907.

[95] Kirkwood CD, Boniface K, Richardson S, Taraporewala ZF, Patton JT, Bishop RF (2008). Non-structural protein NSP2 induces heterotypic antibody responses during primary rotavirus infection and reinfection in children. *J Med Virol*, 80(6):1090-8. https://10.1002/jmv.21160.

[96] Jiang X, Jayaram H, Kumar M, Ludtke SJ, Estes MK, Prasad BV (2006). Cryoelectron microscopy structures of rotavirus NSP2-NSP5 and NSP2-RNA complexes: implications for genome replication. *J Virol*, 80(21):10829-35. https://10.1128/JVI.01347-06.

[97] Donker NC, Foley M, Tamvakis DC, Bishop R, Kirkwood CD (2011). Identification of an antibody-binding epitope on the rotavirus A non-structural protein NSP2 using phage display analysis. *J Gen Virol*, 92(Pt 10):2374-2382. https://10.1099/vir.0.032599-0.

[98] Afrikanova I, Miozzo MC, Giambiagi S, Burrone O (1996). Phosphorylation generates different forms of rotavirus NSP5. *J Gen Virol*, 77 (Pt 9):2059-65. https://10.1099/0022-1317-77-9-2059.

[99] Doytchinova IA, Flower DR (2007). VaxiJen: a server for prediction of protective antigens, tumour antigens and subunit vaccines. *BMC Bioinformatics*, 8:4. https://10.1186/1471-2105-8-4.

[100] Eichwald, C., Rodriguez, J. F., & Burrone, O. R. (2004). Characterization of rotavirus NSP2/NSP5 interactions and the dynamics of viroplasm formation. The Journal of general virology, 85(Pt 3):625–634. https://doi.org/10.1099/vir.0.19611-0.

6.6. Publication of this chapter:

Devi, Y. D., Devi, A., Gogoi, H., Dehingia, B., Doley, R., Buragohain, A. K., Singh, C. S., Borah, P. P., Rao, C. D., Ray, P., Varghese, G. M., Kumar, S., & Namsa, N. D. (2020). Exploring rotavirus proteome to identify potential B- and T-cell epitope using computational immunoinformatics. Heliyon, 6(12):e05760. https://doi.org/10.1016/j.heliyon.2020.e05760.